EVALUATION OF FUEL OXYGENATE DEGRADATION IN THE VADOSE ZONE

David A. Torres, Major, USAF, BSC
AFIT/GES/ENV/05M-05

DEPARTMENT OF THE AIR FORCE
AIR UNIVERSITY

AIR FORCE INSTITUTE OF TECHNOLOGY

Wright-Patterson Air Force Base, Ohio

AFIT/GES/ENV/05M-05

EVALUATION OF FUEL OXYGENATE DEGRADATION IN THE VADOSE ZONE

THESIS

Presented to the Faculty

Department of Systems and Engineering Management

Graduate School of Engineering and Management

Air Force Institute of Technology

Air University

Air Education and Training Command

In Partial Fulfillment of the Requirements for the

Degree of Master of Science in Environmental Engineering and Science

David A. Torres, BS

Major, USAF, BSC

March 2005

AFIT/GES/ENV/05M-05

EVALUATION OF FUEL OXYGENATE DEGRADATION IN THE VADOSE ZONE

David A. Torres, BS
Major, USAF, BSC

Approved:

/signed/	
_____	4 March 05
Dr. Charles A. Bleckmann (Chairman)	date
/signed/	
_____	28 February 05
Dr. Carl G. Enfield (Member)	date
/signed/	
_____	28 February 05
Dr. Ellen C. England (Member)	date
/signed/	
_____	4 March 05
Dr. Mark N. Goltz (Member)	date

Abstract

Groundwater contamination by petroleum products poses a potential human health and safety risk. Methyl tert-butyl ether (MTBE) was a commonly used fuel oxygenate that was added to gasoline to meet environmental regulations. The widespread use of MTBE resulted in significant contamination of drinking water supplies across the United States. Increased scrutiny regarding the use of MTBE has sparked efforts to replace MTBE with alternative fuel oxygenates.

The purpose of this research was to evaluate the degradation characteristics of potential alternative fuel oxygenates in the vadose zone. One fuel oxygenate that is being seriously considered as an alternative to MTBE is diisopropyl ether (DIPE). Specifically, this thesis sought to answer three research questions: what is the potential for DIPE degradation in soil without prior microbial augmentation, how does the presence of co-contaminants, such as ethanol and toluene, impact the biodegradation of DIPE, and will the increased use of DIPE represent a potential environmental risk? Previous research related to fuel oxygenates has focused primarily on oxygenates currently used, such as MTBE and ethanol. This research focused on a potential alternative to MTBE prior to its widespread implementation and use.

An experiment was run for 30 days to assess degradation characteristics for DIPE, ethanol, and toluene in the vadose zone. Due to the short length of the experiment, as well as the experimental difficulties encountered, it is not possible to determine if DIPE degradation occurred. Recommendations for future research to address potential fuel oxygenate impacts on the subsurface environment are discussed.

Table of Contents

Page

Page

List of Figures

Figure Page

Figure Page

List of Tables

Table Page

EVALUATION OF FUEL OXYGENATE DEGRADATION IN THE VADOSE ZONE

1.0 Introduction

1.1 Motivation

The automobile has impacted the environment since its invention and continues to play a major role in current environmental issues. From the invention of the automobile until the mid 1970's, tetra ethyl lead was added to gasoline as an octane enhancer and to reduce engine knock (Kovarik, 2003). However, by the early 1970's, high atmospheric lead levels, ozone depletion and global warming were factors that motivated the Environmental Protection Agency (EPA) to mandate a reduction in the use of lead (USEPA, 2003). In 1979, low levels of methyl tertiary butyl ether (MTBE) replaced lead in gasoline as an octane enhancer and to reduce engine knock. MTBE helped reduce atmospheric lead levels and kept the consumer satisfied. However, in the 1990's, the Clean Air Act Amendments mandated additional changes to gasoline. These changes led to widespread and increased use of MTBE and other fuel additives to increase oxygen content. These fuel additives were aptly named fuel oxygenates.

The widespread use of fuel oxygenates increased opportunities for environmental releases to occur. Releases are inevitable and occur from storage tanks, distribution systems, at the point of use, and also in air emissions (Ahmed, 2001). However, the widespread use of fuel oxygenates was not supported with adequate characterization regarding their environmental fate and transport.

MTBE does not readily degrade in the environment. When released to the soil and subsurface, MTBE is relatively mobile with a relatively high solubility. As a result, significant MTBE surface and groundwater contamination has occurred (Squillace *et al.*, 1996). Additionally, limited understanding of MTBE health effects have shifted regulatory efforts to reducing or even banning MTBE in gasoline.

An alternative fuel oxygenate is needed to fill the void created by MTBE reductions and bans. However, the performance of any replacement is critical to maintain customer satisfaction and continued compliance with regulatory requirements. Several fuel oxygenate alternatives exist and a thorough evaluation, including degradation characteristics under various conditions, is warranted prior to widespread use. The fuel refineries and distributors will ultimately decide the fuel oxygenate that replaces MTBE. Understanding the fate of any replacement oxygenates will not only allow for an informed decision but also provide strategies to control the inevitable releases.

Many different environmental factors affect the degradation of chemicals released to the environment. A chemical would likely encounter both aerobic and anaerobic conditions, each of which has different degradation processes. However, it is likely that most fuel oxygenate releases will initially occur in an aerobic environment. Hence,

aerobic degradation is a good choice to start for an evaluation. An experiment conducted in a laboratory environment affords limited control of certain environmental variables such as whether an aerobic or anaerobic environment exists. Ultimately, the research will provide results that can guide additional research, laboratory or field, eventually leading to an understanding on the environmental fate and transport of a particular chemical.

1.2 Research Objective

Research accomplished by Mares (2004) used a series of eight soil columns to assess potential aerobic degradation of ethyl alcohol, or ethanol. The results indicated ethanol did degrade in the aerobic environment.

To extend this research, the soil columns were maintained in an aerobic state, and an alternative fuel oxygenate, diisopropyl ether (DIPE) was evaluated for potential aerobic degradation. The impact of the presence of co-contaminants, ethanol and toluene, on the aerobic biodegradation of DIPE, was also evaluated. The research addressed the following questions.

1. Does DIPE degradation occur in soils without microbial augmentation?
2. How does the presence of co-contaminants, such as ethanol and toluene, impact the biodegradation of DIPE?
3. Based on the above results, would the use of DIPE as a fuel oxygenate represent an increased long term pollution risk?

1.3 Study Limitations

The experiment was conducted in a laboratory setting which inherently introduces limitations. Key limitations to the study are addressed.

The focus of the study is strictly aerobic degradation. While aerobic degradation is likely to be encountered initially, large or repeated releases can quickly deplete soil oxygen. Anaerobic degradation may still occur, however, anaerobic degradation was not considered in this study.

Due to the short duration of the experiment, optimal microbe adaptation may not have occurred. Microbial populations require adaptation periods to use available substrates. For example, MTBE aerobic degradation can occur, but may require several months, possibly due to slow microbial adaptation and growth (Schirmer *et al.*, 2003).

Since this was a laboratory experiment, the substrate application may not represent a realistic environmental release and therefore any results beyond a controlled laboratory setting may not be represented. The purpose of the laboratory experiment is to determine if degradation can be measured.

2.0 Literature Review

2.1 Fuel Oxygenate History

Automobiles used gasoline blended with lead prior to 1979 primarily to boost octane levels (USEPA, 2003). In 1970, anthropogenic vehicle emissions included nitrogen oxides, sulfur oxides, particulate matter, carbon monoxide, and lead. Vehicle emissions were a major source of atmospheric lead (Godish, 2004). Deteriorating air quality, combined with ozone depletion and global warming, spawned regulatory efforts to control vehicle emissions. In 1973, the Environmental Protection Agency (EPA) issued lead reduction standards requiring the gradual phase down of lead to 0.1 gram per gallon by 1986 (USEPA, 2003). However, lead reductions reduced gasoline octane ratings and increased engine knock. Fuel oxygenates were introduced to replace lead. When blended with gasoline, fuel oxygenates boost octane rating, and reduce engine knock.

In 1990, the Clean Air Act Amendments (CAAA) mandated use of fuel oxygenates to be blended in all grades of gasoline for areas that did not meet ambient air quality standards for carbon monoxide or ozone (Squillace *et al.*, 1996). Two programs, the winter oxygenated fuels program and the reformulated gas program were created to attain these ambient air quality standards. However, a specific fuel oxygenate was not mandated by the CAAA but left to the discretion of the gasoline manufacturers.

The winter oxygenated fuels program requires oxygenated gasoline, also known as oxyfuel, in areas that do not meet carbon monoxide (CO) air quality standards. Started on November 1, 1992, the program included 39 metropolitan areas (USEPA, 2001). Oxyfuel is traditional gasoline blended with at least 2.7% oxygen added by weight (USEPA, 1994). It was used as early as winter 1988 in Denver, CO and in five other metropolitan areas prior to 1992 (USEPA, 1993).

The reformulated fuels program began January 1, 1995, and targeted nine metropolitan areas with the worst ozone pollution. Reformulated gasoline (RFG) is a different chemical formulation than traditional gasoline and contains at least 2.0% oxygen by weight, a maximum of 1.0% benzene, and a maximum of 25% aromatic hydrocarbons by volume (USEPA, 1994). The program was implemented in two phases with the overall goal to reduce vehicle emissions. Phase two of the reformulated fuels program was implemented on January 1, 2000 with additional emissions reductions requirements.

2.2 Fuel Oxygenate Functional Groups

Fuel oxygenates are chemical compounds containing oxygen and hydrogen atoms that are blended with gasoline to increase the oxygen content. Oxygenates increase octane ratings and improve the operating combustion efficiency vehicles. Increased combustion efficiency reduces vehicle carbon monoxide emissions (Godish, 2004).

Additionally, oxygenates reduce the vapor pressure of the mixture, reducing volatilization of aromatic compounds (USEPA, 2003).

Oxygenates include methyl tertiary-butyl ether (MTBE), diisopropyl ether (DIPE), ethyl-tertiary-butyl ether (ETBE), tertiary-amyl-methyl ether (TAME), tertiary-amyl alcohol (TAA) and tertiary-butyl alcohol (TBA), methyl alcohol and ethanol and can be separated into two categories, alcohols and ethers.

Alcohols are derived from aliphatic hydrocarbons by replacing one or more hydrogen atoms with a hydroxyl group, -OH. Alcohols can be produced from naturally occurring substances or synthetic substances. Naturally occurring substances involve fermentation of a carbohydrate source, such as grains, followed by distillation (Boggan, 2005). Synthetic alcohols can be created from natural gas, coal, or oil. Synthetic alcohols are created using ethylene and an acid as a catalyst for hydration (Boggan, 2005). Naturally occurring alcohols can be used in the production of beverage alcohol while synthetic alcohols can only be used for industrial purposes. Due to the polar nature of the oxygen-hydrogen bond, alcohols are more soluble in water than hydrocarbons, however as the carbon chain length increases, the solubility decreases (Brown *et al.*, 1997).

Ethers are two hydrocarbon groups bonded in a carbon-oxygen-carbon sequence and created by a reaction of two alcohol molecules with a strong acid that leads to the elimination of water (Pauling, 1988).

2.2.1 MTBE.

MTBE is an aliphatic ether manufactured by the chemical reaction of methanol and isobutylene. MTBE is a volatile, flammable, colorless liquid that is miscible in gasoline, and soluble in water, alcohol, and other ethers (Squillace *et al.*, 1996). MTBE was originally introduced into gasoline at low levels in the United States in 1979 as an octane enhancer during the phase down of leaded gasoline (USEPA, 2003). Since implementation of the winter oxygenated fuels program, MTBE has been used in gasoline at higher levels. Low-cost, ease of production, and transfer and blending characteristics make MTBE a popular fuel oxygenate (Mormile *et al.*, 1994). MTBE can be produced at a refinery and blended with gasoline prior to distribution without phase separation. The blended gasoline can then be transported through the existing distribution infrastructure (Squillace *et al.*, 1996). To meet the minimum requirements for oxygenated fuels and RFG, gasoline must contain about 15% MTBE by volume (USEPA, 1998). Approximately 30% of all fuel in the United States is blended and MTBE accounts for more than 80% of oxygenated fuels (USEPA, 1998). The structural formula of MTBE is provided below in Figure 2.1.

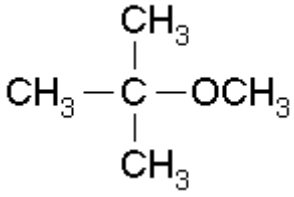

Figure 2.1 Structural Formula of MTBE

2.2.2 ETHANOL.

Ethanol, or ethyl alcohol, can be manufactured from a wide range of naturally occurring materials such as corn, barley or wheat. Early automotive experiments by Nicholas Otto, Henry Ford and others used ethanol (Kovarik, 2003). Ethanol is a volatile, flammable, colorless liquid that is miscible in water. Ethanol used in gasoline requires separate manufacturing near the point of use or must be transported via rail (USEPA, 1998). Distribution systems may contain water and other impurities that ethanol will bring into solution rendering the ethanol-gasoline mixture unusable (USEPA, 1998). Ethanol is the second most common oxygenate in use following MTBE and is used in approximately 15% of oxygenated fuels (USEPA, 1998). The structural formula of ethanol is provided below in Figure 2.2.

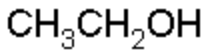

Figure 2.2 Structural Formula of Ethanol

2.2.3 DIPE.

Diisopropyl ether (DIPE) is a byproduct in the production of isopropyl alcohol made from propylene and water (Arce *et al.*, 2000). DIPE is a volatile, highly flammable, colorless liquid that is miscible with most organic solvents, soluble in oxygenated solvents and has limited solubility in water. While MTBE dominates the current fuel oxygenate market, insufficient MTBE supply can increase the interest in the heavier ether DIPE as a suitable replacement (Arce *et al.*, 2000). The structural formula of DIPE is provided below in Figure 2.3.

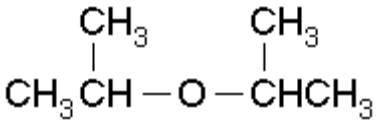

Figure 2.3 Structural Formula of DIPE

2.3 Fuel Oxygenate Health Effects

Risk assessments are a systematic process of hazard identification, dose-response assessment, exposure assessment, and risk characterization. Risk assessments are used to establish an acceptable level of risk which can lead to regulatory guidelines. Reference dose (RfD) for ingestion and reference concentration (RfC) for inhalation are two important values the EPA uses when establishing regulatory guidelines. RfD and RfC are estimates of the levels at which no significant health effects are anticipated due to exposure over a lifetime (USEPA, 2002).

Gasoline blended with fuel oxygenates can be released to the environment via air emissions, accidental discharges, leaking underground storage tanks and others pathways. Potential human exposures to a chemical release can occur through inhalation, ingestion, or dermal contact. For non-occupationally exposed individuals, exposure to gasoline is usually limited to daily activities such as driving, vehicle refueling, parking garages, and homes with attached garages (Ahmed, 2001). Inhalation and dermal contact represent primary exposure risks for non-occupationally exposed individuals. However, the chemical properties of oxygenates combined with accidental discharges and leaking underground storage tanks, has led to the contamination of many surface waters and

drinking water aquifers. If contaminants are not removed from the drinking water, ingestion then becomes a potential pathway.

Traditional gasoline has over 1000 components including fuel oxygenates and aromatic hydrocarbons known as BTEX (benzene, toluene, ethylbenzene, and xylene) (USEPA, 1994). For BTEX and oxygenate components, benzene is the only component classified as a known human carcinogen. MTBE is classified as a confirmed animal carcinogen, but has not been validated as a human carcinogen (ACGIH, 2001). Limited epidemiological and clinical data exists on human health effects related to oxygenate exposures (Ahmed, 2001). Most health effect-related studies use laboratory animals exposed to high dose. Data collected are then extrapolated from an animal exposure to human exposure which would be anticipated to be several orders of magnitudes lower. This dose response assessment produces uncertainty when defining an acceptable risk level for establishing regulatory guidance (Masters, 1998).

2.4 Regulatory Environment for Fuel Oxygenates

Regulatory guidance for non-occupational exposures for fuel oxygenates is limited. MTBE has received the most widespread attention due to its potential as a human carcinogen. However, recommended occupational exposure thresholds for MTBE, DIPE and ethanol do exist. The Occupational Health and Safety Administration (OSHA) is the responsible government organization for establishing occupational exposure limits. The American Conference of Governmental Industrial Hygienists

(ACGIH) augments OSHA limits by providing annually updated recommended exposure thresholds. These thresholds are generally established as either a time weighted average (TWA) or a short term exposure limit (STEL). A TWA is used to define a limit for an occupational employee who works a typical eight hour workday, 40 hours per week. A STEL also establishes a recommended exposure threshold but is for exposure durations over a 15 minute period. STEL values are typically higher than TWA values as the exposure duration is significantly shorter. Table 2.1 is a summary of occupational exposure limits related to several fuel oxygenates and BTEX components.

Table 2.1 Occupational Exposure Standards (ACGIH, 2002)

Component	**Standard**
MTBE	50 ppm (TWA)
DIPE	250 ppm (TWA) 310 ppm (STEL)
Ethanol	1000 ppm (TWA)
Benzene	0.5 ppm (TWA) 2.5 ppm (STEL)
Toluene	50 ppm (TWA)
Ethylbenzene	100 ppm (TWA) 125 ppm (STEL)
Xylene	100 ppm (TWA) 150 ppm (STEL)

Since most individuals do not experience oxygenate exposures in an occupational setting these standards are not designed to protect the general population. As previously mentioned, the bulk of non occupational exposures to BTEX and fuel oxygenates occur through inhalation, dermal contact, and ingestion on an intermittent basis. The EPA has established regulations related to BTEX exposures, however fuel oxygenates do not currently have any regulatory requirements at the national level due to the uncertain

health effects. In December 1997, the EPA issued a drinking water advisory recommending 20-40 μg/L for MTBE to mitigate potential taste and odor effects (USEPA, 1997). This advisory is not enforceable, but many states have used this guidance to establish their own regulatory requirements for MTBE. The standards range from none in Montana to 240 μg/L in Michigan (Delta Environmental Consultants, 2004).

MTBE has received significant attention for its potential health effects. For this reason, the use of MTBE as a fuel oxygenate has been severely restricted in many states. Thirteen states have partially banned MTBE to less than 1% by volume of gasoline; one state is phasing out MTBE; and five have complete MTBE bans (USEPA, 2004). All of these restrictions will be implemented by mid-2005.

2.5 Fate and Transport of Fuel Oxygenates

The 1990 CAA oxygenated fuels and RFG mandate increased the use of oxygenates. The chemical properties of oxygenates and BTEX components are important factors in how much and how far a release will travel in a groundwater aquifer. Two factors that directly impact chemical transport are the pure-phase solubility of the chemical and the octanol-water partition coefficient (K_{OW}). Pure-phase solubility determines how much product can be dissolved into a water solution before free product exists. The partition coefficient provides an indication of the tendency of a solute to partition between an organic medium and water (Clark, 1996). A low K_{OW} indicates a

chemical is unlikely to dissolve in an organic medium. Additionally, the vapor pressure and Henry's Law Constant (K_H) provide valuable information regarding the ability of an oxygenate to reach the soil and stay in the soil. Most oxygenates generally have high vapor pressures that result in volatilization (API, 2000). However, relatively low K_H values cause fuel oxygenates to partition into soil moisture readily (API, 2000). Table 2.2 provides solubility, octanol-water partition coefficient, vapor pressure, and Henry's Law Constant information for common fuel oxygenates as well as toluene.

Table 2.2 Chemical Properties of Common Fuel Oxygenates and Toluene
(Howard *et al.*, 1997)

Oxygenate	**Pure Phase Solubility (mg/L)**	**log K_{OW} (log l/kg)**	**Vapor Pressure (25°C, mm Hg)**	**Henry's Law Constant (Dimensionless)**
Methanol	miscible	-0.75	121.58	1.087E-4
Ethanol	miscible	-0.16 -0.31	49-56.5	2.522E-4
TBA	miscible	0.35	40-42	4.803E-4
MTBE	43,000 - 54,300	1.20	245-256	2.399E-2
DIPE	2,039	1.52	149-151	5.191E-2
ETBE	~26,000	1.74	152	1.087E-1
Toluene	534.8	2.73	28.4	2.428E-1

Due to blending characteristics, ease of distribution, and cost, MTBE became the fuel oxygenate of choice (Mormile *et al.*, 1994). However, due to its relatively high solubility and low $K_{OW,}$ MTBE in the environment dissolves readily in water, and its subsurface transport is not retarded by sorption to soil organics. In areas where MTBE has been used in gasoline at greater than five percent by volume, groundwater detection is five times more likely (Grady, 2001). It is estimated that approximately 5-10 % of

community drinking water supplies in high oxygenate areas have detectable MTBE (USEPA, 1999). Adequate understanding of the attenuation of fuel oxygenates is critical for their continued use. Possible attenuation processes includes sorption, volatilization, abiotic degradation and biodegradation. While the first three are possible with fuel oxygenates, it is unlikely that attenuation by these processes is significant, based upon their chemical properties (Mares, 2004).

2.6 Attenuation of Fuel Oxygenates

Most fuel oxygenate research has focused on the degradation of MTBE, MTBE intermediates, ethanol, and BTEX components as mono-substrates. Past research has identified MTBE as potentially degradable under aerobic and anaerobic conditions. However, these studies sometimes are contradictory and indicate site specific conditions are important to degradation capabilities (Schmidt *et al.*, 2003). Mares (2004) summarized significant aerobic and anaerobic degradation research accomplished pertaining to MTBE, ethanol, and BTEX components. Degradation research continues on MTBE, ethanol, BTEX and also alternative oxygenates.

Schirmer *et al*. (2003) evaluated soil microcosms extracted from the shallow, aerobic sand aquifer located at Canadian Forces Base, Borden Ontario. Soil samples were collected from both uncontaminated and MTBE-contaminated locations in the subsurface. Batch microcosm studies of these soil samples were conducted to evaluate the potential for microbial use of MTBE as a primary carbon source, as well as the potential for MTBE cometabolic degradation with fuel hydrocarbons as the primary

substrate. Results indicated there was potential for MTBE to serve as the primary carbon source; however, this was rare and only occurred after an extended period of at least 68 days. The extended period for degradation could be the result of slow microbial growth or possible genetic mutation changes to utilize MTBE as a sole source of carbon (Schirmer *et al.*, 2003). MTBE degradation by hydrocarbon cometabolism also occurred readily except when toluene and methane were the primary substrates. Additional research into MTBE degradation as a primary carbon source in an aerobic environment could lead to identification of microorganisms that potentially may be capable of degrading alternative oxygenates too.

Other recent MTBE research efforts have focused on identification of microorganisms responsible for the biodegradation of MTBE. Most bacteria are unable to degrade MTBE as the primary growth substrate (Liu *et al.*, 2001). Francois *et al.* (2002) evaluated *Mycobacterium austroafricanum* IFP 2012 for potential MTBE biodegradation. The strain was grown on both MTBE and TBA. Results indicated strains grown on TBA were able to effectively degrade MTBE and that biomass production using TBA was good (Francois *et al.*, 2002). More importantly, *Mycobacterium austroafricanum* IFP 2012 was identified as only the third pure bacterial strain able to grow on and mineralize MTBE as the sole carbon source.

Sedran *et al.* (2002) evaluated the effect of the presence of BTEX on MTBE and TBA degradation. Continuous feed reactor experiments with and without BTEX, indicated the presence of the BTEX compounds did not inhibit the degradation of MTBE or TBA. Batch studies were accomplished using the reactor effluent and biomass. The batch samples were spiked with MTBE, MTBE and BTEX, TBA, and TBA and BTEX.

Batch study results indicated BTEX was preferentially degraded over MTBE and TBA. The BTEX degraded rapidly, and did not impact the MTBE degradation rates. However, the rapid degradation of BTEX may impose a significant oxygen demand that could limit aerobic degradation of MTBE (Sedran *et al.*, 2002).

The degradation of ethanol in an aerobic environment has been previously reported (Da Silva and Alvarez, 2002; Mares, 2004). Ruiz-Aguilar *et al*. (2002) evaluated the effect of ethanol versus MTBE on the degradation of BTEX components. Soil samples were collected from four sites that were either uncontaminated, or had previous exposures to MTBE, BTEX, and ethanol. Aerobic microcosms of these soil samples were studied to evaluate degradation of BTEX alone, BTEX plus ethanol, and BTEX plus MTBE. Results indicated ethanol degradation occurred rapidly in an aerobic environment and that ethanol was more readily degraded than the BTEX compounds. BTEX degradation was inhibited by the presence of ethanol (Ruiz-Aguilar *et al*., 2002). Additionally, the results indicated the presence of MTBE was not likely to affect ethanol or BTEX degradation (Ruiz-Aguilar *et al*., 2002).

Lovanh *et al.* (2002) also evaluated ethanol and BTEX degradation in an aerobic environment. The experiment used four chemostats with ethanol and BTEX compounds exposed to various bacterial cultures. Results indicated ethanol degradation inhibited the degradation of the BTEX compounds. Limited BTEX attenuation due to the presence of ethanol can lead to expanded BTEX plumes if ethanol is used as an oxygenate (Lovanh *et al.*, 2002).

Park *et al.* (2001) evaluated the degradation of toluene in an aerobic environment. Using a known toluene degrading bacteria, *Ralstonia pickettii* PKO1, batch studies and

continuous flow column experiments evaluated toluene degradation when the bacteria were exposed to fluctuating concentrations of toluene. The experiments were conducted in a homogenous saturated sandy porous medium. Michaelis-Menten kinetics were assumed, and kinetic parameters were derived from the batch study data. These parameters were then used to model the continuous flow experimental results. The continuous flow experiments showed significant degradation of toluene. However, when the toluene influent concentrations fluctuated, the observed degradation rates were not consistent with Michaelis-Menten kinetics. Reducing influent toluene concentrations resulted in increasing toluene effluent concentrations. This increased toluene effluent was driven by starvation of the microbial population (Park *et al.*, 2001). When the influent toluene concentrations were increased again, degradation activity increased, thereby reducing effluent concentrations. It appears there is a threshold concentration of toluene required to maintain the microbial population. These results indicated that previous substrate exposure and fluctuating concentrations can significantly impact the degradation capabilities of the microorganisms (Park *et al.*, 2001).

Limited detailed research into DIPE degradation exists. However, an experiment conducted by Church and Tratnyek and reported at a workshop on biodegradation of MTBE in February 2000 (EPA, 2001), used mixed cultures to identify aerobic biodegradation rates of various fuel oxygenates including DIPE. The results of the experiment indicated aerobic degradation rates for DIPE were on the same order of magnitude as the rates for the aerobic degradation of MTBE. The similarity of the chemical structures suggested that similar biodegradation characteristics and constraints would be expected for DIPE and MTBE (EPA, 2001).

3.0 Methodology

3.1 Experiment Design

Operation of the experiment can be broken into 5 categories: the column setup; the feed system; the control system; monitoring equipment; and sampling methods. Mares (2004) discussed specific column construction and equipment details. A brief overview of the system and equipment is provided in this chapter, including system modifications accomplished during the current research.

3.1.1 Column Setup.

The experiment consisted of eight separate soil columns of polyvinyl chloride (PVC) tubing. Each column was constructed in a similar manner and setup to minimize variability from column to column. The columns were eight feet tall and eight inches in diameter. Each column was constructed with one foot of course drain rock at the bottom, followed by approximately six feet of sandy soil on top. Ports were installed in each column at three different elevations, the top, middle, and bottom of the column. The top and middle ports were to sample oxygen and carbon dioxide conditions inside the columns. The bottom port provided column drainage. The sampling ports accessed three 3-foot silicon tubing loops buried in the soil during construction. The top port had two loops, one reinforced with nylon and one with silicon only. The middle port had only one reinforced loop. Silicon is permeable to oxygen and carbon dioxide, allowing an

exchange of gas between the surrounding soil and the silicon loop. Decreased oxygen and increased carbon dioxide indicates microbial activity within the columns. Gas from the top port reinforced loop was pumped to an external oxygen sensor from Japan Battery Co. Ltd. Gas in the remaining loops was analyzed by a Columbus Instruments Micro-Oxymax respirometer. Equipment limitations prevented the use of Micro-Oxymax in previous research.

3.1.2 Feed System.

A chemical and tap water mixture was fed to the soil surface at the top of the column that was open to the atmosphere. Water, in five gallon buckets, was pumped to the columns using a single fixed-speed pump. Test chemicals were stored in a separate reservoir and pumped using a variable speed pump. Mares (2004) recommended increasing the chemical reservoir from a 40 mL vial to ensure a constant chemical feed. A 250 mL amber narrow mouth bottle reservoir capped with a Teflon lined septum replaced the original chemical storage vials. A needle tip was inserted into the septa as had previously been done with the 40 mL vials to equalize pressure. The test chemicals and water were mixed just prior to column application. Previously, the water and chemical feed lines were connected to a 5/16 inch inside diameter (I.D.) tube which then fed the mixture through a stainless steel in-line static tube mixer. This setup created a mini reservoir that was difficult to maintain at consistent water and chemical flow rates. To alleviate the potential flow rate fluctuations, a stainless steel reducing T-connector replaced the 5/16 inch tubing, reducing the volume of the mini reservoir to negligible. The T-connector was then attached to the in-line static tube mixer that fed to the column

top. The feed system pumps were run by a specially developed computer program. (C.G. Enfield, personal communication, August 19, 2004).

3.1.3 Control System.

A dedicated computer, running a visual basic program created by Dr. Enfield, operated the feed system and recorded data from the external oxygen sensor. Originally, the computer program operated the pumps, using data from oxygen sensor. Mares (2004) detailed the pump operation. For the current research, the computer program was revised to operate the pumps for a specified time period independent of the oxygen data. Columns one through four pumped a volumetric flow at 2 % of the volumetric flow rate at saturation, while columns five through eight pumped at 10% of the volumetric flow rate at saturation. The different flow rates were selected to assess potential degradation of the contaminants under varied conditions. The volumetric flow rate at saturation was determined using the constant-head permeameter method described in section 3.2.2.

3.1.4 Monitoring Equipment.

The monitoring equipment consisted of the external Japan Battery Co. Ltd oxygen sensor and the Micro-Oxymax respirometer. Mares (2004) detailed the setup of the external oxygen sensors. As previously discussed, the top and middle ports were also designed to collect oxygen and carbon dioxide data using the Micro-Oxymax respirometer.

The Micro-Oxymax respirometer data can be used to assess microbial activity within the columns. The respirometer was operated as a closed circuit system to measure oxygen and carbon dioxide changes in the experiment. The system was equipped with an

oxygen sensor, range 10-21 percent, and a carbon dioxide sensor, range 0-1 percent. The respirometer had an expansion interface to monitor up to 20 chambers.

The respirometer's primary function was to measure consumption or production of oxygen and carbon dioxide. Once the consumption or production is known, a corresponding rate can then be calculated using Equations 1 and 2 below. These calculations were accomplished by the respirometer.

$$\begin{pmatrix}\text{Consumption}\\ \text{(or production)}\end{pmatrix} = (\text{Gas Volume}) * \begin{pmatrix}\text{Gas concentration change}\\ \text{between 2 consecutive readings}\end{pmatrix} \quad (1)$$

$$\text{Consumption Rate} = \frac{\text{Consumption(or production)}}{\text{Elapsed time between interval}} \quad (2)$$

During operation, gas is pumped from a test chamber through the gas sensors for measurement, returning the air to the test chamber. The three foot silicon loops within each column represented a test chamber in this experiment.

The measured gas concentrations at the sensors can be influenced by temperature fluctuations, barometric pressure changes, and sensor drift. To compensate for these fluctuations, the system can periodically refresh the air in the sensor with external ambient or bottle air. The periodic sensor refresh can be both automatic and user defined.

Since the system operates as a closed circuit, it is critical to eliminate any leaks that could result in measurement errors. Therefore, each connection to the respirometer represents a potential leak. The initial column construction used 1/8 inch I.D. copper tubing to connect the respirometer to the column ports. Each inlet line to the respirometer had a Millipore, Millex-FG 0.20 µm hydrophobic PTFE 50 mm filter with

quick connect fittings, installed to prevent moisture and contaminants from reaching the respirometer. The copper tubing leaked air at the connections into the respirometer sample chambers rendering the system unusable. The copper tubing was replaced with 1/8 inch I.D. nylon tubing. Figure 3.1 below is the soil column experiment.

Figure 3.1 Soil Column Experiment

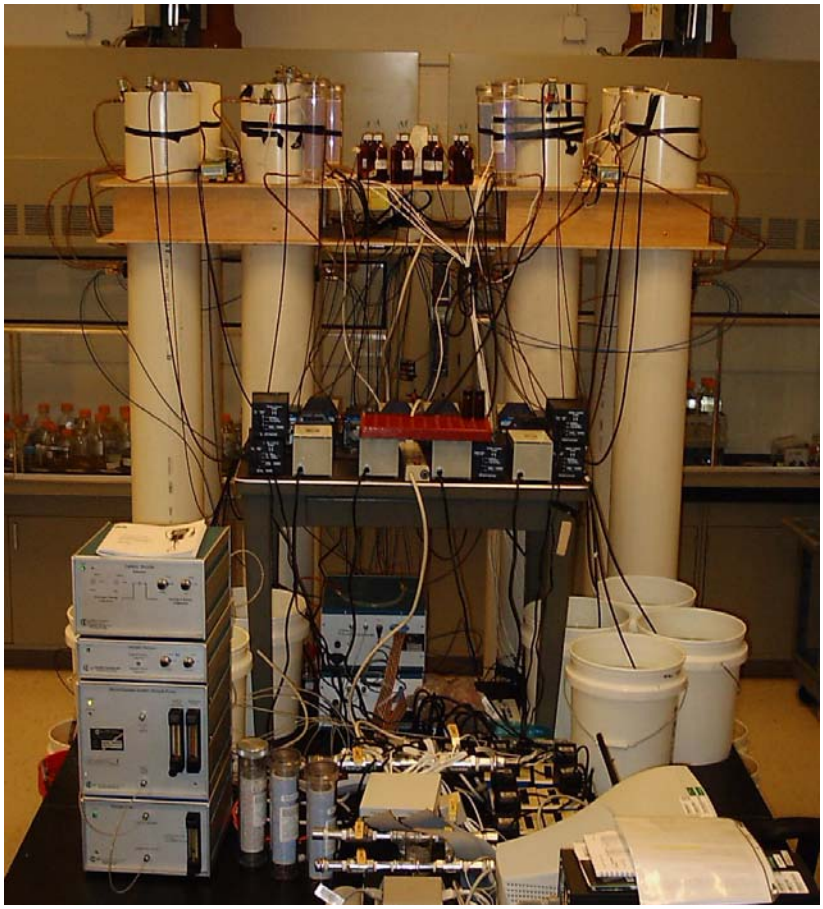

3.1.5 Sampling Methods.

Influent and effluent water was sampled daily. Zero headspace samples were collected into Agilent two mL clear sample vials with PTFE/silicone/PTFE septa screw tops. Influent samples were collected from the influent discharge tube at the top of the

columns. Prior to sample collection, each tube was wiped clean to prevent soil grains from entering the sample vial. Effluent samples were collected using a five mL Hamilton Gastight high performance luer tip syringe with a 22 gauge removable needle. The sample was collected from the effluent discharge tee connector as detailed in Mares (2004). For each sample, a five mL syringe volume was withdrawn and discarded. A second five mL syringe volume was withdrawn and used to fill the two mL vial. The syringe was rinsed three times with deionized water between each sample. Samples were analyzed using an Agilent Gas Chromatograph (GC) 6890 series with a flame ionization detector (FID). Specific GC-FID operating parameters are discussed later in Chapter 3.

3.2 Column Properties

The objective of the research was to determine potential degradation of various organic carbon substrates. Knowledge of the column properties, such as hydraulic mean residence time and pore volume, were important factors in modeling processes in the columns (Mares, 2004). Column properties are needed to establish substrate application rates and determine sampling frequency. These columns were constructed to be identical, but in fact, their properties were different, as discussed in Mares (2004). The goal of this research was to replicate previous results and confirm the following properties for each column: total porosity and pore volume at saturation, hydraulic conditions at saturation, mean residence time and pore volume at less than saturation.

3.2.1 Porosity and Pore Volume at Saturation.

Soil porosity indicates how much liquid a soil can hold. Porosity is typically determined by taking a soil sample, saturating the sample with water, and weighing the sample. The sample is then completely dried and reweighed. The weight difference is used to determine the volume of water in the saturated sample. A traditional porosity determination could not be accomplished for this experiment. The column porosity was estimated from work conducted by a contractor, Jason Lach.

An estimate of the column soil porosity assumed the columns were dry. Influent flow to each column was stopped in the spring of 2004 and only a small amount of water was drained at the base of the column in August 2004 when the contract work was accomplished. Each column was reverse saturated by forcing water up the column through the effluent drain until water completely covered soil at the top of the column. The volume of water used to fill the column was recorded. This volume of water is the volume of voids for the column, or the pore volume. The total volume of the column was calculated using the volume of a cylinder equation. The total porosity was estimated using Equation 3 below.

$$n = \frac{V_V}{V_T}$$

n= Total porosity (3)

V_v =Volume of Voids

V_T =Total Volume of Column

The estimated porosity and pore volume determined using this process assumed 100% soil saturation.

3.2.2 Hydraulic Conditions at Saturation.

The hydraulic conductivity and volumetric flow rate at saturation were determined by the constant-head permeameter method as detailed in Day (2000). Water was forced up the column through the effluent drain until water completely covered the soil at the top of the column. The column was then drained for one-half hour. The column was immediately filled again until the water completely covered the soil. The effluent drain was plugged and additional water added at the top of the column to bring the water level up to one and half inches below the top of the PVC column. A 1000 mL graduated cylinder completely filled with water and plugged with a rubber stopper was then inverted and immersed into the water at the top of the column. When the rubber stopper was removed, the water in the graduated cylinder remained. The height of the water at the top of the inverted graduated cylinder was recorded. The effluent drain plug was then removed. The change in volume and water height for the graduated cylinder and time required was recorded. The volumetric flow rate was calculated using Equation 4 below.

$$Q=\frac{\Delta V}{\Delta t} \quad (4)$$

Q=Volumetric flow rate

ΔV=Change in Volume of Graduated Cylinder

Δt=Change in time

The hydraulic conductivity of the soil was then determined using Equation 5 below.

$$K=\frac{QL}{\Delta hAt} \quad (5)$$

Q=total discharged volume (ml) in a given time t
L=Length of soil column
Δh=total head loss for the constant head permeameter
A=Area of soil column
t=time for change in height
K=Hydraulic Conductivity

3.2.3 Hydraulic Conditions at 2% and 10% of the Volumetric Flow Rate at Saturation.

A non reactive tracer test, using sodium chloride (NaCl), was used to determine the hydraulic mean residence time and pore volume for each column. The volumetric flow rates for the tracer test were 2% of the volumetric flow rate at saturation for columns one through four, and 10% of the volumetric flow rate at saturation for columns five through eight. Three grams of NaCl, A.C.S. crystals from Fisher Scientific, were added to one liter tap water and then stirred for three to five minutes using a stirring plate. A reading was then taken using a Yellow Springs Instrument (YSI) 85 oxygen, conductivity, salinity and temperature probe. The NaCl solution was then fed into the pump system as a pulse input. The duration to feed the pulse was recorded. At the completion of the pulse, the pump line was immediately returned to the five gallon reservoir containing tap water that was run for the duration of the tracer test. Specific conductivity readings were collected at regular time intervals from the effluent discharge using the YSI conductivity probe. Initially, readings were taken at three hour intervals.

Readings were taken hourly when the effluent conductivity started to increase. This was done to capture the peak concentrations related to the pulse input. Data collected from the tracer test for each column was then used to calculate the discrete residence time density function and the mean residence time as detailed in Clark (1996). Additionally, the pore volume and a mass balance for each column were determined using the method of moments as discussed in Mares (2004). The residence density function (Equation 6) and the mean residence time (Equation 7) are listed below.

$$f\left(t_i\right)=\frac{c\left(t_i\right)}{\text{Area}}$$

$$\text{where Area}=\sum_{i=0}^{\text{imax-1}}\left[\frac{c\left(t_{i+1}\right)+c\left(t_i\right)}{2}\right]\left(t_{i+1}\text{-}t_i\right) \tag{6}$$

$f\left(t_i\right)$=Discrete residence time density function

$c\left(t_i\right)$=Effluent concentration at t_i

t_i=Time of effluent sample

$$\bar{t}_{RTD}=\sum_{i=0}^{i\max-1}\left[\frac{t_i+t_{i+1}}{2}\right]\left[\frac{f\left(t_i\right)+f\left(t_{i+1}\right)}{2}\right]\left(t_{i+1}-t_i\right) \tag{7}$$

$\bar{t}_{RTD}$ = Mean residence time

The biodegradation rate in the soil columns can be estimated assuming degradation kinetics can be modeled as a first-order reaction. As such, the mean residence time, and the measured influent (C_0) and effluent (C) concentrations can be used to determine the first-order rate constant (k) using Equation 8 below. Knowing k, the first-order reaction model can then be used to estimate effluent concentrations for any

combination of influent concentration and mean hydraulic residence time. The model can be validated by varying the influent concentration and mean residence time, and comparing how well the first-order model-predicted effluent concentrations compare to measured effluent concentrations. A validated model can be used to develop bench or pilot scale experiments, as well as predict chemical fate in the field due to natural attenuation or engineered processes.

$$k = \frac{1}{\bar{t}_{RTD}} \ln \frac{C_0}{C} \tag{8}$$

The water filled pore volume (V_w) for each column during the tracer test was calculated by multiplying the mean residence time calculated in Equation 7 by the volumetric flow rate.

To validate the tracer test and identify any potential problems with the data, a degree of saturation during the tracer test was calculated for each column. Also, to validate the assumption that the porosity data was collected at saturation, a degree of saturation using Mares (2004) tracer test data was calculated. The degree of saturation was calculated using Equation 9 below.

$$\text{Degree of Saturation} = \frac{V_w}{V_V}$$
$$V_w = \text{Water Filled Pore Volume} \tag{9}$$
$$V_v = \text{Volume of Voids}$$

The water filled pore volume calculated by the tracer tests was used to estimate the volume of water in the column and the volume of voids was measured as described in Section 3.2.1.

3.2.4 Organic Substrates.

The substrates ethanol, toluene, and DIPE were used in this experiment. Four columns received all three chemicals while four columns received only toluene and DIPE. Table 3.1 provides the specific substrate additions to each column.

Table 3.1 Substrates Added to Each Column

Column	Toluene	DIPE	Ethanol
1	X	X	
2	X	X	X
3	X	X	X
4	X	X	
5	X	X	X
6	X	X	
7	X	X	
8	X	X	X

Note: X = chemical added to column

3.3 Flow Rates

The constant-head permeameter test results were used to calculate volumetric flow rates for 2 % and 10% of the volumetric flow rate at saturation. The 2% volumetric flow rate was pumped to columns one through four using 1/16 inch I.D. Norprene tubing for the tap water. The 10% volumetric flow rate was pumped to columns five through eight using 1/8 inch I.D. Norprene tubing for the tap water. As previously discussed, the

control program was revised to allow a specified time period for operation. Based upon manufacturer specifications for pump revolutions per minute and tube flow per revolution for the tap water delivery system, an on/off pump cycle time was calculated. The volumetric flow for the chemical feed system to each column operated at less than 0.05 mL/min. Due to negligible flows for the chemical feed system, these values were not included in the on/off pump cycle calculations. The computer program cycle lasted one minute and for columns one through four the pumps were on 0.4 minutes. For columns five through eight, the pumps were on for 0.44 minutes. These values were entered into the on-screen computer display that controlled the pump operation.

The flow rate of each column was then manually verified using a graduated cylinder and scale. The tap water feed and chemical feed lines were each evaluated separately. For ease of weight conversion, tap water was also used in the chemical feed lines during this portion of work. Each line was sampled three times using a Nalgene 25 ml graduated cylinder (Plastic, Measure, Pour). For each sample, two complete pump cycles were collected into the graduated cylinder. Two pump cycles were collected to minimize possible variations in pump flow. An OHAUS Analytical Plus scale, Model # AP250D was used to weigh the cylinder and water. The scale was zeroed with the dry graduated cylinder prior to taking any samples. The weight was converted as one gram of water equivalent to one milliliter water. A mean flow was calculated for each column. The flow was then divided by two to obtain a mean flow for one pump cycle for each column.

3.4 Calibration Standards

A response-concentration curve for the YSI conductivity probe was created. The curve converted a measured response from the tracer test to a concentration. Certified Fisher Scientific A.C.S. NaCl crystals were added to a one liter graduated cylinder of tap water in increments of 0.01, 0.1, 0.5, 1.0, 1.5, and 2.0 grams. The mass additions correspond to 10, 100, 500, 1000, 1500, and 2000 mg/L of NaCl respectively when added to one liter. The conductivity probe response was then plotted against the concentration added to the tap water. The zero concentration point for the curve used only the tap water conductivity response. Using Microsoft Excel, a best fit line and equation was created.

The equation, $y=0.5172x - 484.07$ with an R^2 value of 0.9999, was calculated for the conductivity-concentration response curve. Since deionized water was not used, this was not a true calibration standard, but provided a good estimation for conductivity values. Tap water was used to eliminate the need to subtract the baseline effluent concentrations throughout the tracer tests. The conductivity-concentration response curve is shown in Appendix B.

Calibration curves for toluene, diisopropyl ether (DIPE), and ethanol were created to correlate a GC-FID response to a known concentration. All chemicals were manufactured by Sigma Aldrich of Milwaukee, WI. Table 3.2 summarizes the chemical grades used in the experiment.

Table 3.2 Chemical Grade Information

Chemical	CAS Number	Grade
Toluene	108-88-3	HPLC grade 99.8%
Diisopropyl Ether	108-20-3	Reagent Plus, 99%
Ethanol	64-17-5	HPLC/Spectrophotometric grade (200 proof)

Chemical standards from 1 mg/L to 1000 mg/L were prepared. The upper limit for the toluene standard was 400 mg/L to ensure the toluene solution was below the solubility limit and provided reproducible results. Each standard was prepared individually using a Finnpipette with disposable 200 μL pipette tips, deionized water, and a 50 mL volumetric flask. The standard solution was gently agitated and then allowed three minutes to reach equilibrium. The standard was then transferred to a 40 mL sample vial with zero headspace and sealed with a Teflon lined septum. A 5 mL Hamilton Gastight high performance luer tip syringe with a 22 gauge removable needle was used to transfer standard solution to a two mL amber sample vial sealed with a PFTE/rubber lined crimp cap. Six samples were analyzed for each standard concentration using the Agilent 6890 GC-FID. The GC-FID response was plotted against the known concentration for each standard. Using Microsoft Excel, a best fit line and equation was developed.

The toluene calibration curve produced the equation y=37021x + 2E+06, with an R^2 value 0.8984. Toluene standards at 1, 10, 100, and 400 mg/L were analyzed. The DIPE calibration curve produced the equation y=115832x + 984100 with an R^2 value 0.9953. DIPE standards at 1, 10, 100, 724, and 1000 mg/L were analyzed. The ethanol

calibration curve produced the equation y=101297x + 636001 with an R^2 value 0.9979. Ethanol standards at 1, 10, 100, 789, and 1000 mg/L were analyzed.

Initially, 36 calibration standards for each chemical were created and analyzed using the GC autoinjector. This process lasted approximately six hours and the samples at the end of the analysis showed potential loss due to volatilization. To minimize loss due to volatilization, standards were run again, and only two concentrations were prepared at a time for analysis. This improved the linear concentration-response. However, all of the calibration curves were not consistent.

The toluene calibration curve R^2 value indicated potential calibration standard issues. First, the GC analytical method could be incorrect. While the GC parameters provided consistent analytical results for the DIPE and ethanol calibration standards, daily GC calibration failed by exceeding the upper and lower 95% confidence limit. Second, and also related to the GC analytical method, was the split inlet used to minimize matrix interference. Split inlets provide good analytical results for higher concentrations. However at low concentrations, a splitless inlet is advantageous. A splitless inlet option was originally considered, however, due to FID difficulties and matrix interference, the analytical method chosen used a split inlet. Third, if the standard had not reached equilibrium when originally placed into the sample vial, some variability could have been introduced. While this possibility exists, the sample standard deviation at a each respective concentration was small. Another possibility included a potentially damaged capillary column. However, GC analysis accomplished for different research during the same period used the same column without any variations. Finally, the most likely explanation for faulty calibration standards was an incorrect GC analytical method

capable of reproducible results across a wide spectrum of concentrations. Therefore, the data collected can only be estimated using the calibration curves. The calibration curves are shown in Appendix B.

3.5 Equipment Settings

3.5.1 Micro-Oxymax Respirometer.

The Micro-Oxymax respirometer allows the user to define variables such as the number of chambers, or in this case tubing loops to sample, sampling interval and duration, refresh frequency, refresh threshold, and refresh duration.

The respirometer samples the chambers, in order, from one to twenty. If a chamber is not functioning properly or is not used it will still be sampled. A chamber not in use is "short circuited" by placing a short length of tube from the input directly to the output on the expansion interface. The experiment sampled all 20 chambers, but only 18 chambers were used for experimental data purposes. The columns required a total of 16 chambers, two chambers per column. The remaining two chambers provided reference points external to the columns that could be used to determine if the system was functioning properly. One external chamber used a single 3 foot loop of silicone tubing exposed to laboratory air. The final external chamber was connected to a 250 mL sealed sample jar.

The sampling interval and duration can be automatically determined by the respirometer or can be user defined. The sample interval determines the sample cycle

frequency. A cycle samples all 20 chambers. Since conditions in the soil columns did not change rapidly, the sampling interval was extended to improve the sensor response capability.

As previously discussed, the user can define the instrument refresh parameters. Refresh frequency, refresh threshold, and refresh duration are three parameters that can be user defined. Refreshing the chamber for every measurement increases the sample cycle time. This can also improve measurement consistency by maintaining a fresh air supply in the sensor to mix with chamber air. A refresh was used for each measurement since the experiment interval was not time constrained. Refresh threshold defines an acceptable upper and lower limit concentration for consecutive samples. If the measured concentration exceeds the upper or lower limit, then the sensor air will be refreshed. This refresh occurs after the current chamber measurement and before the next chamber measurement. The system default parameter was used for the refresh threshold. The refresh duration defines the amount of time the sensor chamber is refreshed with ambient air. This time should be long enough to completely flush the sensor. Specific experiment settings are provided in Appendix A.

Weekly calibration of the oxygen and carbon dioxide sensors was accomplished using a calibration gas from Weiler Welding Company. The gas contained 20.4% oxygen, 0.704% carbon dioxide, and the balance nitrogen. Additionally, all chambers were tested each week to ensure they continued to meet minimum leakage and restriction requirements. If excessive leakage or restriction was identified, the sample chamber required correction. Detailed data regarding the sample chamber's restriction, volume, and leakage are listed in Appendix A.

3.5.2 Agilent 6890 Gas Chromatograph with Flame Ionization Detector.

A gas chromatograph with flame ionization detector (GC-FID) was used to analyze influent and effluent samples. Sample vials were collected, as previously discussed, and placed on a sample vial tray to be analyzed with the Agilent 7683 Auto Injector. The auto injector used a 10 μL gastight syringe rinsed with acetone and deionized water between each sample injection. The capillary column used for analysis was a J&W Scientific DB-624 (#123-1334, Length: 30 m, ID: 0.32 mm, Film: 1.8 um) with a DuraGuard deactivated fused silica column guard (#160-2325-5, Length: 5 m, ID: 0.32 mm). The GC-FID was controlled by a remote computer using the MSD Chemstation Build 75, dated August 26, 2003.

The MSD Chemstation was used to develop calibration curves and also to evaluate influent and effluent concentrations. The software translated the GC-FID response into an area. This area was then converted to a concentration using the linear equations developed from the calibration curves as previously discussed.

The particular GC-FID operating parameters were originally selected based upon Mares (2004). However, due to matrix interferences during elution, the method was revised. The revised method provided for more distinct elution of the three chemicals. The specific parameters of GC-FID operation are detailed in Appendix A.

The method detection limit (MDL) was determined per the Code of Federal Regulations (CFR) (40 CFR 136, 1993). The MDL identifies the lowest quantifiable analytical results for the particular GC method and was determined using Equation 10 below.

$$MDL = SD \times t_{0.99}$$

$$\text{Where } SD = \left\{ \frac{\sum_{i=1}^{n} (x_i - X)^2}{(n-1)} \right\}^{1/2}$$

MDL= method detection limit (mg/L)

SD= standard deviation (10)

$t_{0.99}$ = t-distribution table value for 99% with the degree of freedom (n-1)

x_i = spiking replicates concentration (mg/L) (i = 1 . . . n)

X= the mean of spiking concentrations (mg/L)

A MDL for the GC analytical method was determined for each chemical. However, due to limited reproducibility, the MDL values are also estimated. The MDL values range from 1.14-3.99 mg/L. The MDL calculations are shown in Appendix B.

3.6 Assumptions

The soil column experiment is designed to assess degradation of fuel oxygenates. Several assumptions must be made to determine the amount of degradation, if any that occurs.

The first assumption is that flow and influent concentrations are constant. The pump system is designed to cycle on/off for a specified time each minute. This is done to achieve a desired flow rate, and it is assumed consistent flows and concentrations are applied to the system using this mechanism. Second, it is assumed chemical loss due to volatilization at the top of the columns is negligible. As discussed in Chapter 2, the fuel oxygenates have relatively high vapor pressures which can lead to volatilization of pure phase oxygenate. However, because of the low Henry's Law Constants, we would expect that dissolved oxygenate would largely remain in the aqueous phase. Finally, it is also

assumed the chemical sorption within the soil is minimal. The low K_{OW} associated with the fuel oxygenates indicates the chemicals are unlikely to substantially partition into an organic medium.

4.0 Results and Discussion

4.1 Experimental Results

The research used a series of eight previously constructed soil columns and was accomplished in three phases. Phase one consisted of developing a GC-FID analytical method and creating calibration standards for the equipment used. Next, column properties were determined. Phase three evaluated potential fuel oxygenate degradation.

4.2 Soil Column Properties

Column properties evaluated during the research included the porosity, pore volume, volumetric flow rate and hydraulic conductivity at saturation. The mean residence time and pore volume at less than saturation was also determined. The methods used to evaluate these properties were discussed in Chapter 3.

4.2.1 Porosity and Pore Volume at Saturation.

The columns are constructed with one foot of course drain rock (approximately 1 inch diameter) at the base with 5.5 feet of sandy soil (Mares, 2004). Typical porosity values for sandy soils range from 26 - 53 % total porosity (Domenico and Schwartz, 1998). Porosity values obtained for the columns were 23.2 - 29.7 %. The pore volumes

obtained were 14.9 - 19.1 L. A summary of the porosity and pore volume for each column is provided in Table 4.1. Tabulated porosity values are in Appendix B.

4.2.2 Hydraulic Conditions at Saturation.

The constant-head permeameter method was used to estimate two properties, the volumetric flow rate at saturation and the hydraulic conductivity. The volumetric flow rate at saturation was used to establish a volumetric flow rate at 2% and 10% for the experiment. Volumetric flow rates at saturation were 96.6 - 209 ml/min. Columns one through four were pumped at a volumetric flow rate equal to 2% of volumetric flow at saturation, while columns five through eight pumped a volumetric flow rate equal to 10% of volumetric flow at saturation.. At 2%, the calculated volumetric flow was 3.2 ml/min. At 10%, the calculated volumetric flow was 11.8 ml/min.

Typical hydraulic conductivity values for a sandy soil range $2x10^{-5}$ - 0.6 cm/s (Domenico and Schwartz, 1998). The estimated average hydraulic conductivity values for the columns were $4.40x10^{-3}$ - $9.40x10^{-3}$ cm/s. A summary of the hydraulic conditions at saturation is provided in Table 4.1 below with detailed data and calculations located in Appendix B.

Table 4.1 Summary of Hydraulic Conditions at Saturation

Hydraulic Properties at Saturation				
Column	**Porosity (%)**	**Pore Volume at Saturation**	**Average Volumetric Flow (ml/min)**	**Average Hydraulic Conductivity (cm/s)**
1	28.3	18.2	158	7.27E-03
2	23.2	14.9	143	6.37E-03
3	29.7	19.1	209	9.40E-03
4	25.1	16.1	131	5.91E-03
5	26.6	17.1	96.6	4.40E-03
6	28.3	18.2	103	4.54E-03
7	24.7	15.9	102	4.51E-03
8	27.0	17.4	170	7.49E-03

4.2.3 Hydraulic Conditions at 2% and 10% of Volumetric Flow Rate at Saturation.

Columns 1-4 were pumped at 2% of the volumetric flow rate at saturation during the tracer experiment. The input pulse for each column lasted from a minimum of 4.8 hours to a maximum of 5.0 hours.

A breakthrough curve was plotted for each column. Columns 1-4 all exhibited an extended tailing after reaching a peak effluent concentration. These extended tailings affected the pore volume calculation, mean residence time, and mass balance.

The mean residence times were 63.6 - 77.9 hours and the pore volumes were 12.3 - 15.2 liters. The range of values for the mean residence time and pore volume was narrow and indicated the columns are similar, but not identical, as previously discussed in Chapter 3. A mass balance was also accomplished during the tracer test.

The mass balance errors were -11.1 - 36.0 percent. The wide mass balance fluctuation could be the result of several factors. First, a typical tracer response curve in a saturated medium replicates a bell shaped curve. As the tail extends, the extended area under the curve increases mass recovery for longer than a traditional tracer response curve. Second, the conductivity-concentration curve could also affect the extended tailing. The conductivity-concentration curve used tap water as a base line, establishing 924 μS as the zero point. Columns one, three, and four all had initial effluent concentrations greater than the zero point. The result was positive mass recovery from the start of the tracer experiment. Additionally, at the tail end of the curve, effluent samples were measured until the conductivity dropped below the zero point of the conductivity-concentration curve. This too recovered mass in the effluent. Mares (2004) also hypothesized the extended tailing could be due to inconsistent and low flows. This is most likely. Padilla *et al*. (1999) found that NaCl transport in an unsaturated porous media does not exhibit a traditional breakthrough curve as the degree of saturation decreased, and that both an earlier initial NaCl arrival and an extended tailing were observed. These observations resulted from greater velocity variations and slower solute mixing in the unsaturated media and could result in erroneous calculations (Padilla *et al*.1999).

Columns 5-8 were pumped at 10% of the volumetric flow rate at saturation during the tracer experiment. The input pulse for each column lasted a minimum of 81 minutes to a maximum of 86 minutes.

A breakthrough curve was plotted for each column. Columns 5-8 all exhibited a typical tracer response curve that replicated a bell shaped curve. The mean residence

times were 17.8 - 26.9 hours and the pore volumes were 13.3 - 19.6 liters. The range of values for the mean residence time and pore volume was narrow and also indicated column similarities. The mass balance errors were -20.5 to -34.1 percent.

The pore volumes calculated from the tracer tests conducted during this research effort, were expected to be lower than the pore volumes obtained at saturation. These lower values were assumed since the tracer tests were conducted at less than saturation. For pore volume data collected during this research, the assumption was correct with the exception of columns five and seven. As discussed above, velocity variations and slower solute mixing could lead to erroneous calculations for tracer tests conducted at less than saturation. This is the most likely cause for the results in columns five and seven. When the pore volume data at saturation was compared against the tracer test pore volume data from Mares (2004), columns two, four, and five through eight all were greater than the pore volumes calculated at saturation. Again, as discussed previously, the differences in pore volume data could be the result of velocity variations and slower solute mixing. Erroneous assumptions related to the pore volumes calculated at saturation should also be considered as a possible reason. The calculated pore volumes at saturation and from the tracer tests are compared below in Table 4.2. Results for the tracer test for columns 1-8 are detailed in Appendix B.

Table 4.2 Estimated Pore Volume Comparison

	Pore Volume, L		
Column	**Saturated Column Test**	**Tracer Tests (Nov/Dec 2004)**	**Tracer Tests (Mares, 2004)**
1	18.2	14.0	17.0
2	14.9	12.3	15.7
3	19.1	14.5	17.5
4	16.1	15.2	19.3
5	17.1	19.6	27.3
6	18.2	13.3	23.4
7	15.9	17.5	27.8
8	17.4	14.6	23.8

The degree of saturation during the tracer test was also determined for each column as discussed in Chapter 3. Again, the results indicated errors in columns five and seven for the tracer data collected during the current research, as these two columns exceeded 100% saturation which is not possible. When the degree of saturation was calculated using tracer test pore volume data from Mares (2004), columns two and four through eight, indicated errors within the data collected. Table 4.3 below provides degree of saturation results.

Table 4.3 Estimated Pore Volume Comparison

Column	Tracer Test (Nov/Dec 2004) Degree of Saturation (%)	Tracer Test (Mares, 2004) Degree of Saturation (%)
1	76.9	93.5
2	82.3	105.3
3	76.1	91.7
4	94.3	119.9
5	115	159.7
6	73.2	128.3
7	110	174.7
8	84.2	136.9

4.3 Respirometer Results

Respirometer data were collected for only one week during the experiment. Setup of the system required extensive time and effort to eliminate leaks both inside the column and with the connecting tubing. The original setup used copper tubing to connect the respirometer to the sample loops inside the column. As previously discussed, the copper tubing leaked air into the respirometer sample chamber rendering the system unusable, and the copper tubing was changed to nylon tubing. The nylon tubing worked well and eliminated leaks with the respirometer at exterior connections. However, internal connections with the silicon tubing leaked. Water was visible in column four tubing and air leaked excessively in columns five and seven. Approximately one foot of soil was removed from the top of each column to repair the tubing. The leaks in these three columns were repaired. Also, near the conclusion of the experiment, column three developed an internal leak, and rendered chamber three data unusable. Other problems

encountered with the respirometer included the oxygen sensor. When the respirometer was placed in service, the original oxygen sensor configuration quickly reached the lower limit of detection, 19%. The sensor was replaced with an oxygen sensor capable of 10-21% oxygen detection. This provided a good range to observe potential aerobic activity in the columns. If aerobic activity occurred near the top of the columns, it was anticipated that the available oxygen in the soil would continue to decrease as the depth of the column increased. However, the oxygen content actually increased with depth in columns two through eight indicating potential equipment problems. Additionally, the respirometer top sensor data and the external oxygen sensor data for each column were compared. Only column five data had comparable values for both the respirometer and external oxygen sensor. The remaining columns indicated either the respirometer or external sensor was not functioning properly. Data results for the respirometer and external oxygen sensor are provided in Appendix B.

4.4 Organic Substrate Analysis

Organic substrate was added to the columns in December 2004 for 14 days. Due to a chemical shortage, the chemical additions were stopped for approximately two weeks. During this time, tap water continuously pumped through the columns. When sufficient chemicals were available, the chemicals ran continuously for the duration of the experiment.

Thirty days of data were collected during the experiment. Influent and effluent samples were analyzed for DIPE, toluene, and ethanol. Daily samples were taken rather than sampling based upon estimated pore volumes to determine when the system stabilized.

Due to fluctuations in the influent concentration, the system did not fully stabilize. Column seven toluene influent and effluent concentrations provided a good example of the complexity for the substrate application. The toluene influent concentrations during the 30 days fluctuated between 28 mg/L and 200 mg/L. A peak sample influent concentration of 678 mg/L was even recorded one time. However, the toluene effluent sample concentrations consistently exceeded 500 mg/L during the experiment and only in the last week of data collection, did toluene effluent concentrations approach influent concentrations indicating potential column stabilization. The high effluent concentrations could be the result of possible sorption associated with the December 2004 initial substrate application. Unfortunately, no influent data exist to substantiate this possibility. Figure 4.1 below highlights the difference between the toluene influent and effluent concentrations.

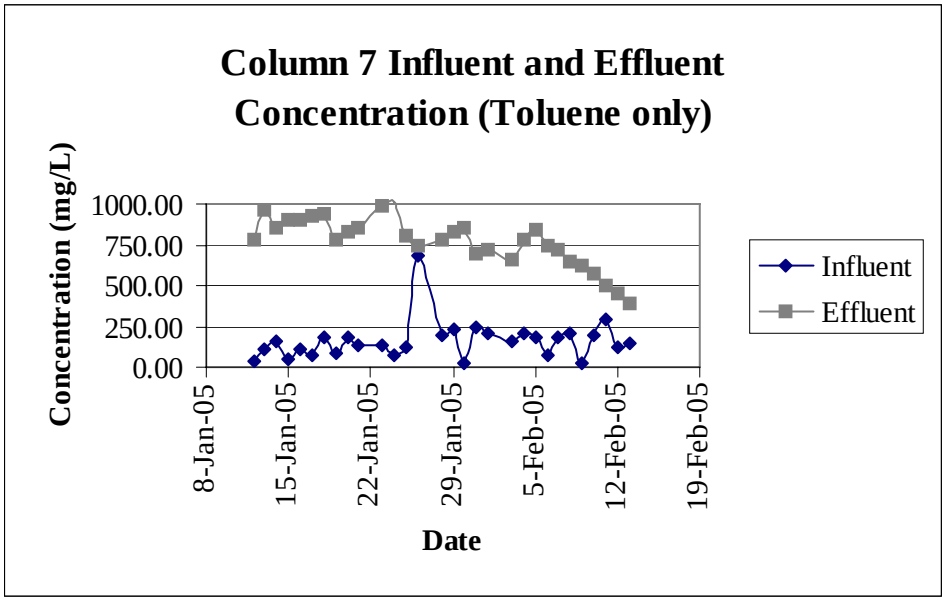

Figure 4.1 Column 7 Toluene Influent and Effluent Concentrations

Previous research using the soil columns evaluated ethanol degradation. Mares (2004) reported ethanol degradation did occur, therefore, it was anticipated that ethanol would degrade again in the soil columns during this experiment. Ethanol degradation did occur in all four columns within approximately one week after sampling started. However, due to the short experiment length, toluene and DIPE degradation were not observed in any column. The potential inhibition of DIPE degradation due to the presence of toluene and ethanol could not be resolved. Table 4.4 below provides a range of influent and effluent concentrations for each soil column. Tabulated influent and effluent data and charts for each column are provided in Appendix B.

Table 4.4 Influent and Effluent Concentrations Summary

	Influent, mg/L			Effluent, mg/L		
Column	**Toluene**	**DIPE**	**Ethanol**	**Toluene**	**DIPE**	**Ethanol**
1	22.2-333	120-406		155-1.63x10^3	303-822	
2	277-792	385-900	757-1.48x10^3	0-339	278-850	0-265
3	0-929	0-635	0-1.22x10^3	0-134	0-684	0-1.79x10^3
4	49.1-356	110-423		0-364	0-1.50x10^3	
5	0-411	0-277	0-564	0-182	0-994	0
6	36.9-257	57.6-233		156-816	118-296	
7	28.7-679	83.1-339		394-1.01x10^3	139-485	
8	76.5-500	82.5-387	33.8-623	152-790	97.5-470	0-490

5.0 Conclusions

5.1 Summary

The focus of this research was to evaluate aerobic degradation of alternative fuel oxygenates. The hydraulic properties provided insight into the possible environmental fate and transport of the substrates applied. Unfortunately, due to equipment limitations and time, the full focus of the research was not accomplished.

5.2 Conclusions

Does DIPE degradation occur in soils without microbial augmentation?

Due to the short length of the experiment, as well as the experimental difficulties encountered, it is not possible to determine if DIPE degradation will occur in soils without microbial augmentation. However, aerobic degradation of DIPE in soils without microbial augmentation may still occur. As previously discussed, aerobic degradation of MTBE was originally believed to not occur but recent studies have proven MTBE degradation over periods greater than sixty days. DIPE may also require extended periods for the microbial population to grow and adapt for adequate degradation to occur.

How does the presence of co-contaminants, such as ethanol and toluene, impact the biodegradation of DIPE?

The introduction of toluene did not show any impact on the degradation process. Degradation of the ethanol was evident. Multiple substrates have the potential to impact degradation processes and the preferential degradation of ethanol likely inhibits the growth of a microbial population capable of degrading DIPE and toluene. It is likely that DIPE degradation would occur last for the three substrates.

Based on the above results, would the use of DIPE as a fuel oxygenate represent an increased long term pollution risk?

Again, due to the short length of the experiment, as well as the experimental difficulties encountered, any conclusions regarding the potential long term risks related to DIPE would be difficult to support. As previously discussed in Chapter 2, MTBE does not degrade rapidly under aerobic conditions and MTBE and DIPE potentially share similar degradation characteristics. Therefore, we can speculate that DIPE, like MTBE, will not rapidly degrade under aerobic conditions.

5.3 Future Research

Initially, research efforts should focus on long term aerobic studies to determine if DIPE or other fuel oxygenate degradation can occur. If degradation does occur over extended periods, additional potential research topics could be addressed.

First, batch studies using soil from the columns could be accomplished to evaluate potential degradation of the contaminants. Data collected from the batch studies could then be used to determine substrate utilization rates. The batch studies could also be used to evaluate the types of microorganisms responsible for degradation. Knowing the microbial population responsible for degradation and substrate utilization rates could lead to potential soil bioaugmentation as a cleanup method. Second, various combinations of fuel oxygenates, BTEX compounds, and various degradation intermediates are likely to be encountered at a contaminated site. Understanding how multiple contaminants impact attenuation rates is critical. Finally, if aerobic degradation does occur, studying the potential degradation effects under anaerobic conditions would provide valuable information.

Within the scope of the column experiment, four areas could be improved. First, is substrate application. The current setup does not provide consistent influent concentrations. Variations in the concentrations make it difficult to establish when, if any, degradation occurs. A modified system to provide consistent concentrations is recommended. Second, the respirometer will only provide carbon dioxide respiration to one percent. Beyond this value it is not possible to determine how much biological activity is occurring within the soil columns. To provide useful data that can be

correlated with analytical results, the carbon dioxide sensor range will need to be extended. Third, any points of potential leaks for the respirometer need to be adequately repaired including the internal sampling loops. Finally, a method to allow for water supply and adequate drainage will allow the system to be operated at various flow rates with minimal maintenance. The current system is manually filled and drained each day. If the application rates are increased, the existing setup would become cumbersome and difficult for a single individual to maintain. This could limit potential experiment variations.

Appendix A

Table A.1 Micro-Oxymax Respirometer Experiment Settings

Parameter	Value
Start Channel	1
Stop Channel	20
Sample Interval	5 hours
Sample Duration	0
Refresh Interval	1
Refresh Threshold	0.5
Refresh Window	30
Auto Volume Measurement	No
Purge Sensor Enabled	No
Switch Drier Enabled	N.A.
Gas Data Units	μL
Time Units	Min
Normalization Units	N.A.
Aux Temp Start at Ch	0
Enable Open Flow	No

Table A.2 Typical Micro-Oxymax Respirometer Values

Channel Label	Channel	Volume (mL)	Restriction (mmHg)	Leakage (ml/min)
1 - Top	1	76	38.7	-0.141
2 - Top	2	66	32.5	-0.174
3 - Top	3	68	38.8	-0.190
4 - Top	4	65	31.5	-0.138
Short Circuit	5	10	19.7	-0.871
1 - Bottom	6	47	35.1	-0.118
2 - Bottom	7	41	32.9	-0.162
3 - Bottom	8	49	38.7	-0.143
4 - Bottom	9	35	28.5	-0.139
Exterior Silicon Loop	10	47	23.7	-0.352
5 - Top	11	70	38.2	-0.202
6 - Top	12	72	38.5	-0.198
7 - Top	13	78	41.6	-0.242
8 - Top	14	71	40.8	-0.110
Closed 250 mL Jar	15	320	22.9	-0.241
5 - Bottom	16	43	33.6	-0.243
6 - Bottom	17	36	28.7	-0.238
7 - Bottom	18	46	36.7	-0.232
8 - Bottom	19	45	39.0	-0.169
Short Circuit	20	1	20.1	-0.118

Note: Values for January 30, 2005

Table A.3 Agilent 6890 Gas Chromatograph with Flame Ionization Detector Instrument Control Parameters

6890 Gas Chromatograph

Serial Number	US 10339021

Oven

Initial temperature	50 'C (On)
Maximum temperature	260 'C
Initial time	1.00 min
Equilibration time	1.00 min
Post temperature	0 'C
Post time	0.00 min
Run time	10.00 min

Ramp	Rate (ºC/min)	Final Temperature (ºC)	Final Time (min)
1	10.00	110	1.0
2	20.00	130	1.0

Front Inlet (Split/Splitless)

Mode	Split
Initial temperature	75 'C (On)
Pressure	13.00 psi (On)
Split ratio	15:1
Split flow	42.8 mL/min
Total flow	48.3 mL/min
Gas saver	Off
Gas type	Helium

Capillary Column

Model Number DB-624, Agilent part number 123-1334

Inside Diameter	0.32 mm
Length	30 m
Film Thickness	1.8 um

Dura-Guard deactivated silica column guard

Inside Diameter	0.32 mm
Length	5 m

Maximum temperature	260 'C
Nominal length	30.0 m
Nominal diameter	320.00 um

Table A.3 Agilent 6890 Gas Chromatograph with Flame Ionization Detector Instrument Control Parameters (Continued)

Nominal film thickness	1.80 um
Mode	Constant Pressure
Pressure	13.00 psi
Nominal initial flow	2.9 mL/min
Average velocity	44 cm/sec
Inlet	Front Inlet
Outlet	Front Detector
Outlet pressure	Ambient

Flame Ionization Detector

Temperature	250 'C (On)
Hydrogen flow	40.0 mL/min (On)
Air flow	400.0 mL/min (On)
Mode	Constant makeup flow Makeup flow 25.0 mL/min (On)
Makeup Gas Type	Nitrogen
Flame	On
Electrometer	On
Lit offset	2.0

SIGNAL 1

Data rate	20 Hz
Type	Front Detector
Save Data	On
Zero	0.0 (Off)
Range	0
Fast Peaks	Off
Attenuation	0

7673 Auto Injector Parameters

Serial Number	US 33821606
Injector Location	Front
Sample Washes	3
Sample Pumps	6
Injection Volume	1.0 microliters
Syringe Size	10.0 microliters
Post Injection Solvent A Washes (Acetone)	3
Post Injection Solvent B Washes (Deionized Water)	9
Viscosity Delay	6 seconds

Plunger Speed	Slow
Pre Injection Dwell	0.00 minutes
Post Injection Dwell	0.00 minutes

Appendix B

Table B.1 Estimated Porosity

Column	1	2	3	4	5	6	7	8
Water Added to Dry Column, L	18.2	14.9	19.1	16.1	17.1	18.2	15.9	17.4
Total Column Volume, L	64.3	64.3	64.3	64.3	64.3	64.3	64.3	64.3
Total Porosity, %	28.3	23.2	29.7	25.1	26.6	28.3	24.7	27.0

Table B.2 Hydraulic Conductivity and Volumetric Flow Rates at Saturation

Run 1														
Column	Column Length L (cm)	Distance from top of column to soil (cm)	ΔL (cm)	Distance from top of Column to water (cm)	Height at effluent flow (cm)	Head ΔH (cm)	Permeameter Volume Change (ml)	Column Area (cm2)	Elapsed Time (s)	Hydraulic Conductivity K (cm/s)	Volumetric Flow Rate Q (ml/sec)	Volumetric Flow Rate Q (ml/min)	10% Vol Flow Rate (ml/min)	2% Vol Flow Rate (ml/min)
1a	254	26.7	227	3.8	36.8	213.4	1000	324.3	375	7.34E-03	2.67	160	16.0	3.20
1b	254	26.7	227	3.8	36.8	213.4	1010	324.3	394	7.06E-03	2.56	154	15.4	3.08
2a	254	31.8	222	3.8	36.8	213.4	970	324.3	412	6.31E-03	2.35	141	14.1	2.83
2b	254	31.8	222	3.8	36.8	213.4	1000	324.3	422	6.35E-03	2.37	142	14.2	2.84
3a	254	30.5	224	3.8	36.8	213.4	1000	324.3	296	9.12E-03	3.38	203	20.3	4.05
3b	254	30.5	224	3.8	36.8	213.4	1010	324.3	292	9.33E-03	3.46	208	20.8	4.15
4a	254	30.5	224	3.8	36.8	213.4	830	324.3	389	5.76E-03	2.13	128	12.8	2.56
4b	254	30.5	224	3.8	36.8	213.4	1000	324.3	440	6.13E-03	2.27	136	13.6	2.73
5a	254	27.9	226	3.8	36.8	213.4	1010	324.3	655	4.22E-03	1.54	92.5	9.25	1.85
5b	254	27.9	226	3.8	36.8	213.4	980	324.3	677	3.96E-03	1.45	86.9	8.69	1.74
6a	254	34.3	220	3.8	36.8	213.4	1010	324.3	589	4.53E-03	1.71	103	10.3	2.06
6b	254	34.3	220	3.8	36.8	213.4	830	324.3	517	4.24E-03	1.61	96.3	9.63	1.93
7a	254	34.3	220	3.8	36.8	213.4	990	324.3	551	4.75E-03	1.80	108	10.8	2.16
7b	254	34.3	220	3.8	36.8	213.4	960	324.3	551	4.60E-03	1.74	105	10.5	2.09
8a	254	34.3	220	3.8	36.8	213.4	990	324.3	355	7.37E-03	2.79	167	16.7	3.35
8b	254	34.3	220	3.8	36.8	213.4	990	324.3	345	7.58E-03	2.87	172	17.2	3.44

Table B.2 Hydraulic Conductivity and Saturated Flow Data (Continued)

Run 2														
Column	Column Length L (cm)	Distance from top of column to soil (cm)	ΔL (cm)	Distance from top of Column to water (cm)	Height at effluent flow (cm)	Head ΔH (cm)	Permeameter Volume Change (ml)	Column Area (cm2)	Elapsed Time (s)	Hydraulic Conductivity K (cm/s)	Volumetric Flow Rate Q (ml/sec)	Volumetric Flow Rate Q (ml/min)	10% Vol Flow Rate (ml/min)	2% Vol Flow Rate (ml/min)
1a	254	26.7	227	3.8	36.8	213.4	1000	324.3	385	7.15E-03	2.60	156	15.6	3.12
1b	254	26.7	227	3.8	36.8	213.4	990	324.3	345	7.90E-03	2.87	172	17.2	3.44
2a	254	31.8	222	3.8	36.8	213.4	990	324.3	425	6.24E-03	2.33	140	14.0	2.80
2b	254	31.8	222	3.8	36.8	213.4	970	324.3	410	6.34E-03	2.37	142	14.2	2.84
3a	254	30.5	224	3.8	36.8	213.4	1010	324.3	276	9.87E-03	3.66	220	22.0	4.39
3b	254	30.5	224	3.8	36.8	213.4	1010	324.3	279	9.77E-03	3.62	217	21.7	4.34
4a	254	30.5	224	3.8	36.8	213.4	1000	324.3	426	6.33E-03	2.35	141	14.1	2.82
4b	254	30.5	224	3.8	36.8	213.4	1010	324.3	483	5.64E-03	2.09	125	12.5	2.51
5a	254	27.9	226	3.8	36.8	213.4	980	324.3	602	4.45E-03	1.63	98	9.8	1.95
5b	254	27.9	226	3.8	36.8	213.4	970	324.3	541	4.90E-03	1.79	108	10.8	2.15
6a	254	34.3	220	3.8	36.8	213.4	1000	324.3	518	5.10E-03	1.93	116	11.6	2.32
6b	254	34.3	220	3.8	36.8	213.4	940	324.3	483	5.14E-03	1.95	117	11.7	2.34
7a	254	34.3	220	3.8	36.8	213.4	960	324.3	578	4.39E-03	1.66	99.7	9.97	1.99
7b	254	34.3	220	3.8	36.8	213.4	980	324.3	567	4.57E-03	1.73	104	10.4	2.07
8a	254	34.3	220	3.8	36.8	213.4	980	324.3	350	7.40E-03	2.80	168	16.8	3.36
8b	254	34.3	220	3.8	36.8	213.4	1000	324.3	346	7.64E-03	2.89	173	17.3	3.47

TableB.2 Hydraulic Conductivity and Saturated Flow Data (Continued)

Run 3														
Column	Column Length L (cm)	Distance from top of column to soil (cm)	ΔL (cm)	Distance from top of Column to water (cm)	Height at effluent flow (cm)	Head ΔH (cm)	Permeameter Volume Change (ml)	Column Area (cm2)	Elapsed Time (s)	Hydraulic Conductivity K (cm/s)	Volumetric Flow Rate Q (ml/sec)	Volumetric Flow Rate Q (ml/min)	10% Vol Flow Rate (ml/min)	2% Vol Flow Rate (ml/min)
1a	254	26.7	227	3.8	36.8	213.4	960	324.3	364	7.26E-03	2.64	158	15.8	3.16
1b	254	26.7	227	3.8	36.8	213.4	940	324.3	375	6.90E-03	2.51	150	15.0	3.01
2a	254	31.8	222	3.8	36.8	213.4	990	324.3	417	6.36E-03	2.37	142	14.2	2.85
2b	254	31.8	222	3.8	36.8	213.4	990	324.3	400	6.63E-03	2.48	149	14.9	2.97
3a	254	30.5	224	3.8	36.8	213.4	970	324.3	284	9.22E-03	3.42	205	20.5	4.10
3b	254	30.5	224	3.8	36.8	213.4	960	324.3	285	9.09E-03	3.37	202	20.2	4.04
4a	254	30.5	224	3.8	36.8	213.4	970	324.3	461	5.68E-03	2.10	126	12.6	2.52
4b	254	30.5	224	3.8	36.8	213.4	1000	324.3	458	5.89E-03	2.18	131	13.1	2.62
5a	254	27.9	226	3.8	36.8	213.4	970	324.3	651	4.07E-03	1.49	89.4	8.94	1.79
5b	254	27.9	226	3.8	36.8	213.4	980	324.3	556	4.82E-03	1.76	106	10.6	2.12
6a	254	34.3	220	3.8	36.8	213.4	990	324.3	635	4.12E-03	1.56	93.5	9.35	1.87
6b	254	34.3	220	3.8	36.8	213.4	990	324.3	641	4.08E-03	1.54	92.7	9.27	1.85
7a	254	34.3	220	3.8	36.8	213.4	980	324.3	591	4.38E-03	1.66	99.5	9.95	1.99
7b	254	34.3	220	3.8	36.8	213.4	950	324.3	578	4.34E-03	1.64	98.6	9.86	1.97
8a	254	34.3	220	3.8	36.8	213.4	1000	324.3	354	7.47E-03	2.82	169	16.9	3.39
8b	254	34.3	220	3.8	36.8	213.4	1010	324.3	356	7.50E-03	2.84	170	17.0	3.40

Table B.3 Spreadsheet Cell Formulas for Table B.2

B	C	D	E	F	G	H	I	J	K	L	M	N	O	P
Column	**Column Length L (cm)**	**Distance from top of column to soil (cm)**	**ΔL (cm)**	**Distance from top of column to water (cm)**	**Height at effluent flow (cm)**	**Head ΔH (cm)**	**Permeameter Volume Change (ml)**	**Column Area (cm2)**	**Elapsed Time (s)**	**Hydraulic Conductivity K (cm/s)**	**Volumetric Flow Rate Q (ml/sec)**	**Volumetric Flow Rate Q (ml/min)**	**10% Vol Flow Rate (ml/min)**	**2% Vol Flow Rate (ml/min)**
1a	254	26.67	=+C3-D3	3.8	36.8	=+C3-F3-G3	1000	=+((4*2.54)^2)*PI( )	375	=+(M3*(E3-G3))/(((C3-F3-G3)*J3	=+I3/K3	=+M3*60	=+N3*0.1	=+N3*0.02
1b	254	26.67	=+C4-D4	3.8	36.8	=+C4-F4-G4	1010	=+((4*2.54)^2)*PI( )	394	=+(M4*(E4-G4))/(((C4-F4-G4)*J4	=+I4/K4	=+M4*60	=+N4*0.1	=+N4*0.02
2a	254	31.75	=+C5-D5	3.8	36.8	=+C5-F5-G5	970	=+((4*2.54)^2)*PI( )	412	=+(M5*(E5-G5))/(((C5-F5-G5)*J5	=+I5/K5	=+M5*60	=+N5*0.1	=+N5*0.02
2b	254	31.75	=+C6-D6	3.8	36.8	=+C6-F6-G6	1000	=+((4*2.54)^2)*PI( )	422	=+(M6*(E6-G6))/(((C6-F6-G6)*J6	=+I6/K6	=+M6*60	=+N6*0.1	=+N6*0.02
3a	254	30.48	=+C7-D7	3.8	36.8	=+C7-F7-G7	1000	=+((4*2.54)^2)*PI( )	296	=+(M7*(E7-G7))/(((C7-F7-G7)*J7	=+I7/K7	=+M7*60	=+N7*0.1	=+N7*0.02
3b	254	30.48	=+C8-D8	3.8	36.8	=+C8-F8-G8	1010	=+((4*2.54)^2)*PI( )	292	=+(M8*(E8-G8))/(((C8-F8-G8)*J8	=+I8/K8	=+M8*60	=+N8*0.1	=+N8*0.02
Note:Datum is the height of the effluent drain														

Table B.4 Maximum, Minimum and Averages for 2%, 10% and Saturated Column Flow

2 % OF VOLUMETRIC FLOW AT SATURATION (ml/min)			
COLUMN	**MAX**	**MIN**	**MEAN**
1	3.44	3.01	3.17
2	2.97	2.80	2.85
3	4.39	4.04	4.18
4	2.82	2.51	2.63
5	2.15	1.74	1.93
6	2.34	1.85	2.06
7	2.16	1.97	2.05
8	3.47	3.35	3.40
1-4	**4.39**	**2.51**	**3.21**
5-8	**3.47**	**1.74**	**2.36**

10 % OF VOLUMETRIC FLOW AT SATURATION (ml/min)			
COLUMN	**MAX**	**MIN**	**MEAN**
1	17.2	15.0	15.8
2	14.9	14.0	14.3
3	22.0	20.2	20.9
4	14.1	12.5	13.1
5	10.8	8.7	9.7
6	11.7	9.3	10.3
7	10.8	9.9	10.2
8	17.3	16.7	17.0
1-4	**22.0**	**12.5**	**16.0**
5-8	**17.3**	**8.7**	**11.8**

VOLUMETRIC FLOW, SATURATION (ml/min)			
COLUMN	**MAX**	**MIN**	**MEAN**
1	172	150	158
2	149	140	143
3	220	202	209
4	141	125	131
5	108	87	97
6	117	93	103
7	108	99	102
8	173	167	170
1-4	**220**	**125**	**160**
5-8	**173**	**87**	**118**

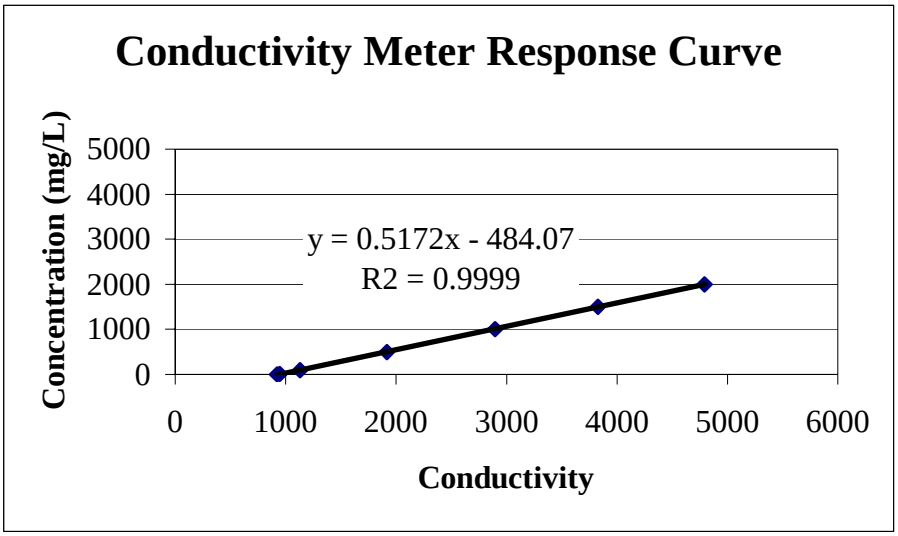

Figure B.1 Conductivity Meter Response Curve

Table B.5 Average Water Flows

	Column							
	1	**2**	**3**	**4**	**5**	**6**	**7**	**8**
Run 1	6.52	6.12	6.47	6.36	24.3	25.0	24.4	24.8
Run 2	6.27	6.61	6.64	6.54	24.3	25.2	24.2	24.8
Run 3	6.74	6.58	6.66	6.61	24.1	24.8	24.4	24.8
Mean	6.51	6.44	6.59	6.50	24.2	25.0	24.3	24.8
Flow (ml/min)	3.26	3.22	3.30	3.25	12.1	12.5	12.2	12.4

Pre Tracer Test - 27 Nov 04

	Column							
	1	**2**	**3**	**4**	**5**	**6**	**7**	**8**
Run 1	6.59	6.45	6.70	6.38	22.8	23.6	23.6	23.3
Run 2	6.45	6.49	6.74	6.48	22.8	23.7	23.7	23.7
Run 3	6.47	6.57	6.71	6.65	23.1	23.6	23.6	23.4
Mean	6.50	6.50	6.72	6.50	22.9	23.6	23.6	23.4
Flow (ml/min)	3.25	3.25	3.36	3.25	11.4	11.8	11.8	11.7

Post Tracer Test - 4 Dec 04

Note:Each run collected a sample from two pump cycles. The final flow is the mean of three runs divided by two

Table B.6 Average Chemical Flows

	Column							
	1	**2**	**3**	**4**	**5**	**6**	**7**	**8**
Run 1	0.0701	0.0720	0.0630	0.0674	0.0769	0.0745	0.0745	0.0733
Run 2	0.0739	0.0718	0.0647	0.0668	0.0794	0.0720	0.0778	0.0805
Run 3	0.0735	0.0695	0.0645	0.0653	0.0772	0.0745	0.0690	0.0756
Mean	0.0725	0.0711	0.0641	0.0665	0.0778	0.0737	0.0738	0.0765
ml/min	0.0363	0.0356	0.0320	0.0333	0.0389	0.0368	0.0369	0.0382

9 Dec 04

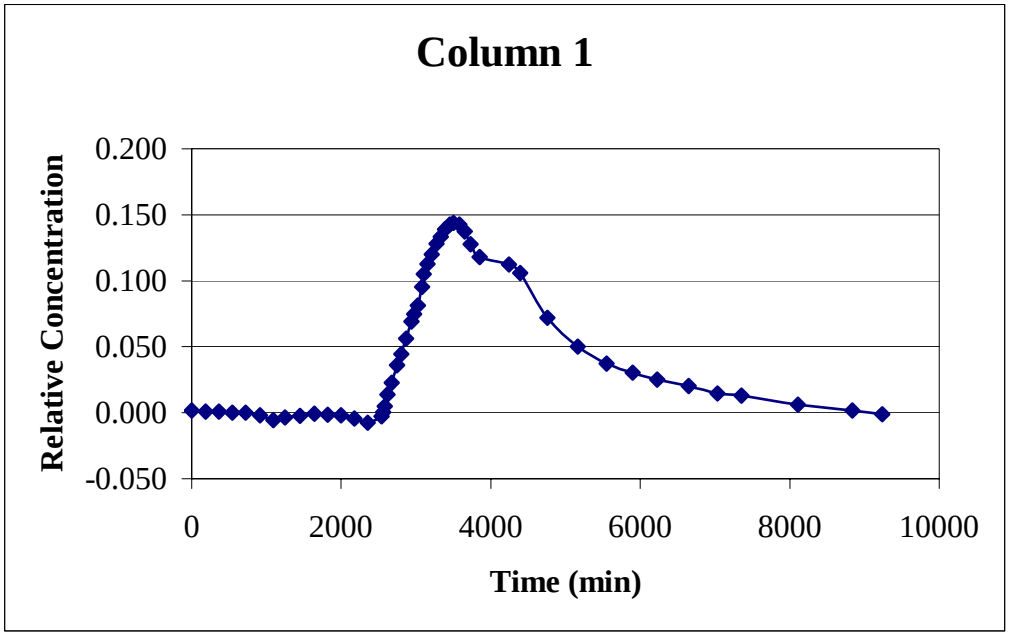

Figure B.2 Column 1 Tracer Results (27 Nov 04)

Table B.7 Column 1 Tracer Results (27 Nov 04)

Specific Conductivity (uS/cm)	Initial Concentration (mg/L)	Mass (g)	Mass Balance Error
6650	2955.3	2.9	3.5

Time (min)	Specific Conductivity (uS/cm)	Concentration (mg/L)	Relative Concentration	Area	f(t)	t_i
0	946	5.2	0.0	734.7	0.0000	0.1
188	941	2.6	0.0009	457.7	0.0000	0.1
363	941	2.6	0.0009	284.5	0.0000	0.1
543	937	0.5	0.0002	51.8	0.0000	0.0
723	936	0.0	0.0000	-534.9	0.0000	-0.5
913	925	-5.7	-0.0019	-1986.1	0.0000	-2.2
1088	903	-17.0	-0.0058	-2215.6	0.0000	-2.9
1250	916	-10.3	-0.0035	-1735.1	0.0000	-2.6
1448	922	-7.2	-0.0024	-928.0	0.0000	-1.6
1638	931	-2.6	-0.0009	-599.9	0.0000	-1.1
1818	928	-4.1	-0.0014	-879.2	0.0000	-1.8
1998	925	-5.7	-0.0019	-1614.9	0.0000	-3.7
2177	912	-12.4	-0.0042	-3160.0	0.0000	-7.9
2357	892	-22.7	-0.0077	-2818.6	0.0000	-7.6
2539	920	-8.2	-0.0028	-79.0	0.0000	-0.2
2561	938	1.1	0.0004	169.0	0.0000	0.5
2582	965	15.0	0.0051	987.6	0.0000	2.8
2617	1016	41.4	0.0140	3244.6	0.0000	9.5
2677	1065	66.7	0.0226	5719.6	0.0001	17.1
2743	1142	106.6	0.0361	7154.6	0.0001	21.8
2803	1191	131.9	0.0446	9683.9	0.0001	30.2
2868	1257	166.1	0.0562	13499.8	0.0002	43.2
2941	1330	203.8	0.0690	6370.2	0.0002	20.7
2971	1363	220.9	0.0747	12227.1	0.0002	40.4
3024	1401	240.5	0.0814	15688.4	0.0003	52.8
3084	1482	282.4	0.0956	5042.9	0.0003	17.2

Table B.7 Column 1 Tracer Results (27 Nov 04) (Continued)

Time (min)	Specific Conductivity (uS/cm)	Concentration (mg/L)	Relative Concentration	Area	f(t)	t_i
3101	1537	310.9	0.1052	16112.2	0.0003	55.5
3151	1581	333.6	0.1129	20638.0	0.0004	72.3
3211	1621	354.3	0.1199	21987.9	0.0004	78.5
3271	1668	378.6	0.1281	23198.2	0.0004	84.3
3331	1699	394.7	0.1335	24175.7	0.0004	89.5
3391	1731	411.2	0.1391	24982.5	0.0005	94.1
3451	1751	421.5	0.1426	22847.3	0.0005	87.5
3505	1757	424.7	0.1437	30867.3	0.0005	120.4
3578	1750	421.0	0.1425	30187.7	0.0005	120.1
3651	1721	406.0	0.1374	30169.2	0.0004	122.6
3728	1666	377.6	0.1278	45420.3	0.0004	189.6
3853	1611	349.1	0.1181	132255.2	0.0004	589.3
4241	1579	332.6	0.1125	49988.0	0.0004	237.7
4396	1540	312.4	0.1057	94596.0	0.0003	476.6
4756	1348	213.1	0.0721	73220.2	0.0002	399.7
5161	1223	148.5	0.0502	49921.1	0.0002	294.3
5547	1149	110.2	0.0373	35146.8	0.0001	221.5
5899	1109	89.5	0.0303	26649.5	0.0001	177.9
6225	1079	74.0	0.0250	28034.2	0.0001	198.6
6645	1051	59.5	0.0201	20081.3	0.0001	151.2
7035	1020	43.5	0.0147	12920.6	0.0000	102.3
7351	1010	38.3	0.0130	21501.0	0.0000	183.0
8113	971	18.1	0.0061	8247.7	0.0000	77.0
8836	945	4.7	0.0016	321.2	0.0000	3.2
9235	930	-3.1	-0.0010		0.0000	

Area (mg*min/L)	Retention Time t_{RTD}(min)	Pulse Duration (min)	Flow Rate (ml/min)	Calculated Mass (g)	Pore Volume (L)
908234	4302.4	297	3.3	3.0	14.0

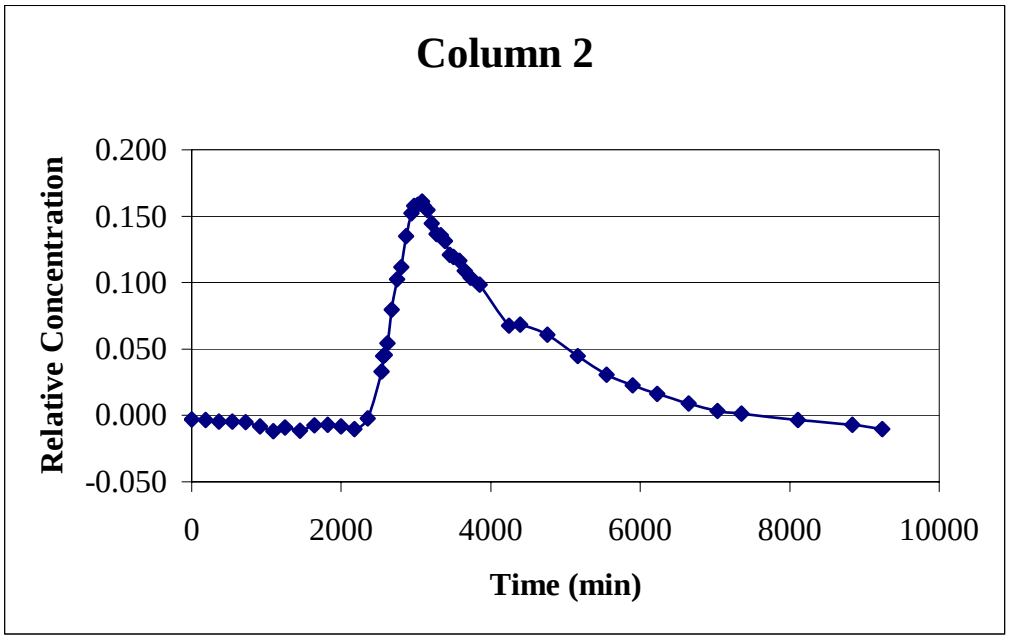

Figure B.3 Column 2 Tracer Results (27 Nov 04)

Table B.8 Column 2 Tracer Results (27 Nov 04)

Specific Conductivity (uS/cm)	Initial Concentration (mg/L)	Mass (g)	Mass Balance Error
6730	2996.7	2.8	-11.1

Time (min)	Specific Conductivity (uS/cm)	Concentration (mg/L)	Relative Concentration	Area	f(t)	t_i
0	919	-8.8	-0.0029	-1793.3	0.0000	-0.2
188	916	-10.3	-0.0034	-2121.9	0.0000	-0.7
363	909	-13.9	-0.0047	-2554.9	0.0000	-1.5
543	908	-14.5	-0.0048	-2648.0	0.0000	-2.1
723	907	-15.0	-0.0050	-3777.8	0.0000	-4.0
913	888	-24.8	-0.0083	-5289.7	0.0000	-6.8
1088	867	-35.7	-0.0119	-5106.2	0.0000	-7.6
1250	883	-27.4	-0.0091	-6087.4	0.0000	-10.5
1448	870	-34.1	-0.0114	-5350.1	0.0000	-10.6
1638	893	-22.2	-0.0074	-3951.3	0.0000	-8.7
1818	894	-21.7	-0.0072	-4137.5	0.0000	-10.1
1998	889	-24.3	-0.0081	-4901.4	0.0000	-13.1
2177	877	-30.5	-0.0102	-3299.7	0.0000	-9.6
2357	924	-6.2	-0.0021	8430.0	0.0000	26.4
2539	1127	98.8	0.0330	2560.8	0.0001	8.4
2561	1195	134.0	0.0447	2840.8	0.0002	9.4
2582	1200	136.6	0.0456	5241.6	0.0002	17.4
2617	1251	162.9	0.0544	12042.2	0.0002	40.8
2677	1397	238.5	0.0796	17991.2	0.0003	62.4
2743	1529	306.7	0.1024	19241.6	0.0004	68.3
2803	1583	334.7	0.1117	24005.2	0.0004	87.2
2868	1717	404.0	0.1348	31414.8	0.0005	116.9
2941	1819	456.7	0.1524	13949.8	0.0006	52.8
2971	1851	473.3	0.1579	25138.0	0.0006	96.5
3024	1855	475.3	0.1586	28737.4	0.0006	112.4
3084	1869	482.6	0.1610	8124.7	0.0006	32.2

TableB.8 Column 2 Tracer Results (27 Nov 04) (Continued)

Time (min)	Specific Conductivity (uS/cm)	Concentration (mg/L)	Relative Concentration	Area	f(t)	t_i
3101	1851	473.3	0.1579	23404.8	0.0006	93.7
3151	1831	462.9	0.1545	26891.0	0.0006	109.5
3211	1774	433.4	0.1446	25292.8	0.0006	105.0
3271	1728	409.7	0.1367	24486.0	0.0005	103.5
3331	1722	406.5	0.1357	24020.5	0.0005	103.4
3391	1698	394.1	0.1315	22686.1	0.0005	99.4
3451	1636	362.1	0.1208	19440.0	0.0005	86.6
3505	1628	357.9	0.1194	25789.2	0.0005	117.0
3578	1610	348.6	0.1163	24618.8	0.0004	114.0
3651	1566	325.9	0.1087	24514.2	0.0004	115.8
3728	1537	310.9	0.1037	37888.6	0.0004	183.9
3853	1507	295.4	0.0986	96635.7	0.0004	500.9
4241	1328	202.8	0.0677	31549.8	0.0003	174.5
4396	1331	204.3	0.0682	69553.2	0.0003	407.6
4756	1288	182.1	0.0608	63899.0	0.0002	405.8
5161	1194	133.5	0.0445	43432.8	0.0002	297.8
5547	1113	91.6	0.0306	28046.7	0.0001	205.6
5899	1067	67.8	0.0226	18977.8	0.0001	147.3
6225	1030	48.6	0.0162	15761.0	0.0001	129.9
6645	987	26.4	0.0088	7172.0	0.0000	62.8
7035	956	10.4	0.0035	2215.6	0.0000	20.4
7351	943	3.6	0.0012	-2342.4	0.0000	-23.2
8113	917	-9.8	-0.0033	-11383.9	0.0000	-123.6
8836	894	-21.7	-0.0072	-10409.7	0.0000	-120.5
9235	877	-30.5	-0.0102		0.0000	

Area (mg*min/L)	Retention Time t_{RTD}(min)	Pulse Duration (min)	Flow Rate (ml/min)	Calculated Mass (g)	Pore Volume (L)
780838	3816.2	293	3.2	2.5	12.3

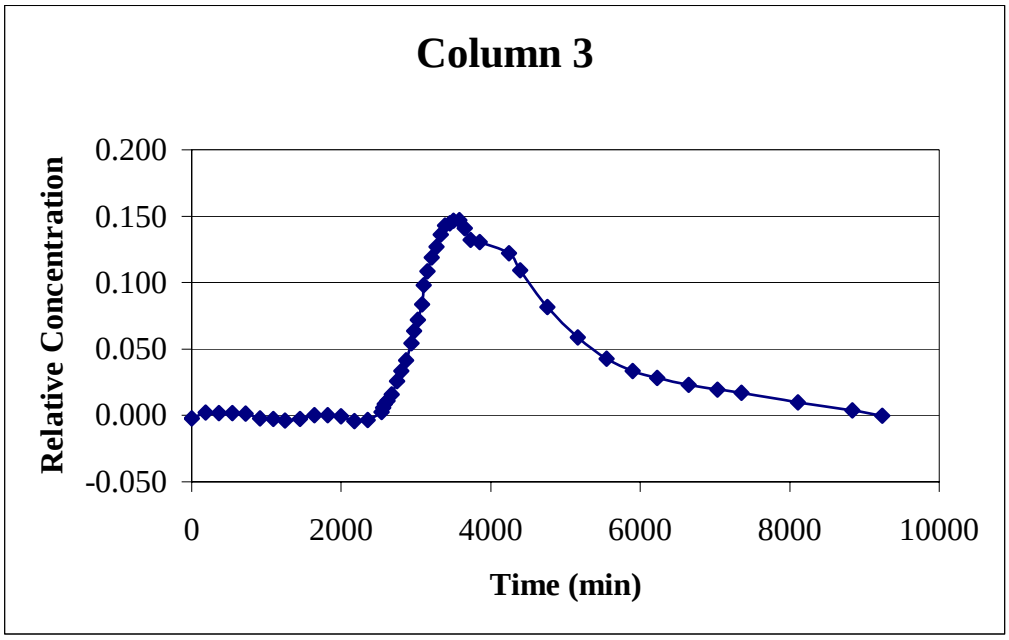

Figure B.4 Column 3 Tracer Results (27 Nov 04)

Table B.9 Column 3 Tracer Results (27 Nov 04)

Specific Conductivity (uS/cm)	Initial Concentration (mg/L)	Mass (g)	Mass Balance Error
6670	2965.7	2.8	15.5

Time (min)	Specific Conductivity (uS/cm)	Concentration (mg/L)	Relative Concentration	Area	f(t)	t_i
0	924	-6.2	-0.0021	5.5	0.0000	0.0
188	948	6.2	0.0021	1046.0	0.0000	0.3
363	947	5.7	0.0019	936.2	0.0000	0.4
543	945	4.7	0.0016	796.6	0.0000	0.5
723	944	4.2	0.0014	-191.0	0.0000	-0.2
913	924	-6.2	-0.0021	-1216.8	0.0000	-1.2
1088	921	-7.7	-0.0026	-1503.4	0.0000	-1.8
1250	915	-10.8	-0.0037	-1837.5	0.0000	-2.5
1448	921	-7.7	-0.0026	-731.5	0.0000	-1.1
1638	936	0.0	0.0000	5.3	0.0000	0.0
1818	936	0.0	0.0000	-134.4	0.0000	-0.3
1998	933	-1.5	-0.0005	-1244.6	0.0000	-2.6
2177	912	-12.4	-0.0042	-1996.3	0.0000	-4.6
2357	917	-9.8	-0.0033	-182.9	0.0000	-0.5
2539	951	7.8	0.0026	279.4	0.0000	0.7
2561	970	17.6	0.0059	456.8	0.0000	1.2
2582	986	25.9	0.0087	1023.8	0.0000	2.7
2617	999	32.6	0.0110	2375.7	0.0000	6.4
2677	1026	46.6	0.0157	4046.9	0.0000	11.1
2743	1083	76.1	0.0256	5261.7	0.0001	14.7
2803	1128	99.3	0.0335	7229.8	0.0001	20.7
2868	1174	123.1	0.0415	10366.0	0.0001	30.4
2941	1247	160.9	0.0542	5237.5	0.0002	15.6
2971	1300	188.3	0.0635	10651.0	0.0002	32.2
3024	1349	213.6	0.0720	13857.5	0.0002	42.7
3084	1416	248.3	0.0837	4581.3	0.0003	14.3

Table B.9 Column 3 Tracer Results (27 Nov 04) (Continued)

Time (min)	Specific Conductivity (uS/cm)	Concentration (mg/L)	Relative Concentration	Area	f(t)	t_i
3101	1498	290.7	0.0980	15323.5	0.0003	48.4
3151	1559	322.2	0.1087	20265.6	0.0003	65.1
3211	1619	353.3	0.1191	21910.3	0.0004	71.7
3271	1665	377.1	0.1271	23446.4	0.0004	78.2
3331	1718	404.5	0.1364	24858.4	0.0004	84.4
3391	1756	424.1	0.1430	25603.2	0.0004	88.4
3451	1766	429.3	0.1448	23336.1	0.0004	82.0
3505	1777	435.0	0.1467	31773.5	0.0004	113.6
3578	1778	435.5	0.1469	31150.5	0.0004	113.7
3651	1744	417.9	0.1409	31204.7	0.0004	116.3
3728	1695	392.6	0.1324	48749.8	0.0004	186.6
3853	1685	387.4	0.1306	145399.4	0.0004	594.2
4241	1636	362.1	0.1221	53194.7	0.0004	232.0
4396	1563	324.3	0.1094	102043.7	0.0003	471.5
4756	1405	242.6	0.0818	84426.6	0.0002	422.7
5161	1273	174.3	0.0588	58106.3	0.0002	314.2
5547	1181	126.7	0.0427	39789.2	0.0001	229.9
5899	1128	99.3	0.0335	29853.0	0.0001	182.7
6225	1098	83.8	0.0283	32052.8	0.0001	208.3
6645	1069	68.8	0.0232	24619.8	0.0001	170.1
7035	1047	57.4	0.0194	17006.5	0.0001	123.5
7351	1033	50.2	0.0169	30368.4	0.0001	237.1
8113	993	29.5	0.0100	14604.6	0.0000	125.0
8836	957	10.9	0.0037	2075.3	0.0000	18.9
9235	935	-0.5	-0.0002		0.0000	

Area (mg*min/L)	Retention Time t_{RTD}(min)	Pulse Duration (min)	Flow Rate (ml/min)	Calculated Mass (g)	Pore Volume (L)
990281	4413.3	289	3.295	3.3	14.5

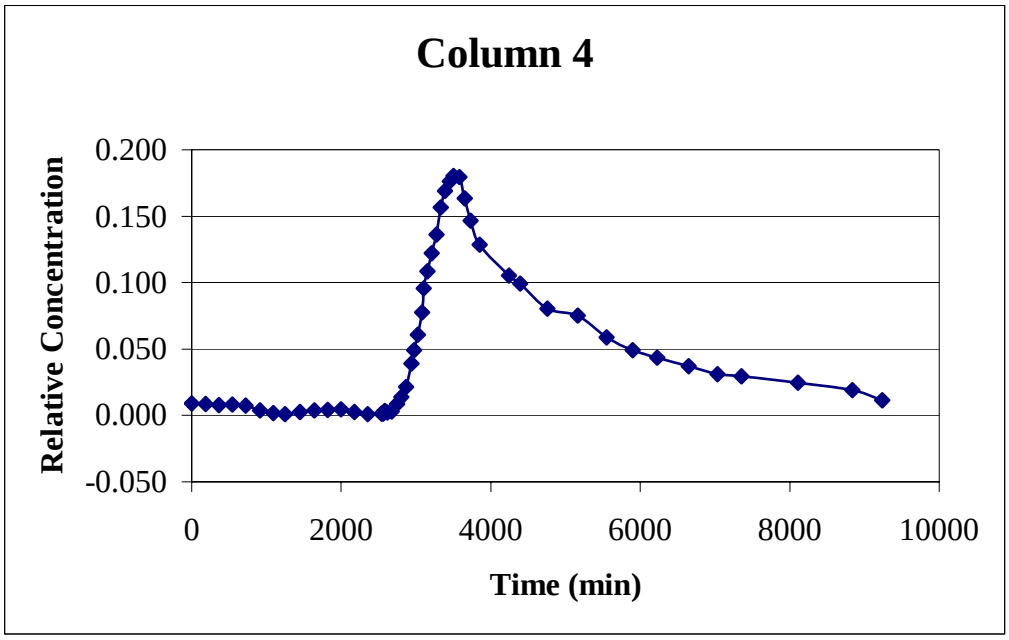

Figure B.5 Column 4 Tracer Results (27 Nov 04)

Table B.10 Column 4 Tracer Results (27 Nov 04)

Specific Conductivity (uS/cm)	Initial Concentration (mg/L)	Mass (g)	Mass Balance Error
6780	3022.5	2.9	36.0

Time (min)	Specific Conductivity (uS/cm)	Concentration (mg/L)	Relative Concentration	Area	f(t)	t_i
0	988	26.9	0.0089	5013.0	0.0000	0.4
188	987	26.4	0.0087	4394.8	0.0000	1.0
363	982	23.8	0.0079	4334.2	0.0000	1.6
543	983	24.3	0.0081	4194.6	0.0000	2.2
723	979	22.3	0.0074	3199.3	0.0000	2.1
913	958	11.4	0.0038	1498.5	0.0000	1.2
1088	947	5.7	0.0019	716.9	0.0000	0.7
1250	942	3.1	0.0010	1081.0	0.0000	1.2
1448	951	7.8	0.0026	1823.5	0.0000	2.3
1638	958	11.4	0.0038	2193.0	0.0000	3.1
1818	961	13.0	0.0043	2379.2	0.0000	3.7
1998	962	13.5	0.0045	1949.4	0.0000	3.3
2177	952	8.3	0.0027	982.8	0.0000	1.8
2357	941	2.6	0.0009	664.2	0.0000	1.3
2539	945	4.7	0.0015	97.4	0.0000	0.2
2561	944	4.2	0.0014	152.7	0.0000	0.3
2582	956	10.4	0.0034	299.7	0.0000	0.6
2617	949	6.8	0.0022	482.7	0.0000	1.0
2677	954	9.3	0.0031	1162.5	0.0000	2.6
2743	986	25.9	0.0086	2018.8	0.0000	4.6
2803	1016	41.4	0.0137	3447.7	0.0000	8.0
2868	1061	64.7	0.0214	6666.0	0.0001	15.8
2941	1164	118.0	0.0390	3996.2	0.0001	9.6
2971	1223	148.5	0.0491	8814.4	0.0001	21.5
3024	1292	184.2	0.0609	12569.7	0.0001	31.2
3084	1390	234.8	0.0777	4449.5	0.0002	11.2

Table B.10 Column 4 Tracer Results (27 Nov 04) (Continued)

Time (min)	Specific Conductivity (uS/cm)	Concentration (mg/L)	Relative Concentration	Area	f(t)	t_i
3101	1494	288.6	0.0955	15427.0	0.0002	39.2
3151	1571	328.5	0.1087	20932.8	0.0003	54.2
3211	1650	369.3	0.1222	23415.4	0.0003	61.7
3271	1731	411.2	0.1360	26549.6	0.0003	71.3
3331	1852	473.8	0.1568	29544.2	0.0004	80.8
3391	1924	511.0	0.1691	31328.6	0.0004	87.2
3451	1967	533.3	0.1764	29117.4	0.0004	82.4
3505	1990	545.2	0.1804	39721.0	0.0004	114.5
3578	1986	543.1	0.1797	37871.0	0.0004	111.4
3651	1892	494.5	0.1636	36123.0	0.0004	108.4
3728	1794	443.8	0.1468	52046.9	0.0004	160.5
3853	1688	389.0	0.1287	137171.7	0.0003	451.7
4241	1551	318.1	0.1052	47903.7	0.0003	168.3
4396	1516	300.0	0.0993	97761.3	0.0002	364.0
4756	1406	243.1	0.0804	95318.9	0.0002	384.6
5161	1376	227.6	0.0753	78170.0	0.0002	340.5
5547	1279	177.4	0.0587	57448.4	0.0001	267.5
5899	1224	149.0	0.0493	45702.1	0.0001	225.4
6225	1190	131.4	0.0435	51059.9	0.0001	267.3
6645	1152	111.7	0.0370	40151.3	0.0001	223.5
7035	1118	94.2	0.0312	28937.3	0.0001	169.4
7351	1108	89.0	0.0294	62488.1	0.0001	393.1
8113	1081	75.0	0.0248	47884.9	0.0001	330.2
8836	1047	57.4	0.0190	18377.9	0.0000	135.1
9235	1003	34.7	0.0115		0.0000	

Area (mg*min/L)	Retention Time t_{RTD}(min)	Pulse Duration (min)	Flow Rate (ml/min)	Calculated Mass (g)	Pore Volume (L)
1229034	4675.1	299	3.3	4.0	15.2

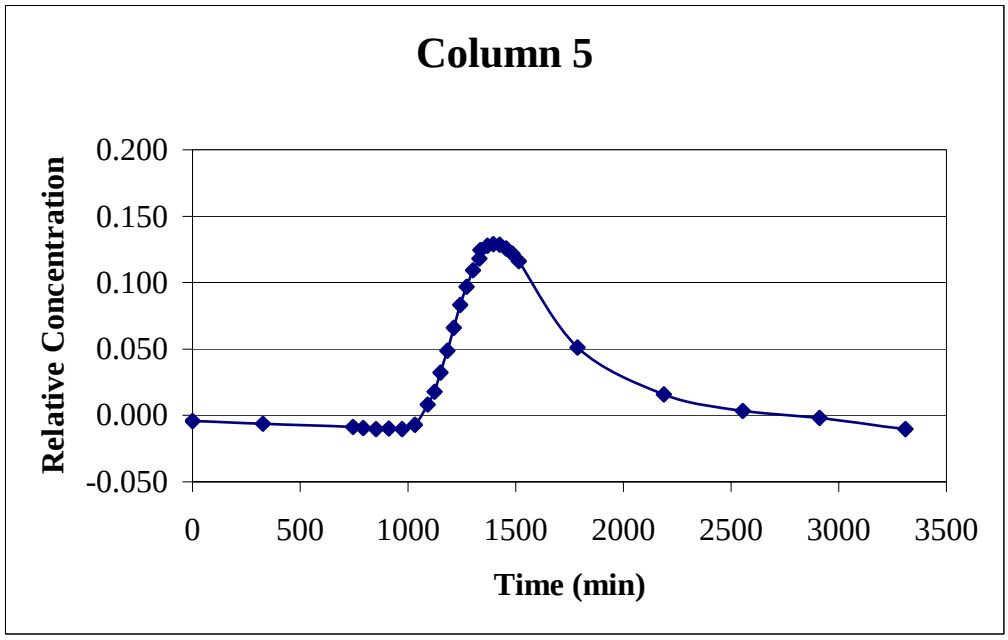

Figure B.6 Column 5 Tracer Results (1 Dec 04)

Table B.11 Column 5 Tracer Results (1 Dec 04)

Specific Conductivity (uS/cm)	Initial Concentration (mg/L)	Mass (g)	Mass Balance Error
6580	2919.1	3.0	-20.5

Time (min)	Specific Conductivity (uS/cm)	Concentration (mg/L)	Relative Concentration	Area	f(t)	t_i
0	911	-12.9	-0.0044	-5133.0	-0.0001	-4.2
326	900	-18.6	-0.0064	-9328.4	-0.0001	-25.1
746	886	-25.8	-0.0088	-1235.8	-0.0001	-4.8
792	882	-27.9	-0.0096	-1720.5	-0.0001	-7.1
852	879	-29.5	-0.0101	-1751.6	-0.0001	-7.7
912	880	-28.9	-0.0099	-1842.0	-0.0001	-8.7
974	877	-30.5	-0.0104	-1483.2	-0.0002	-7.5
1032	896	-20.7	-0.0071	94.8	-0.0001	0.5
1092	982	23.8	0.0082	1179.3	0.0001	6.5
1123	1037	52.3	0.0179	2130.7	0.0003	12.1
1152	1119	94.7	0.0324	3561.8	0.0005	20.8
1182	1212	142.8	0.0489	5035.8	0.0007	30.2
1212	1309	192.9	0.0661	6758.9	0.0010	41.6
1243	1406	243.1	0.0833	7627.7	0.0012	48.1
1272	1483	282.9	0.0969	9023.4	0.0014	58.2

Table B.11 Column 5 Tracer Results (1 Dec 04) (Continued)

Time (min)	Specific Conductivity (uS/cm)	Concentration (mg/L)	Relative Concentration	Area	f(t)	t_i
1302	1552	318.6	0.1092	9954.4	0.0016	65.7
1332	1603	345.0	0.1182	1416.2	0.0017	9.5
1336	1638	363.1	0.1244	11768.3	0.0018	79.8
1368	1656	372.4	0.1276	10485.5	0.0019	72.6
1396	1664	376.6	0.1290	11281.0	0.0019	79.8
1426	1662	375.5	0.1286	11133.6	0.0019	80.4
1456	1645	366.7	0.1256	10831.0	0.0018	79.9
1486	1623	355.3	0.1217	10419.9	0.0018	78.4
1516	1592	339.3	0.1162	65989.7	0.0017	546.1
1786	1225	149.5	0.0512	39307.6	0.0007	391.5
2188	1025	46.1	0.0158	10260.6	0.0002	122.0
2555	955	9.9	0.0034	838.9	0.0000	11.5
2911	926	-5.1	-0.0018	-7107.9	0.0000	-110.8
3310	877	-30.5	-0.0104		-0.0002	

Area (mg*min/L)	Retention Time t_{RTD}(min)	Pulse Duration (min)	Flow Rate (ml/min)	Calculated Mass (g)	Pore Volume (L)
199497	1616.4	86	12.1	2.4	19.6

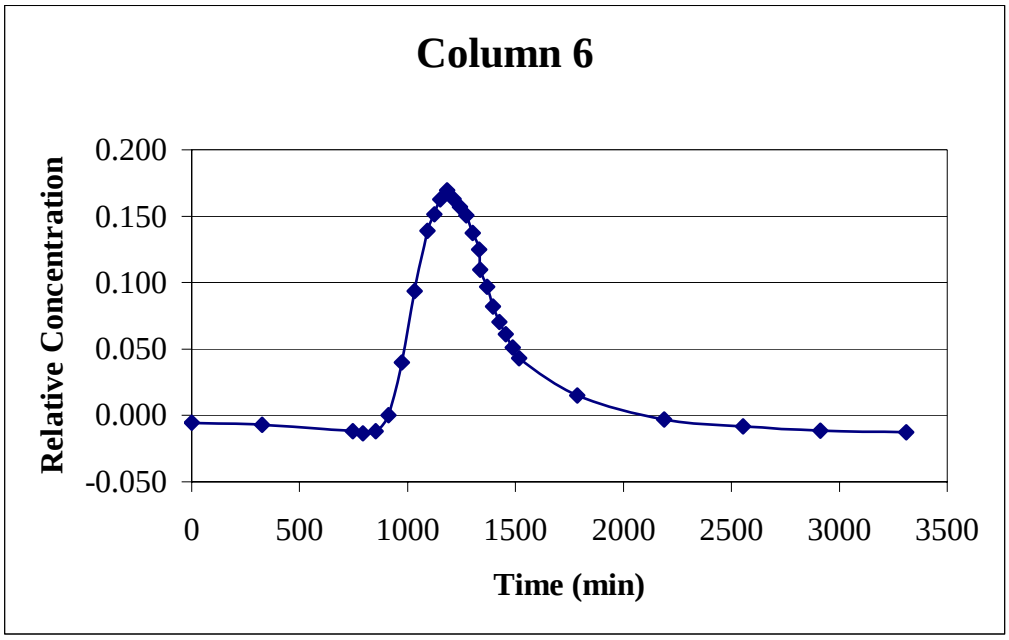

Figure B.7 Column 6 Tracer Results (1 Dec 04)

Table B.12 Column 6 Tracer Results (1 Dec 04)

Specific Conductivity (uS/cm)	Initial Concentration (mg/L)	Mass (g)	Mass Balance Error
6600	2929.5	3.0	-32.5

Time (min)	Specific Conductivity (uS/cm)	Concentration (mg/L)	Relative Concentration	Area	f(t)	t_i
0	906	-15.49	-0.0053	-5807.4	-0.0001	-5.9
326	897	-20.14	-0.0069	-11609.2	-0.0001	-38.9
746	868	-35.14	-0.0120	-1711.6	-0.0002	-8.2
792	860	-39.28	-0.0134	-2217.0	-0.0002	-11.4
852	869	-34.62	-0.0118	-1022.3	-0.0002	-5.6
912	937	0.55	0.0002	3625.3	0.0000	21.4
974	1161	116.40	0.0397	11325.8	0.0007	71.0
1032	1466	274.15	0.0936	20436.3	0.0017	135.6
1092	1723	407.07	0.1390	13180.2	0.0025	91.2
1123	1793	443.27	0.1513	13342.3	0.0028	94.8
1152	1858	476.89	0.1628	14609.2	0.0030	106.5
1182	1897	497.06	0.1697	14616.9	0.0031	109.3
1212	1859	477.40	0.1630	14535.0	0.0030	111.4
1243	1826	460.34	0.1571	13072.3	0.0029	102.7
1272	1789	441.20	0.1506	12654.2	0.0028	101.7

Table B.12 Column 6 Tracer Results (1 Dec 04) (Continued)

Time (min)	Specific Conductivity (uS/cm)	Concentration (mg/L)	Relative Concentration	Area	f(t)	t_i
1302	1714	402.41	0.1374	11521.5	0.0025	94.8
1332	1643	365.69	0.1248	1373.8	0.0023	11.4
1336	1557	321.21	0.1096	9682.9	0.0020	81.8
1368	1485	283.97	0.0969	7335.7	0.0018	63.3
1396	1400	240.01	0.0819	6696.0	0.0015	59.0
1426	1335	206.39	0.0705	5788.3	0.0013	52.1
1456	1283	179.50	0.0613	4942.7	0.0011	45.4
1486	1226	150.02	0.0512	4143.6	0.0009	38.8
1516	1180	126.23	0.0431	22979.3	0.0008	237.0
1786	1021	43.99	0.0150	7080.8	0.0003	87.9
2188	919	-8.76	-0.0030	-6158.2	-0.0001	-91.2
2555	888	-24.80	-0.0085	-10300.5	-0.0002	-175.8
2911	872	-33.07	-0.0113	-14021.0	-0.0002	-272.4
3310	864	-37.21	-0.0127		-0.0002	

Area (mg*min/L)	Retention Time t_{RTD}(min)	Pulse Duration (min)	Flow Rate (ml/min)	Calculated Mass (g)	Pore Volume (L)
160095	1067.1	81	12.5	2.0	13.3

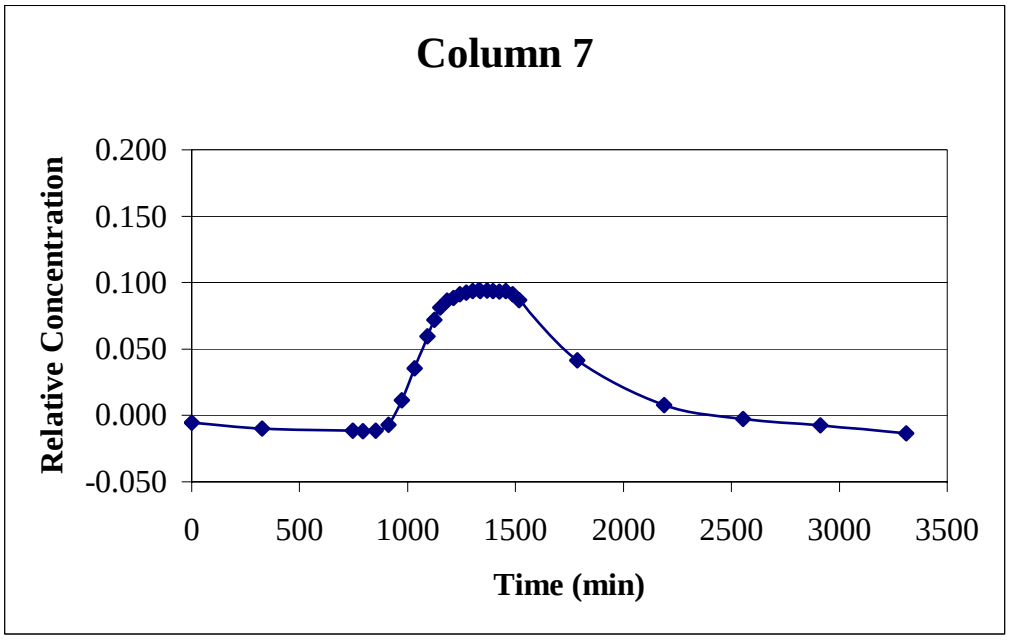

Figure B.8 Column 7 Tracer Results (1 Dec 04)

Table B.13 Column 7 Tracer Results (1 Dec 04)

Specific Conductivity (uS/cm)	Initial Concentration (mg/L)	Mass (g)	Mass Balance Error
6580	2919.1	3.0	-34.1

Time (min)	Specific Conductivity (uS/cm)	Concentration (mg/L)	Relative Concentration	Area	f(t)	t_i
0	905	-16.0	-0.0055	-7324.9	-0.0001	-7.4
326	880	-28.9	-0.0099	-13021.2	-0.0002	-43.2
746	872	-33.1	-0.0113	-1545.1	-0.0002	-7.3
792	870	-34.1	-0.0117	-2015.3	-0.0002	-10.2
852	872	-33.1	-0.0113	-1627.4	-0.0002	-8.9
912	895	-21.2	-0.0073	370.6	-0.0001	2.2
974	1000	33.1	0.0113	3961.4	0.0002	24.6
1032	1136	103.5	0.0354	8318.3	0.0006	54.6
1092	1272	173.8	0.0595	5957.2	0.0011	40.8
1123	1343	210.5	0.0721	6495.3	0.0013	45.7
1152	1395	237.4	0.0813	7339.9	0.0015	53.0
1182	1423	251.9	0.0863	7658.0	0.0016	56.7
1212	1436	258.6	0.0886	8137.8	0.0016	61.8
1243	1451	266.4	0.0913	7770.2	0.0016	60.4
1272	1457	269.5	0.0923	8139.0	0.0017	64.8

Table B.13 Column 7 Tracer Results (1 Dec 04) (Continued)

Time (min)	Specific Conductivity (uS/cm)	Concentration (mg/L)	Relative Concentration	Area	f(t)	t_i
1302	1464	273.1	0.0936	8239.9	0.0017	67.1
1332	1470	276.2	0.0946	1099.7	0.0017	9.1
1336	1465	273.6	0.0937	8764.4	0.0017	73.3
1368	1466	274.1	0.0939	7668.8	0.0017	65.6
1396	1465	273.6	0.0937	8193.3	0.0017	71.5
1426	1463	272.6	0.0934	8185.6	0.0017	73.0
1456	1464	273.1	0.0936	8092.5	0.0017	73.6
1486	1451	266.4	0.0913	7789.9	0.0016	72.3
1516	1425	252.9	0.0866	50559.0	0.0016	516.3
1786	1171	121.6	0.0416	29119.8	0.0008	357.9
2188	981	23.3	0.0080	2952.8	0.0001	43.3
2555	922	-7.2	-0.0025	-5237.1	0.0000	-88.5
2911	893	-22.2	-0.0076	-12370.1	-0.0001	-238.0
3310	859	-39.8	-0.0136		-0.0002	

Area (mg*min/L)	Retention Time t_{RTD}(min)	Pulse Duration (min)	Flow Rate (ml/min)	Calculated Mass (g)	Pore Volume (L)
161672	1442.0	84	12.2	2.0	17.5

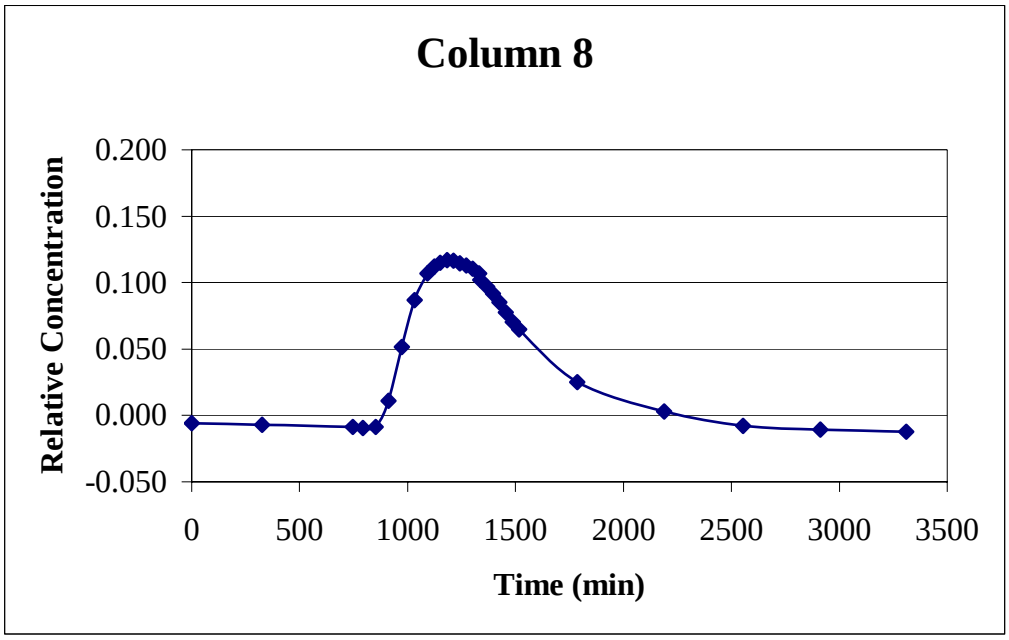

Figure B.9 Column 8 Tracer Results (1 Dec 04)

Table B.14 Column 8 Tracer Results (1 Dec 04)

Specific Conductivity (uS/cm)	Initial Concentration (mg/L)	Mass (g)	Mass Balance Error
6580	2919.1	3.0	-31.3

Time (min)	Specific Conductivity (uS/cm)	Concentration (mg/L)	Relative Concentration	Area	f(t)	t_i
0	903	-17.0	-0.006	-6228.9	-0.0001	-6.1
326	895	-21.2	-0.007	-9871.4	-0.0001	-31.8
746	886	-25.8	-0.009	-1235.8	-0.0002	-5.7
792	882	-27.9	-0.010	-1596.4	-0.0002	-7.9
852	887	-25.3	-0.009	219.0	-0.0002	1.2
912	999	32.6	0.011	5661.5	0.0002	32.1
974	1226	150.0	0.051	11715.8	0.0009	70.6
1032	1427	254.0	0.087	16991.8	0.0015	108.4
1092	1540	312.4	0.107	9909.4	0.0019	66.0
1123	1568	326.9	0.112	9607.6	0.0020	65.7
1152	1585	335.7	0.115	10156.1	0.0020	71.2
1182	1596	341.4	0.117	10225.9	0.0021	73.6
1212	1594	340.3	0.117	10462.6	0.0020	77.2
1243	1583	334.7	0.115	9630.1	0.0020	72.8
1272	1573	329.5	0.113	9783.7	0.0020	75.7

Table B.14 Column 8 Tracer Results (1 Dec 04)(Continued)

Time (min)	Specific Conductivity (uS/cm)	Concentration (mg/L)	Relative Concentration	Area	f(t)	t_i
1302	1560	322.8	0.111	9519.9	0.0019	75.3
1332	1539	311.9	0.107	1218.6	0.0019	9.8
1336	1511	297.4	0.102	9285.7	0.0018	75.4
1368	1483	282.9	0.097	7712.3	0.0017	64.1
1396	1454	267.9	0.092	7758.9	0.0016	65.8
1426	1418	249.3	0.085	7138.2	0.0015	61.8
1456	1374	226.6	0.078	6478.8	0.0014	57.3
1486	1333	205.4	0.070	5920.2	0.0012	53.4
1516	1302	189.3	0.065	35407.6	0.0011	351.3
1786	1077	73.0	0.025	16333.0	0.0004	195.0
2188	952	8.3	0.003	-2646.7	0.0000	-37.7
2555	892	-22.7	-0.008	-9656.1	-0.0001	-158.6
2911	875	-31.5	-0.011	-13505.1	-0.0002	-252.5
3310	866	-36.2	-0.012		-0.0002	

Area (mg*min/L)	Retention Time t_{RTD}(min)	Pulse Duration (min)	Flow Rate (ml/min)	Calculated Mass (g)	Pore Volume (L)
166396	1181.9	83	12.4	2.1	14.6

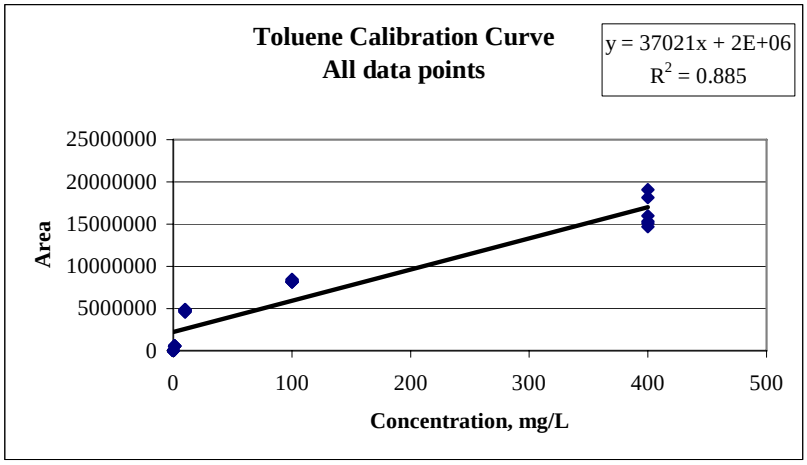

Figure B.10 Toluene Calibration Curve

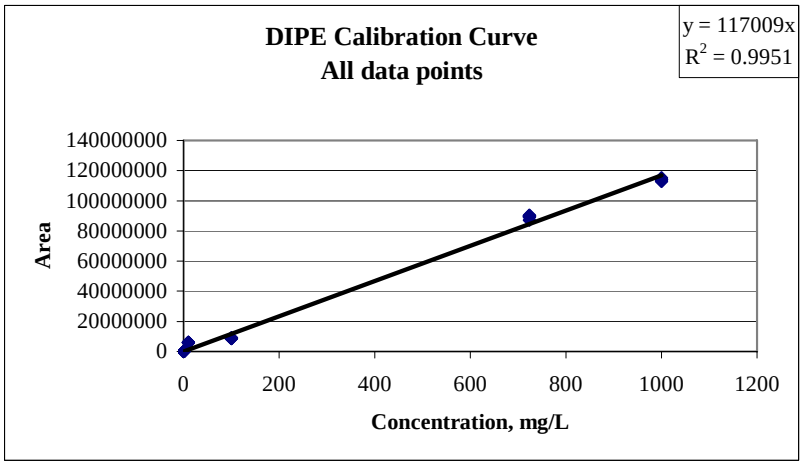

Figure B.11 Diisopropyl Ether Calibration Curve

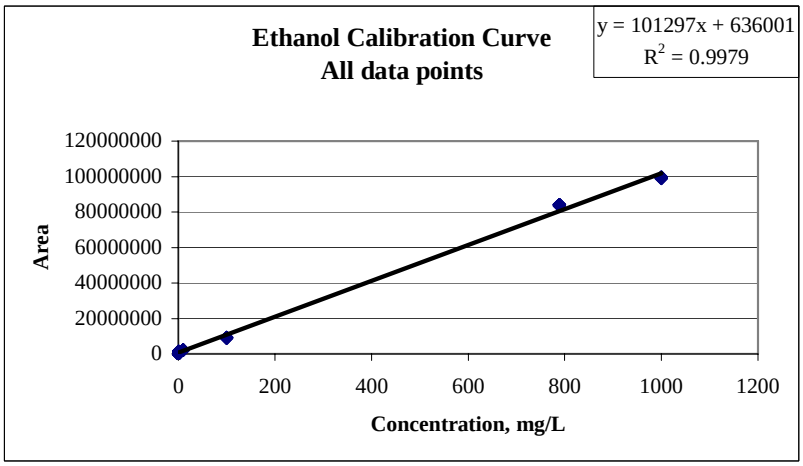

Figure B.12 Ethanol Calibration Curve

Table B.15 Method Detection Limit Calculations for Toluene, DIPE, and Ethanol

Toluene	Concentration	x_i-X	$(x_i-X)^2$
1	-38.29	0.25	0.06
2	-38.37	0.16	0.02
3	-38.67	-0.13	0.02
4	-38.08	0.45	0.20
5	-38.97	-0.43	0.19
6	-38.82	-0.28	0.08
Total	-231.19		0.58
X=	-38.53		
SD=	0.34		
t_{99}(n=6)=	3.37		
MDL=	1.14		

DIPE	Concentration	x_i-X	$(x_i-X)^2$
1	44.24	0.78	0.61
2	43.67	0.22	0.05
3	43.77	0.32	0.10
4	43.98	0.53	0.28
5	43.99	0.54	0.29
6	41.07	-2.39	5.69
Total	260.73		7.02
X=	43.45		
SD=	1.18		
t_{99}(n=6)=	3.37		
MDL=	3.99		

Ethanol	Concentration	x_i-X	$(x_i-X)^2$
1	8.71	0.27	0.07
2	8.92	0.48	0.23
3	8.16	-0.27	0.07
4	7.78	-0.66	0.43
5	8.85	0.41	0.17
6	8.20	-0.23	0.05
Total	50.63		1.04
X=	8.44		
SD=	0.46		
t_{99}(n=6)=	3.37		
MDL=	1.53		

Table B.16 Column 1 Influent Concentrations

Date	Toluene Influent mg/L	DIPE Influent mg/L		Toluene Effluent mg/L	DIPE Effluent mg/L
12-Jan-05	164.67	337.07		205.25	483.71
13-Jan-05	332.90	260.33		346.82	822.20
14-Jan-05	47.84	157.24		284.05	596.12
15-Jan-05	90.07	263.32		283.37	619.32
16-Jan-05	189.22	387.07		196.95	530.05
17-Jan-05	221.82	374.37		1631.00	503.43
18-Jan-05	224.32	333.27		182.90	459.79
19-Jan-05	203.12	286.65		217.34	537.70
20-Jan-05	141.33	271.93		200.33	528.12
21-Jan-05	71.82	240.35		216.03	558.41
23-Jan-05	204.14	382.75		200.03	546.49
24-Jan-05	95.14	248.12		286.32	624.49
25-Jan-05	300.95	362.68		251.72	571.88
26-Jan-05	143.58	304.59		199.05	532.82
28-Jan-05	142.14	239.83		257.45	575.61
29-Jan-05	188.01	231.77		193.70	464.19
30-Jan-05	22.23	144.42		233.16	520.56
31-Jan-05	245.16	120.50		272.79	597.24
1-Feb-05	298.85	406.35		257.90	556.69
3-Feb-05	158.32	347.94		203.99	408.66
4-Feb-05	150.69	353.73		225.21	398.43
5-Feb-05	76.81	293.62		226.39	360.61
6-Feb-05	111.63	324.83		183.09	302.80
7-Feb-05	281.83	157.49		195.08	317.72
8-Feb-05	116.88	182.94		180.28	306.59
9-Feb-05	116.08	226.92		186.10	333.34
10-Feb-05	183.06	275.37		203.22	381.30
11-Feb-05	134.91	270.81		177.32	373.83
12-Feb-05	134.83	304.30		179.03	360.32
13-Feb-05	226.56	356.59		154.94	329.49

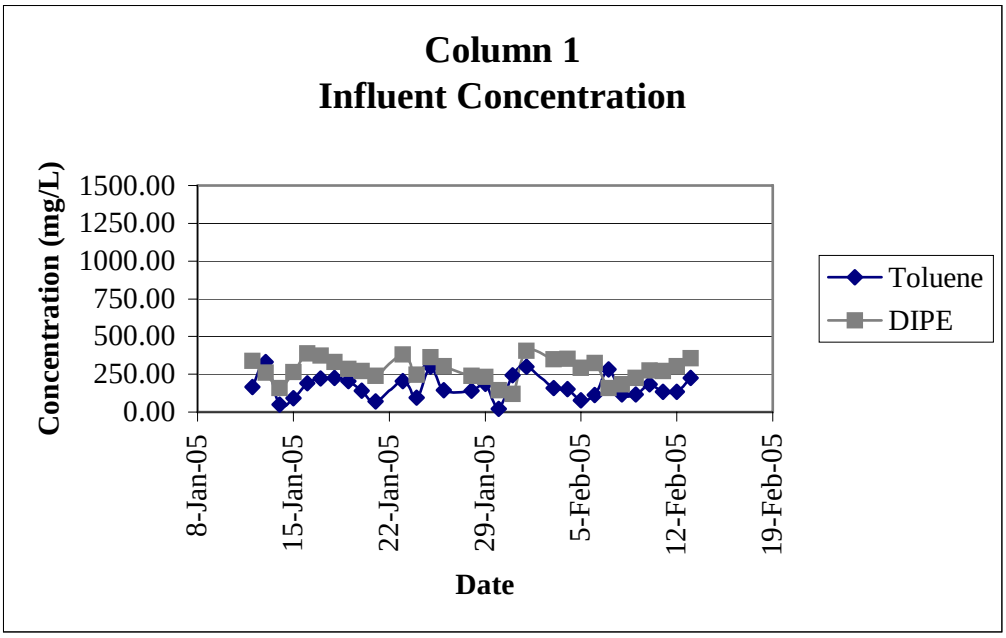

Figure B.13 Column 1 Influent Concentration

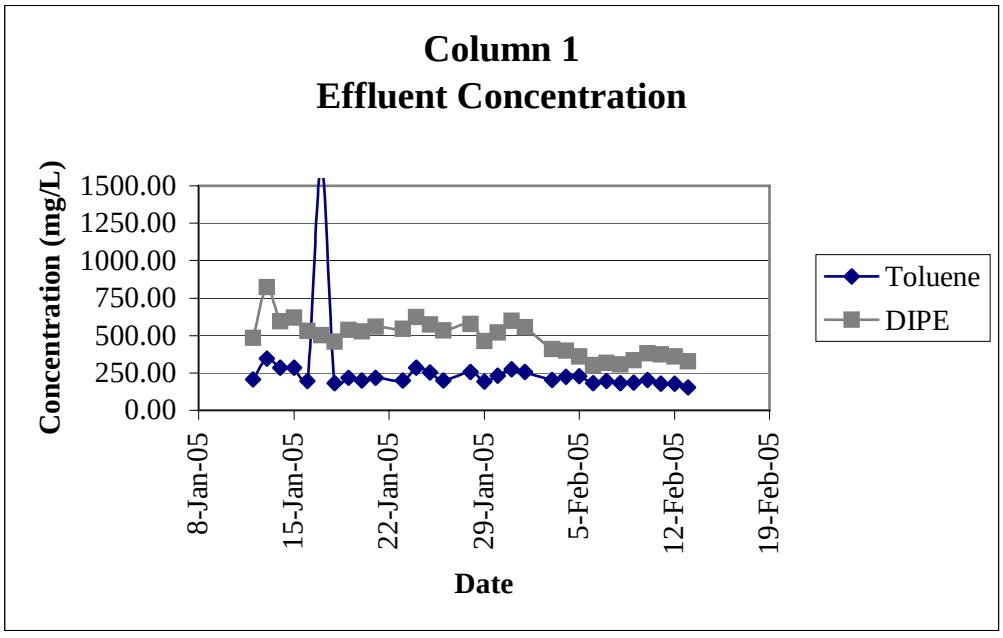

Figure B.14 Column 1 Effluent Concentration

Table B.17 Column 2 Influent Concentrations

Date	Toluene Influent mg/L	DIPE Influent mg/L	Ethanol Effluent mg/L
12-Jan-05	394.24	576.30	1261.97
13-Jan-05	791.54	862.26	1478.75
14-Jan-05	549.50	689.00	1199.82
15-Jan-05	660.75	821.55	1373.90
16-Jan-05	605.25	899.94	1380.16
17-Jan-05	553.56	808.48	1239.14
18-Jan-05	433.40	668.41	1271.64
19-Jan-05	547.24	745.00	1037.81
20-Jan-05	496.79	409.65	947.83
21-Jan-05	526.81	641.72	990.32
23-Jan-05	536.18	612.89	1152.91
24-Jan-05	377.51	420.08	864.70
25-Jan-05	357.16	474.82	873.71
26-Jan-05	505.54	715.65	1042.05
28-Jan-05	620.02	690.12	1049.03
29-Jan-05	352.92	522.40	891.35
30-Jan-05	343.86	428.00	862.39
31-Jan-05	340.73	496.48	990.03
1-Feb-05	579.55	646.98	1074.84
3-Feb-05	570.81	548.50	948.83
4-Feb-05	526.41	549.76	934.98
5-Feb-05	384.67	482.36	934.41
6-Feb-05	516.34	585.12	983.51
7-Feb-05	445.71	621.11	1122.62
8-Feb-05	325.52	414.15	889.64
9-Feb-05	305.45	387.29	879.12
10-Feb-05	447.54	478.52	981.19
11-Feb-05	401.21	457.62	930.38
12-Feb-05	294.71	440.94	897.44
13-Feb-05	277.07	384.82	756.79

Table B.18 Column 2 Effluent Concentrations

Date	Toluene Effluent mg/L	DIPE Effluent mg/L	Ethanol Effluent mg/L
12-Jan-05	-36.57	566.37	-1.60
13-Jan-05	338.99	850.31	2.99
14-Jan-05	-32.54	487.41	-4.77
15-Jan-05	-18.92	460.84	11.59
16-Jan-05	-0.35	475.05	30.84
17-Jan-05	-2.79	423.96	133.45
18-Jan-05	27.01	548.00	204.18
19-Jan-05	46.62	549.20	254.70
20-Jan-05	50.43	570.02	264.94
21-Jan-05	76.72	617.95	210.00
23-Jan-05	82.35	512.86	27.65
24-Jan-05	115.94	557.42	4.75
25-Jan-05	146.37	515.62	-6.28
26-Jan-05	133.57	537.35	-6.28
28-Jan-05	177.02	527.41	-6.28
29-Jan-05	157.18	421.22	-6.28
30-Jan-05	170.37	381.14	-6.28
31-Jan-05	187.83	395.68	-6.16
1-Feb-05	163.02	353.79	-6.28
3-Feb-05	201.52	346.56	-6.12
4-Feb-05	213.56	329.98	-6.28
5-Feb-05	188.09	308.83	-6.16
6-Feb-05	191.70	313.05	-6.28
7-Feb-05	176.79	290.22	-6.28
8-Feb-05	163.04	287.85	-6.28
9-Feb-05	160.43	283.24	-6.28
10-Feb-05	157.41	292.15	-6.28
11-Feb-05	142.96	280.32	-6.28
12-Feb-05	139.98	291.96	-6.28
13-Feb-05	148.48	278.43	-6.28

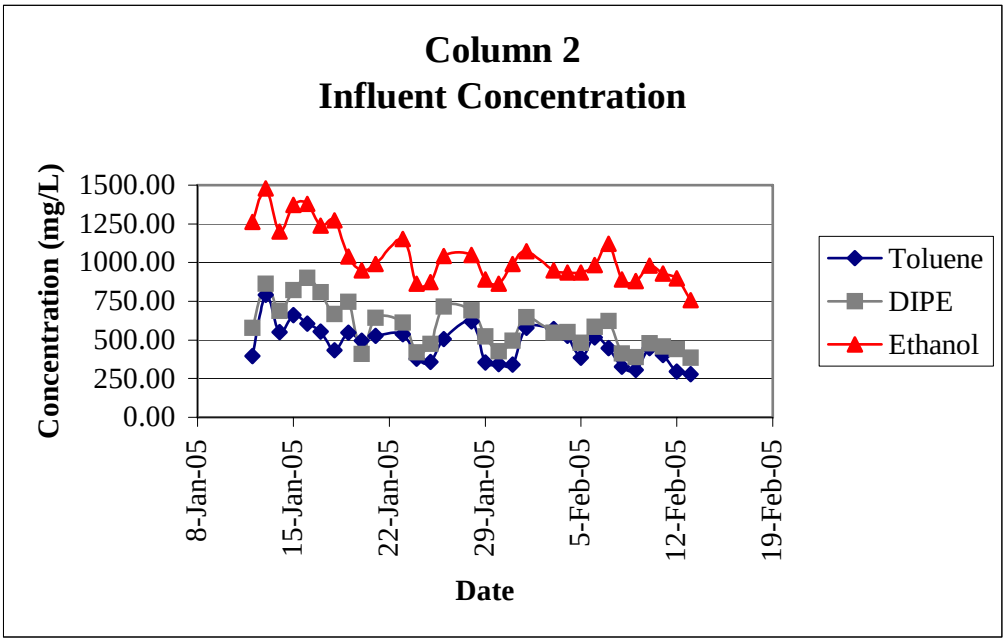

Figure B.15 Column 2 Influent Concentration

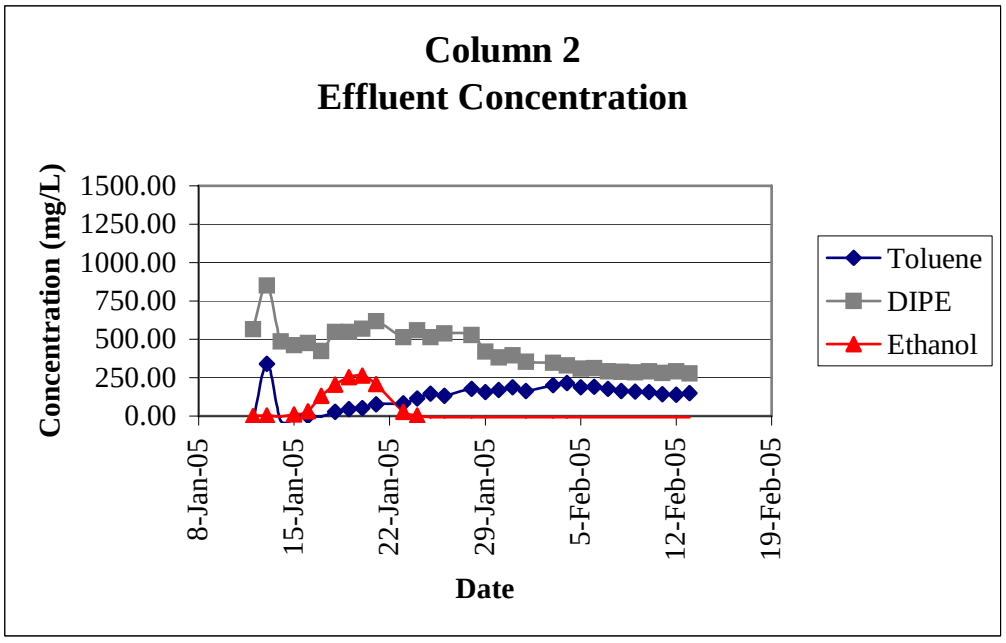

Figure B.16 Column 2 Effluent Concentration

Table B.19 Column 3 Influent Concentrations

Date	Toluene Influent mg/L	DIPE Influent mg/L	Ethanol Influent mg/L
12-Jan-05	-49.63	-8.50	-6.28
13-Jan-05	-54.02	-8.50	-6.28
14-Jan-05	489.60	575.69	1164.53
15-Jan-05	929.33	607.26	1183.34
16-Jan-05	343.33	550.92	1219.64
17-Jan-05	397.05	515.83	1134.86
18-Jan-05	485.70	634.66	1198.86
19-Jan-05	460.17	514.15	1019.32
20-Jan-05	368.88	450.92	949.51
21-Jan-05	435.17	552.87	876.17
23-Jan-05	454.34	553.90	991.23
24-Jan-05	362.43	525.12	1122.54
25-Jan-05	400.10	496.19	872.46
26-Jan-05	285.67	424.39	962.95
28-Jan-05	338.52	500.81	1131.84
29-Jan-05	261.75	346.38	774.25
30-Jan-05	413.39	387.01	721.19
31-Jan-05	541.61	540.44	862.32
1-Feb-05	272.14	432.09	875.68
3-Feb-05	473.11	497.16	845.08
4-Feb-05	421.90	446.82	936.33
5-Feb-05	478.71	477.12	759.81
6-Feb-05	303.39	342.53	817.55
7-Feb-05	321.79	442.23	869.29
8-Feb-05	437.80	462.07	697.13
9-Feb-05	281.40	372.25	806.84
10-Feb-05	485.37	456.66	635.96
11-Feb-05	243.81	361.97	941.23
12-Feb-05	357.43	257.96	838.02
13-Feb-05	208.19	295.66	810.74

Table B.20 Column 3 Effluent Concentrations

Date	Toluene Effluent mg/L	DIPE Effluent mg/L	Ethanol Effluent mg/L
12-Jan-05	-39.81	-2.37	-6.28
13-Jan-05	-54.02	-2.45	-6.28
14-Jan-05	-19.66	-4.85	-6.28
15-Jan-05	-9.17	-5.14	11.59
16-Jan-05	-54.02	-0.37	132.33
17-Jan-05	-54.02	268.91	1787.97
18-Jan-05	-35.64	494.77	1332.64
19-Jan-05	-49.75	644.65	946.20
20-Jan-05	-49.14	683.54	920.01
21-Jan-05	-52.00	389.84	413.07
23-Jan-05	-50.23	499.38	0.44
24-Jan-05	-43.82	562.21	-6.03
25-Jan-05	-36.05	434.24	-6.28
26-Jan-05	-29.71	559.93	-6.28
28-Jan-05	-3.16	439.82	-6.28
29-Jan-05	15.44	456.63	-6.28
30-Jan-05	37.12	402.43	-3.02
31-Jan-05	54.89	398.92	14.33
1-Feb-05	39.28	402.67	16.47
3-Feb-05	84.28	332.00	-5.69
4-Feb-05	101.87	336.82	-6.10
5-Feb-05	104.32	314.38	-6.28
6-Feb-05	113.37	306.64	-6.28
7-Feb-05	112.74	279.61	-6.28
8-Feb-05	82.06	256.66	-6.28
9-Feb-05	108.71	268.96	-6.28
10-Feb-05	126.60	280.68	-6.16
11-Feb-05	85.67	279.87	-6.28
12-Feb-05	133.93	260.55	-6.28
13-Feb-05	125.99	259.05	-6.28

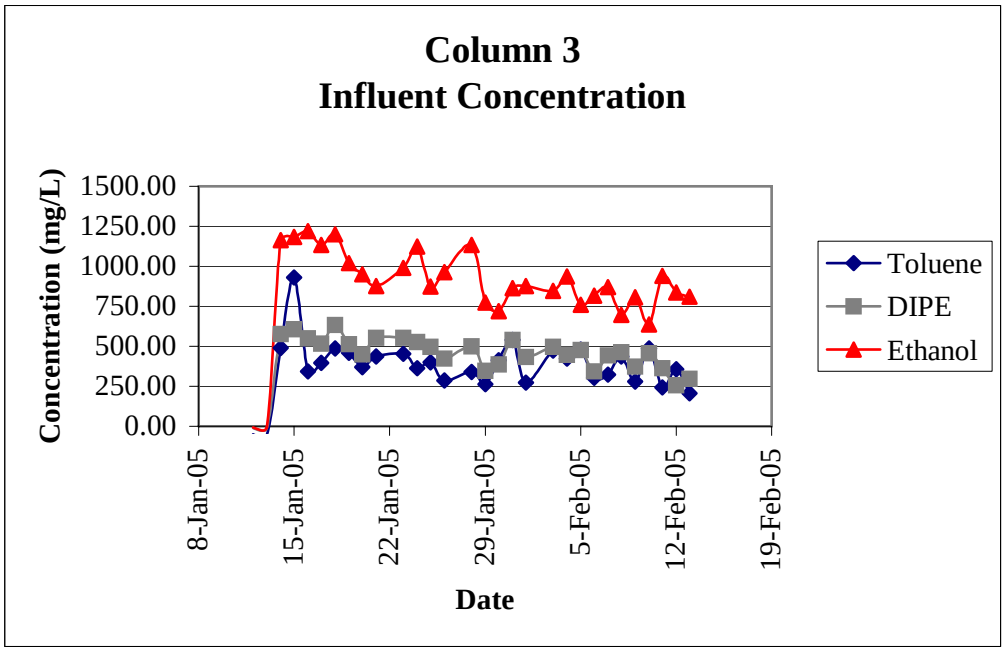

Figure B.17 Column 3 Influent Concentration

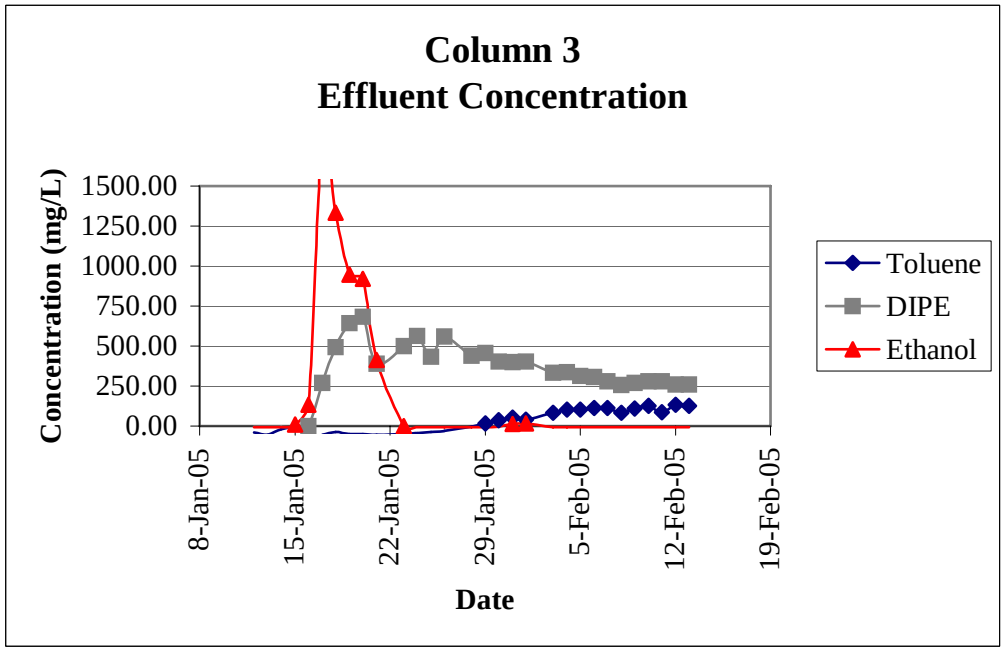

Figure B.18 Column 3 Effluent Concentration

Table B.21 Column 4 Influent and Effluent Concentrations

Date	Toluene Influent mg/L	DIPE Influent mg/L		Toluene Effluent mg/L	DIPE Effluent mg/L
12-Jan-05	121.46	251.84		92.31	1113.39
13-Jan-05	355.85	253.69		126.64	1502.74
14-Jan-05	74.83	109.69		64.97	977.66
15-Jan-05	202.69	290.49		80.27	993.82
16-Jan-05	316.65	336.25		89.96	989.68
17-Jan-05	49.12	204.54		113.89	906.35
18-Jan-05	275.50	361.15		126.70	807.61
19-Jan-05	184.73	392.17		-48.31	-8.50
20-Jan-05	174.17	343.86		185.51	692.37
21-Jan-05	49.89	213.44		231.84	686.20
23-Jan-05	125.50	289.42		265.01	632.27
24-Jan-05	252.80	188.27		244.46	552.56
25-Jan-05	207.50	346.28		322.97	616.10
26-Jan-05	197.72	263.21		345.32	697.35
28-Jan-05	219.34	379.66		305.07	515.05
29-Jan-05	106.08	337.25		309.19	464.97
30-Jan-05	125.28	292.88		349.58	439.34
31-Jan-05	306.50	143.34		351.15	434.64
1-Feb-05	263.91	319.65		364.07	436.52
3-Feb-05	284.69	388.70		335.36	433.03
4-Feb-05	161.90	355.93		348.72	462.78
5-Feb-05	265.75	422.91		319.08	400.06
6-Feb-05	158.91	324.80		310.57	384.42
7-Feb-05	234.27	186.08		357.41	399.93
8-Feb-05	163.61	251.69		326.54	373.98
9-Feb-05	112.77	218.63		309.80	356.80
10-Feb-05	164.43	247.93		297.96	353.43
11-Feb-05	140.41	289.40		312.78	390.68
12-Feb-05	131.35	257.96		350.90	418.18
13-Feb-05	164.01	288.37		294.40	338.78

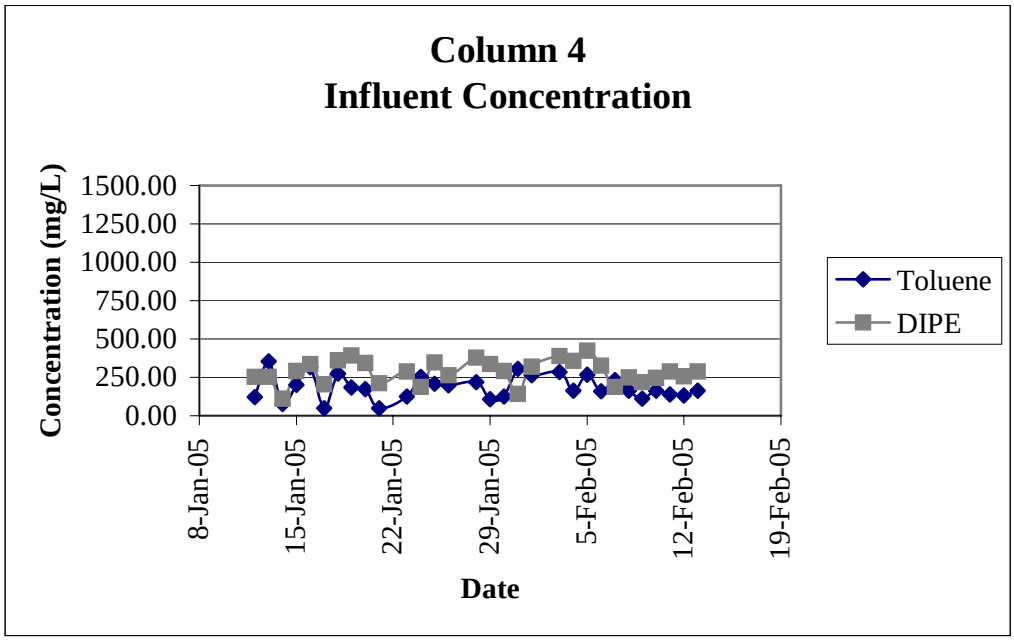

Figure B.19 Column 4 Influent Concentration

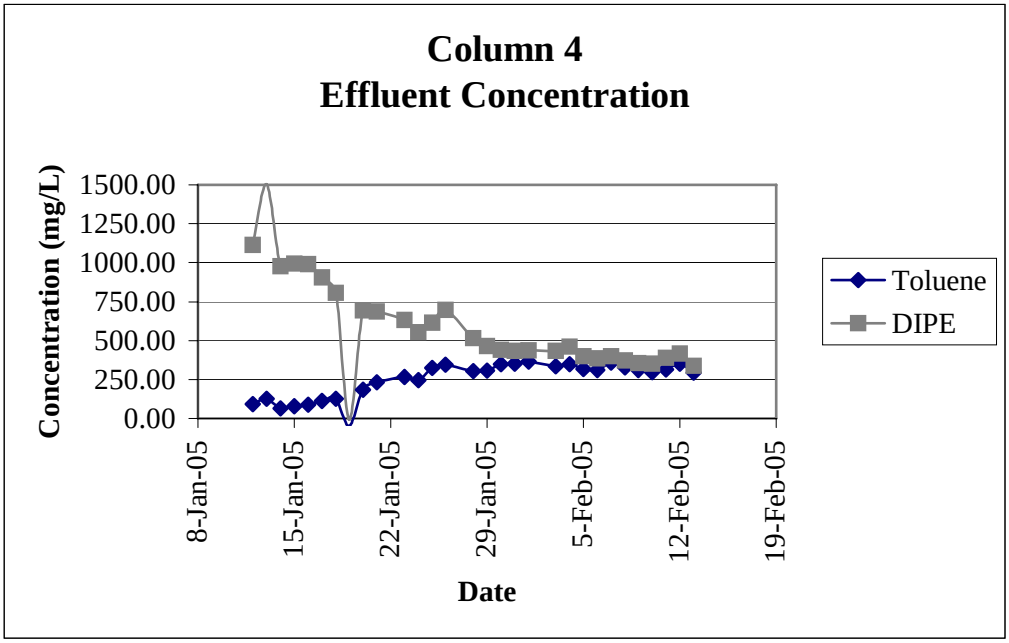

Figure B.20 Column 4 Effluent Concentration

Table B.22 Column 5 Influent Concentrations

Date	Toluene Influent mg/L	DIPE Influent mg/L	Ethanol Influent mg/L
12-Jan-05	-50.01	-8.50	-6.28
13-Jan-05	-54.02	-8.50	-6.28
14-Jan-05	82.56	67.75	563.60
15-Jan-05	103.00	101.58	260.13
16-Jan-05	208.01	177.85	165.55
17-Jan-05	89.28	154.82	46.09
18-Jan-05	72.32	143.73	209.40
19-Jan-05	117.66	131.58	272.70
20-Jan-05	184.05	152.05	187.40
21-Jan-05	102.35	143.60	277.09
23-Jan-05	359.36	176.05	304.80
24-Jan-05	88.76	144.63	194.14
25-Jan-05	207.14	190.92	112.78
26-Jan-05	410.76	210.13	298.65
28-Jan-05	119.57	127.31	279.91
29-Jan-05	82.52	114.37	290.46
30-Jan-05	91.84	133.78	271.95
31-Jan-05	236.30	137.76	173.20
1-Feb-05	376.79	277.04	338.85
3-Feb-05	37.69	96.67	198.28
4-Feb-05	65.47	114.67	297.37
5-Feb-05	116.47	130.87	228.76
6-Feb-05	91.51	118.42	263.64
7-Feb-05	204.86	202.63	244.41
8-Feb-05	184.01	163.18	181.54
9-Feb-05	22.84	64.08	114.18
10-Feb-05	94.40	102.41	132.27
11-Feb-05	40.36	80.97	169.38
12-Feb-05	107.11	131.69	171.11
13-Feb-05	50.89	56.99	158.18

Table B.23Column 5 Effluent Concentrations

Date	Toluene Effluent mg/L	DIPE Effluent mg/L	Ethanol Effluent mg/L
12-Jan-05	-21.85	-7.26	-6.28
13-Jan-05	-23.13	-8.50	-6.28
14-Jan-05	-54.02	-7.25	-6.28
15-Jan-05	80.27	993.82	-6.28
16-Jan-05	-34.95	102.87	-0.61
17-Jan-05	-1.43	111.29	-5.23
18-Jan-05	62.41	135.08	-6.28
19-Jan-05	135.35	160.93	-6.28
20-Jan-05	143.86	157.30	-6.28
21-Jan-05	143.68	174.14	-6.28
23-Jan-05	170.25	144.94	-6.28
24-Jan-05	161.55	128.33	-6.28
25-Jan-05	134.86	110.57	-6.28
26-Jan-05	174.16	134.41	-6.28
28-Jan-05	181.80	143.02	-6.28
29-Jan-05	172.80	125.99	-6.28
30-Jan-05	155.28	120.16	-6.28
31-Jan-05	164.81	127.47	-6.28
1-Feb-05	140.16	120.41	-6.28
3-Feb-05	115.34	130.94	-6.28
4-Feb-05	130.35	137.70	-6.28
5-Feb-05	124.63	134.58	-6.28
6-Feb-05	116.78	110.12	-6.28
7-Feb-05	143.26	116.07	-6.28
8-Feb-05	134.09	110.65	-6.28
9-Feb-05	115.70	112.46	-6.28
10-Feb-05	147.90	133.61	-6.28
11-Feb-05	94.53	99.61	-6.28
12-Feb-05	108.50	106.73	-6.28
13-Feb-05	76.60	83.75	-6.28

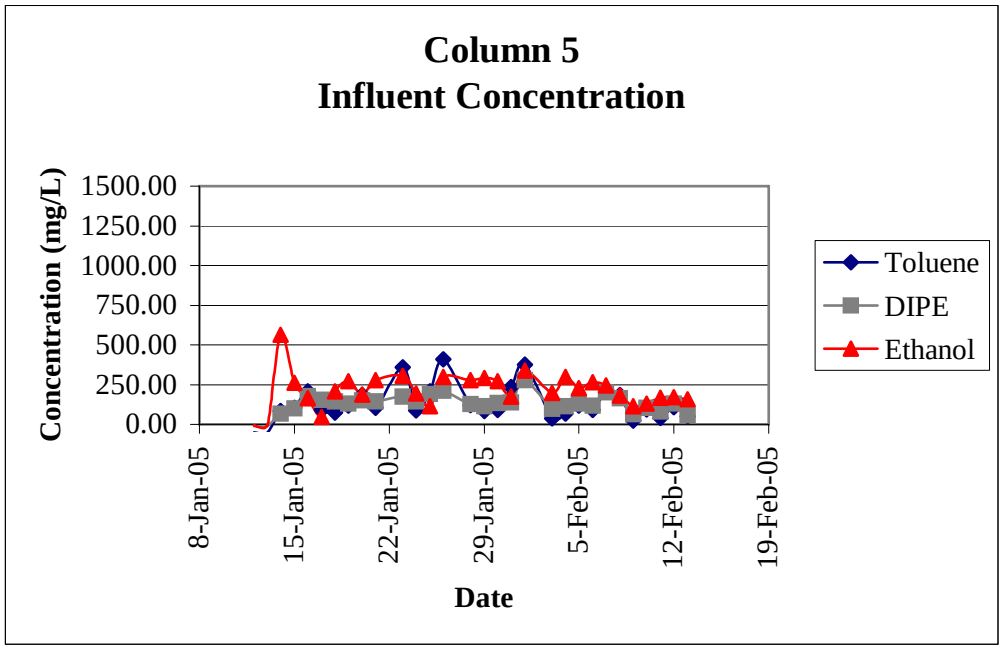

Figure B.21 Column 5 Influent Concentration

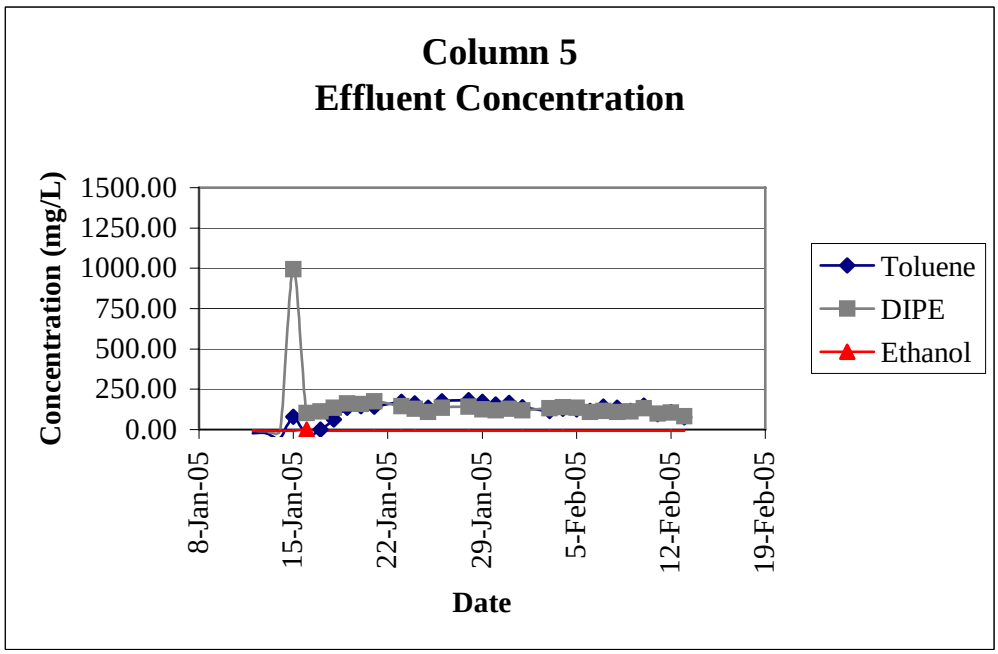

Figure B.22 Column 5 Effluent Concentration

Table B.24 Column 6 Influent and Effluent Concentrations

Date	Toluene Influent mg/L	DIPE Influent mg/L		Toluene Effluent mg/L	DIPE Effluent mg/L
12-Jan-05	36.95	83.56		586.52	246.66
13-Jan-05	100.97	146.61		815.97	296.00
14-Jan-05	71.26	105.76		676.09	184.81
15-Jan-05	155.83	173.04		697.61	214.27
16-Jan-05	174.71	231.47		677.75	219.78
17-Jan-05	87.82	212.38		596.86	200.06
18-Jan-05	49.37	132.32		678.14	217.88
19-Jan-05	80.53	133.86		673.01	275.21
20-Jan-05	89.29	135.01		674.77	286.68
21-Jan-05	125.21	170.58		564.67	213.41
23-Jan-05	150.39	168.98		694.28	267.34
24-Jan-05	256.73	198.21		406.62	178.49
25-Jan-05	123.68	141.73		442.95	148.82
26-Jan-05	59.47	131.22		628.54	231.68
28-Jan-05	76.44	185.74		523.55	197.65
29-Jan-05	133.52	181.68		451.34	190.17
30-Jan-05	89.62	128.18		398.66	191.68
31-Jan-05	53.28	126.56		387.03	231.53
1-Feb-05	73.90	149.97		320.74	201.45
3-Feb-05	207.20	160.87		346.65	207.45
4-Feb-05	61.55	123.88		340.13	217.94
5-Feb-05	221.24	232.38		297.85	178.91
6-Feb-05	128.39	142.65		309.93	198.61
7-Feb-05	62.41	57.60		268.90	190.86
8-Feb-05	240.96	130.29		218.57	130.94
9-Feb-05	38.51	86.35		197.92	117.70
10-Feb-05	100.29	115.16		183.91	117.88
11-Feb-05	79.64	123.09		234.61	117.64
12-Feb-05	122.31	148.84		223.87	130.86
13-Feb-05	84.38	158.62		156.10	126.00

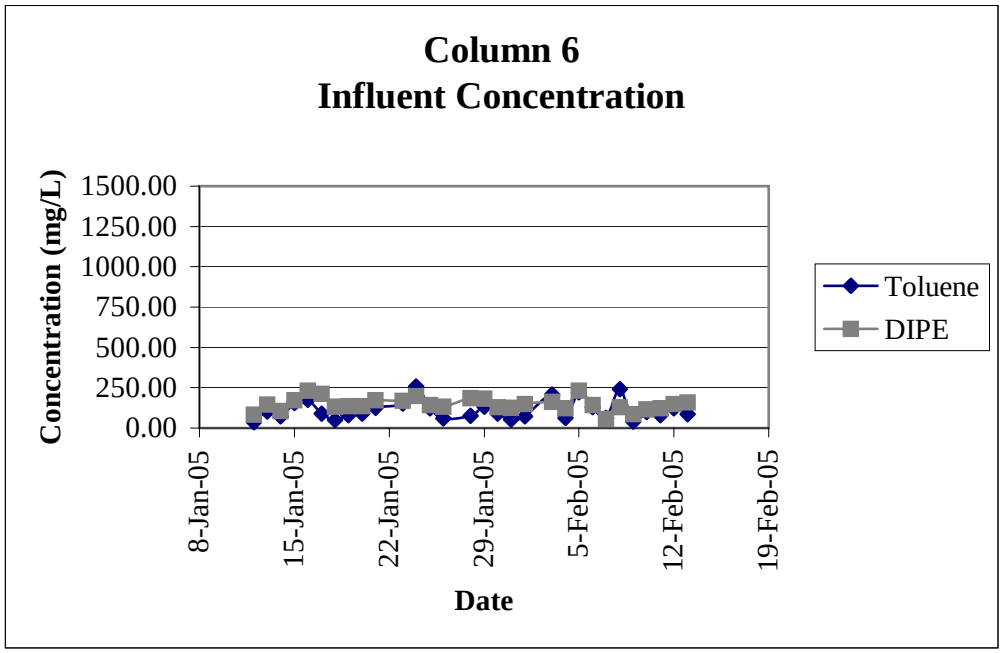

Figure B.23 Column 6 Influent Concentration

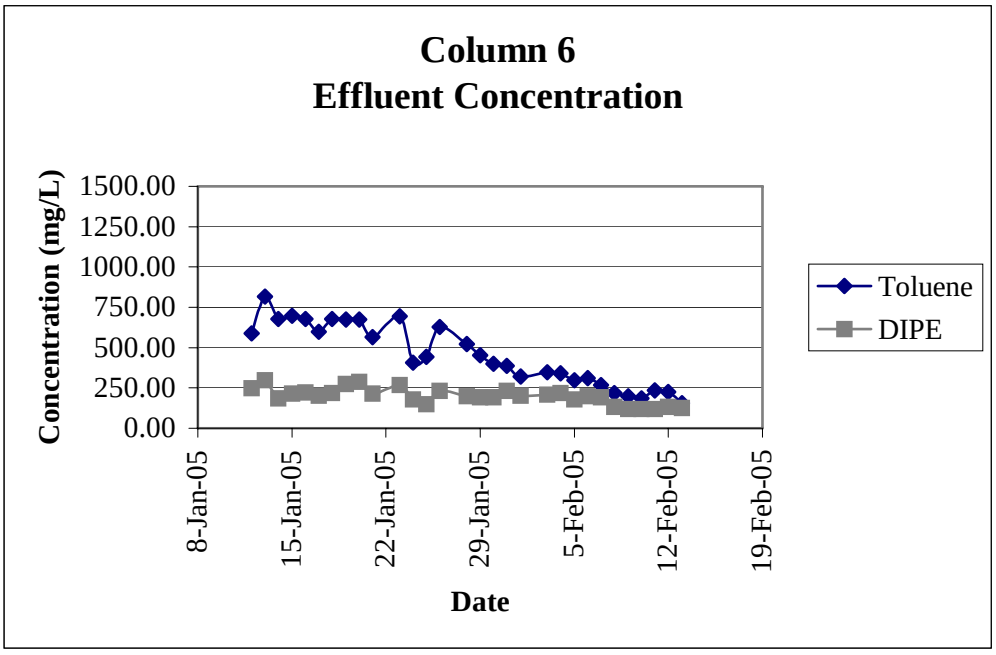

Figure B.24 Column 6 Effluent Concentration

Table B.25 Column 7 Influent and Effluent Concentrations

Date	Toluene Influent mg/L	DIPE Influent mg/L		Toluene Effluent mg/L	DIPE Effluent mg/L
12-Jan-05	35.01	127.84		784.31	436.72
13-Jan-05	113.47	245.33		964.67	485.47
14-Jan-05	160.04	164.41		856.17	363.57
15-Jan-05	43.63	90.47		896.37	273.38
16-Jan-05	111.33	197.52		898.88	261.69
17-Jan-05	69.56	197.16		931.75	253.76
18-Jan-05	184.03	231.69		934.71	270.18
19-Jan-05	87.41	110.47		779.76	139.20
20-Jan-05	188.06	224.46		833.40	245.78
21-Jan-05	134.35	219.73		849.47	240.82
23-Jan-05	132.94	139.08		993.62	297.74
24-Jan-05	67.46	115.73		1011.49	317.64
25-Jan-05	119.80	157.47		805.94	222.15
26-Jan-05	678.75	289.22		743.52	203.71
28-Jan-05	200.87	339.17		777.02	233.48
29-Jan-05	228.63	311.32		827.03	264.33
30-Jan-05	28.73	119.92		858.28	283.20
31-Jan-05	242.38	84.68		699.96	226.59
1-Feb-05	203.45	110.73		721.22	185.31
3-Feb-05	163.03	235.13		663.85	150.15
4-Feb-05	207.81	297.68		779.14	197.72
5-Feb-05	186.22	274.15		844.02	230.18
6-Feb-05	68.13	212.65		743.95	224.09
7-Feb-05	188.27	226.38		713.84	223.81
8-Feb-05	205.37	258.34		646.52	226.09
9-Feb-05	29.40	83.08		623.96	208.08
10-Feb-05	196.92	267.10		569.80	190.92
11-Feb-05	293.33	243.08		501.34	187.97
12-Feb-05	122.31	148.84		448.11	185.45
13-Feb-05	149.12	204.67		393.76	197.81

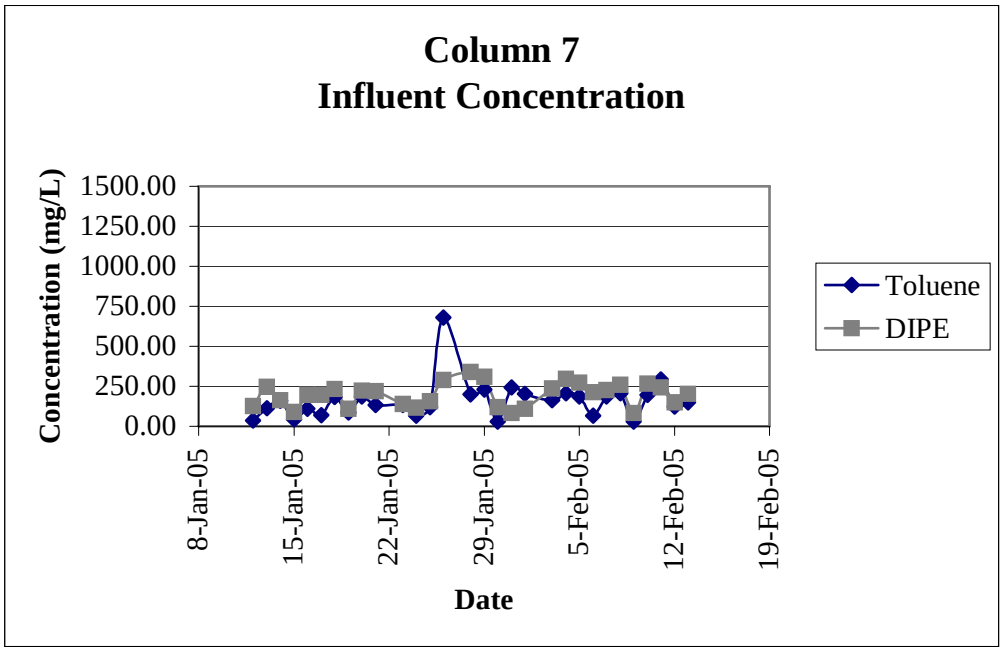

Figure B.25 Column 7 Influent Concentration

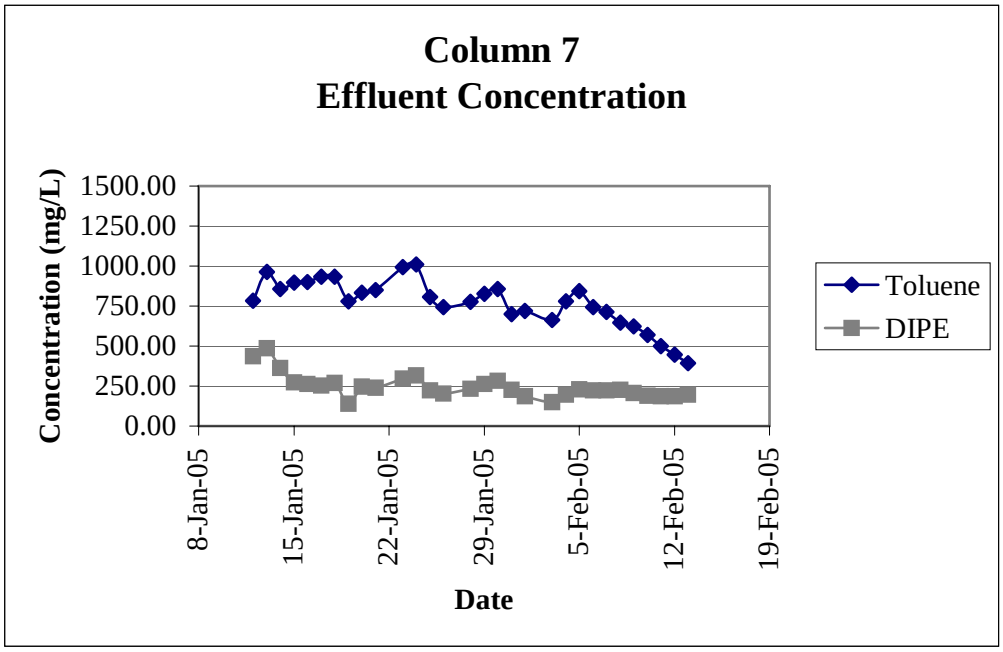

Figure B.26 Column 7 Effluent Concentration

Table B.26 Column 8 Influent Concentrations

Date	Toluene Influent mg/L	DIPE Influent mg/L	Ethanol Influent mg/L
12-Jan-05	160.95	207.64	491.56
13-Jan-05	416.82	316.67	623.33
14-Jan-05	429.09	387.35	471.86
15-Jan-05	254.24	117.31	112.66
16-Jan-05	192.80	196.88	154.24
17-Jan-05	153.41	162.73	170.35
18-Jan-05	83.38	114.57	163.25
19-Jan-05	76.53	82.47	87.25
20-Jan-05	95.62	122.77	146.90
21-Jan-05	149.21	155.34	136.45
23-Jan-05	194.36	185.43	56.91
24-Jan-05	156.59	137.04	227.71
25-Jan-05	108.61	109.92	92.89
26-Jan-05	134.85	159.60	182.95
28-Jan-05	116.39	165.91	270.47
29-Jan-05	83.50	112.18	227.55
30-Jan-05	106.77	143.04	189.38
31-Jan-05	84.27	117.87	164.84
1-Feb-05	500.07	255.31	64.05
3-Feb-05	144.73	165.70	230.06
4-Feb-05	177.92	136.41	55.73
5-Feb-05	143.70	138.30	165.64
6-Feb-05	83.94	110.62	119.50
7-Feb-05	87.60	96.20	185.43
8-Feb-05	115.82	119.83	214.94
9-Feb-05	123.24	95.45	71.82
10-Feb-05	97.66	102.39	33.78
11-Feb-05	108.37	108.00	148.31
12-Feb-05	140.91	96.23	68.91
13-Feb-05	94.83	90.54	79.01

Table B.27 Column 8 Effluent Concentrations

Date	Toluene Effluent mg/L	DIPE Effluent mg/L	Ethanol Effluent mg/L
12-Jan-05	586.83	354.09	190.80
13-Jan-05	578.61	364.49	490.33
14-Jan-05	683.56	469.84	325.99
15-Jan-05	739.89	281.40	183.37
16-Jan-05	660.78	156.17	74.96
17-Jan-05	710.83	136.79	78.22
18-Jan-05	757.05	110.42	81.04
19-Jan-05	790.03	139.20	65.94
20-Jan-05	656.60	120.09	22.02
21-Jan-05	617.28	123.64	36.70
23-Jan-05	464.59	141.00	41.00
24-Jan-05	436.02	148.08	-6.12
25-Jan-05	382.28	113.84	10.86
26-Jan-05	413.71	144.86	4.94
28-Jan-05	343.58	101.00	-6.28
29-Jan-05	330.91	102.61	-6.28
30-Jan-05	365.91	163.71	-6.28
31-Jan-05	240.31	103.32	-6.28
1-Feb-05	241.23	109.62	-6.28
3-Feb-05	214.93	112.44	-6.15
4-Feb-05	247.62	135.12	-6.20
5-Feb-05	230.06	118.20	-6.17
6-Feb-05	238.56	116.98	-6.08
7-Feb-05	221.24	111.78	-6.19
8-Feb-05	209.22	111.60	-6.18
9-Feb-05	173.14	120.01	-6.18
10-Feb-05	166.11	110.75	-6.17
11-Feb-05	190.23	105.53	-6.19
12-Feb-05	203.56	99.81	-6.28
13-Feb-05	152.43	97.45	-6.28

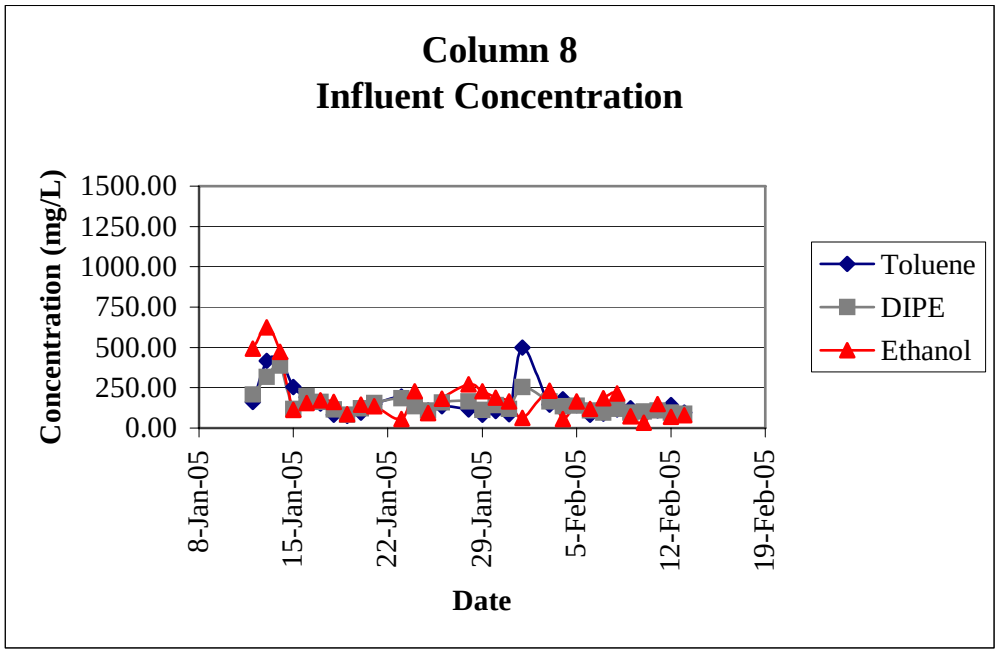

Figure B.27 Column 8 Influent Concentration

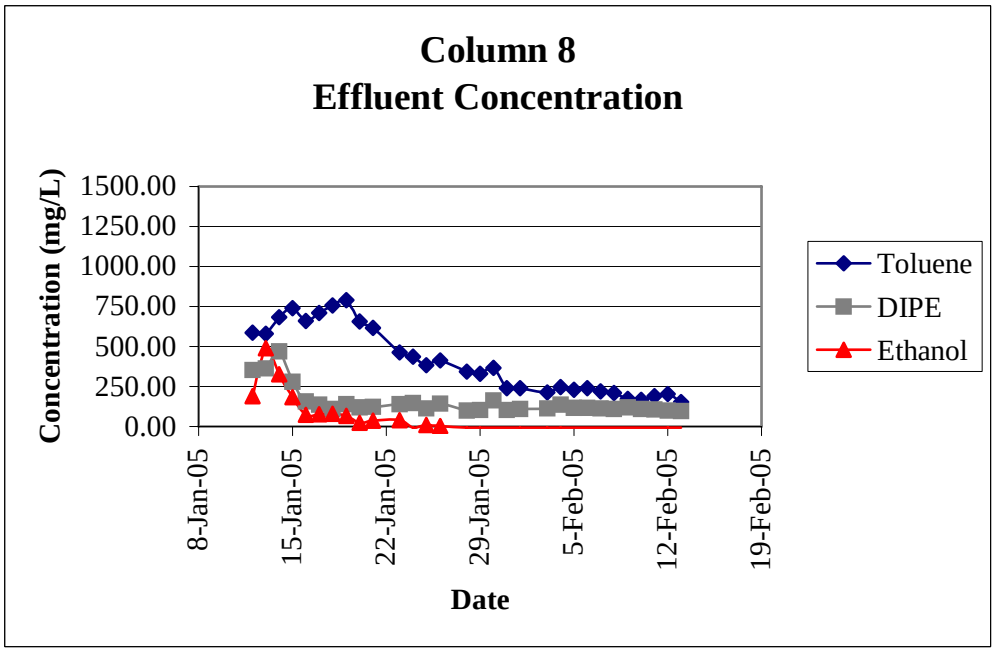

Figure B.28 Column 8 Effluent Concentration

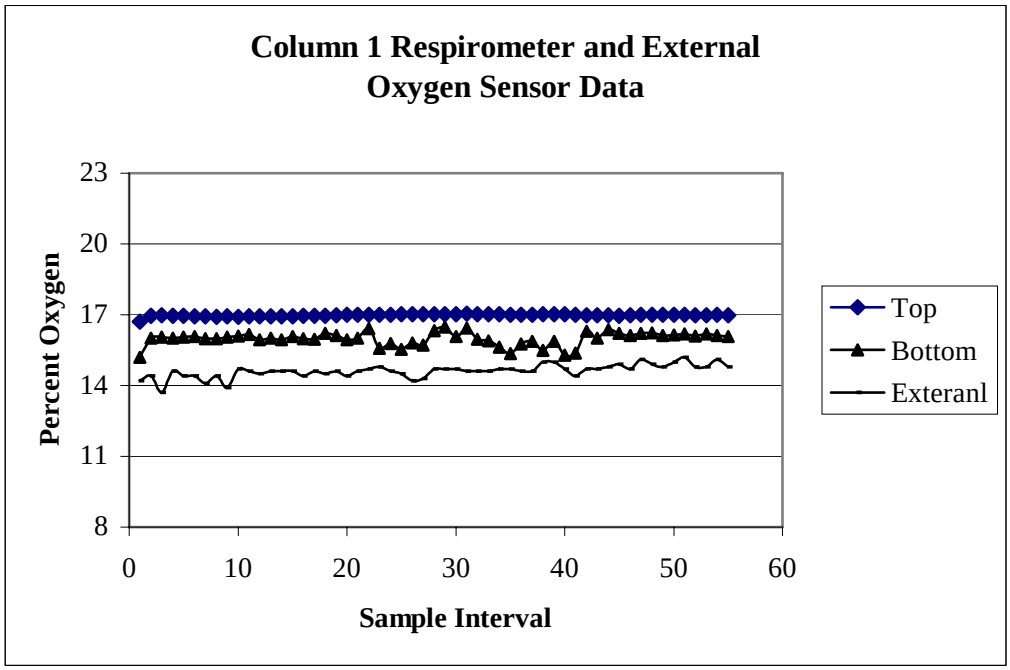

Figure B.29 Column 1 Respirometer and External Oxygen Sensor Data

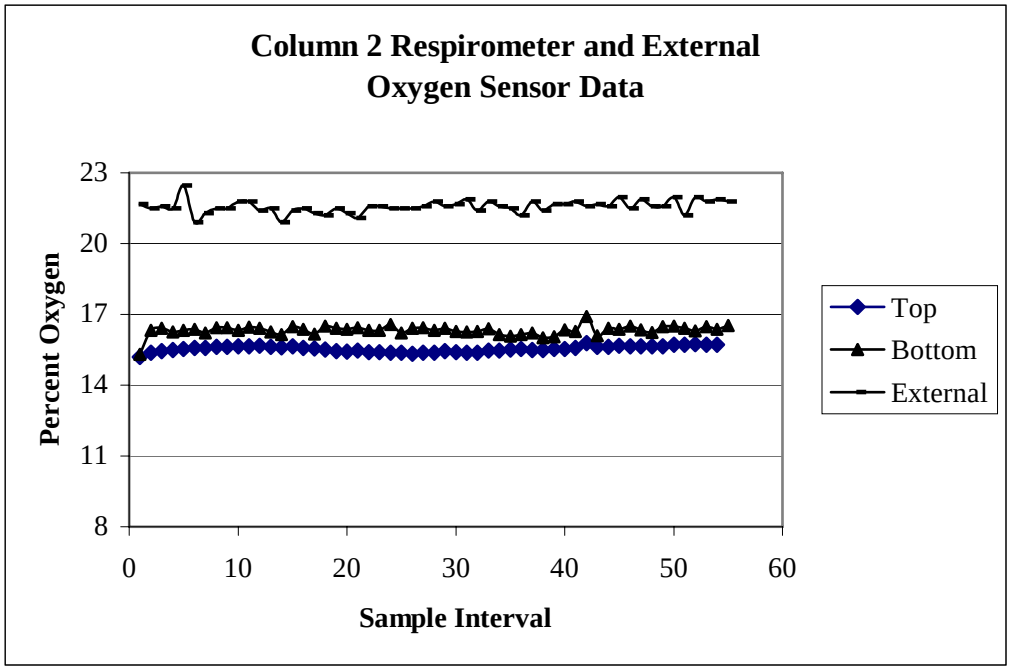

Figure B.30 Column 2 Respirometer and External Oxygen Sensor Data

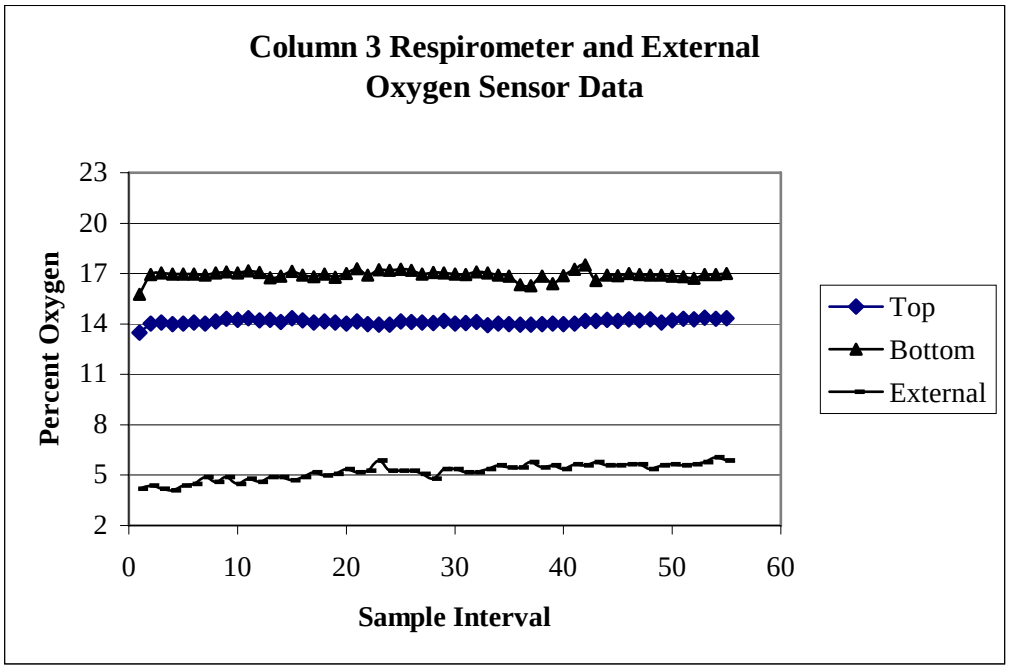

Figure B.31 Column 3 Respirometer and External Oxygen Sensor Data

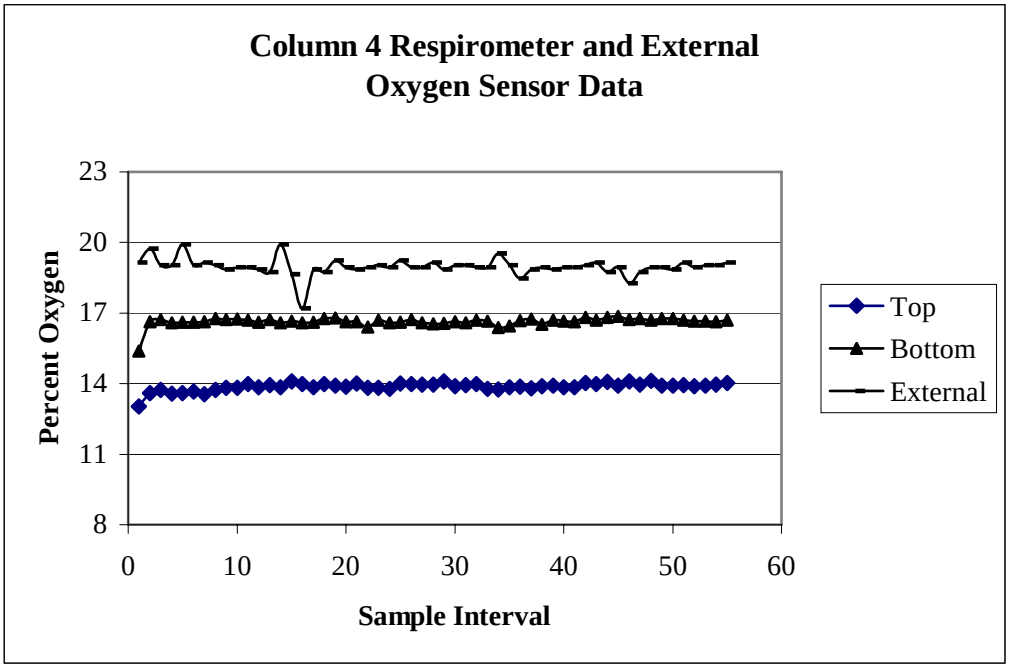

Figure B.32 Column 4 Respirometer and External Oxygen Sensor Data

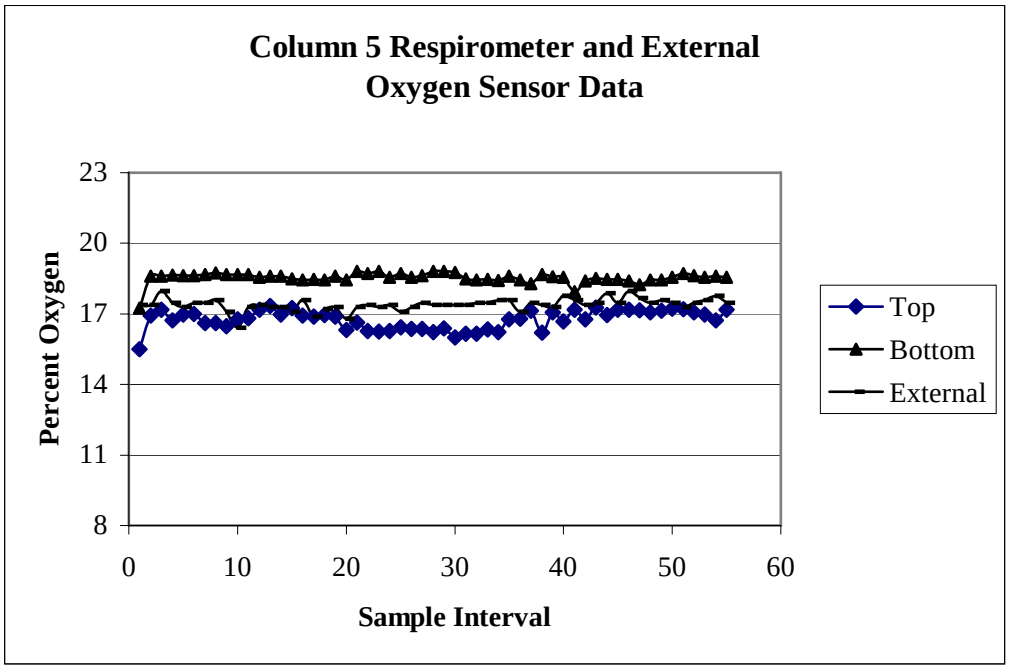

Figure B.33 Column 5 Respirometer and External Oxygen Sensor Data

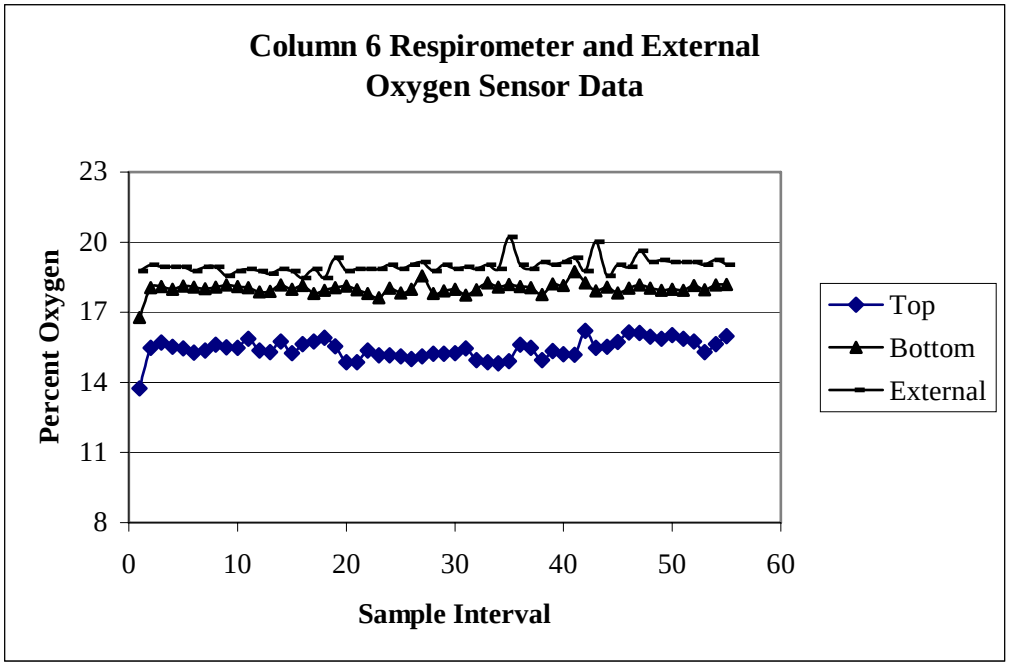

Figure B.34 Column 6 Respirometer and External Oxygen Sensor Data

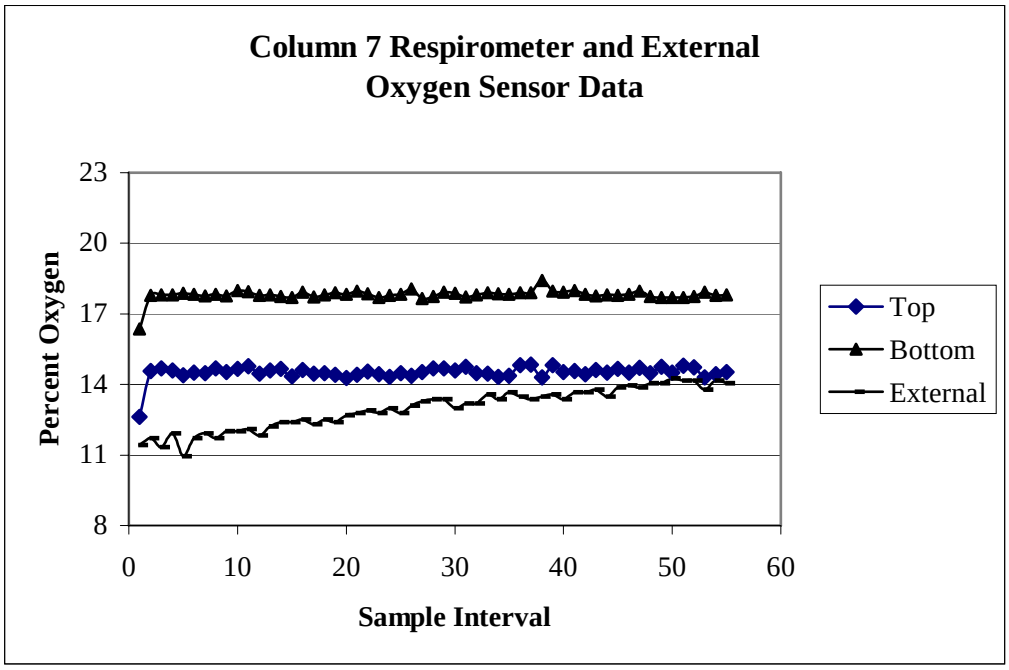

Figure B.35 Column 7 Respirometer and External Oxygen Sensor Data

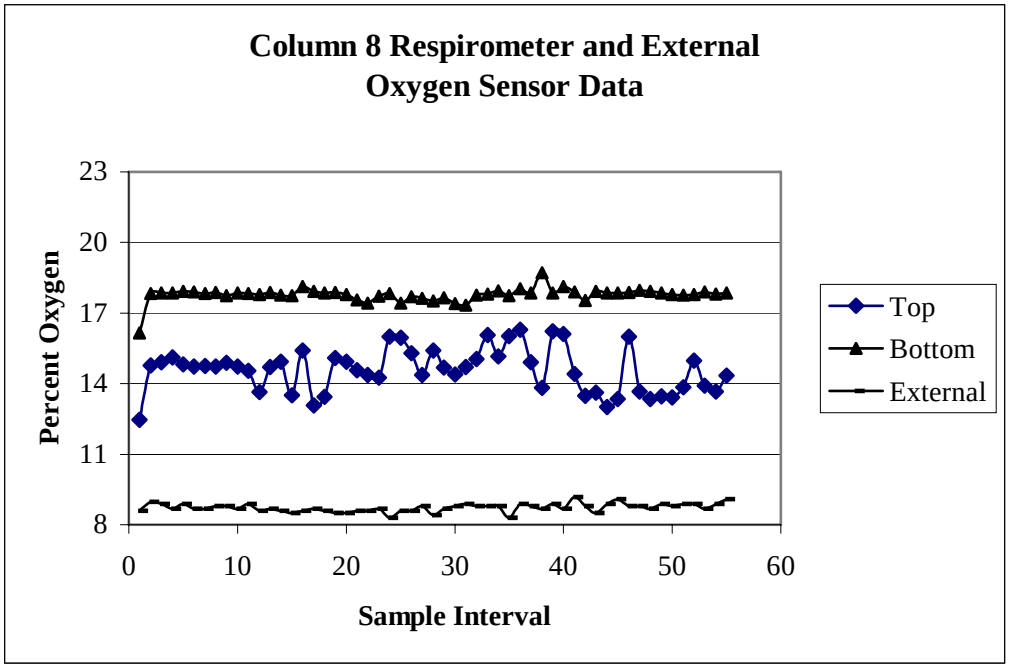

Figure B.36 Column 8 Respirometer and External Oxygen Sensor Data

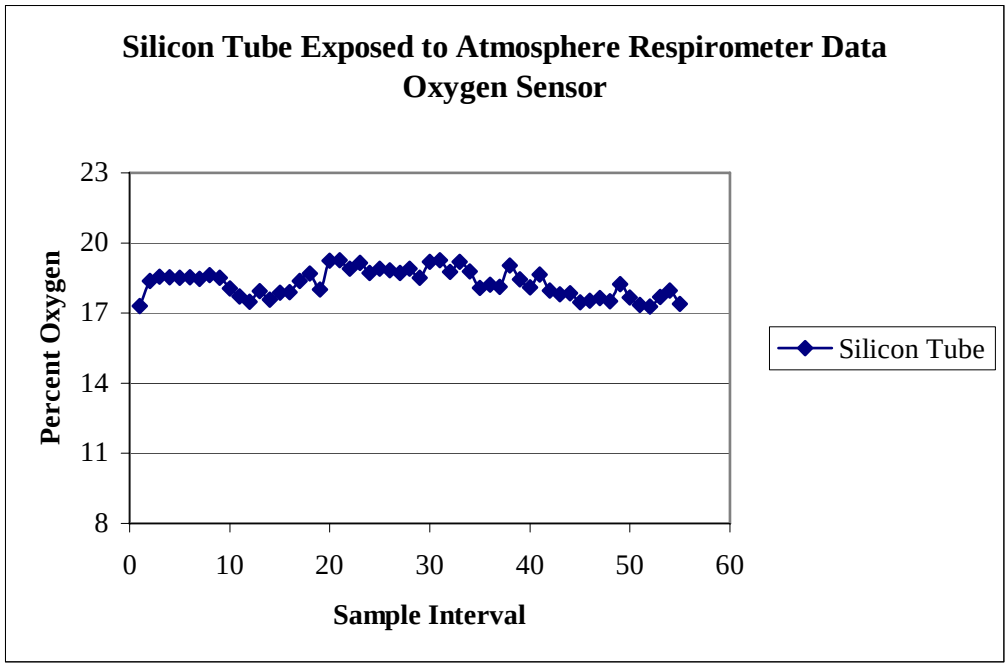

Figure B.37 Silicon Tube Exposed to Atmosphere Respirometer Data, Oxygen Sensor

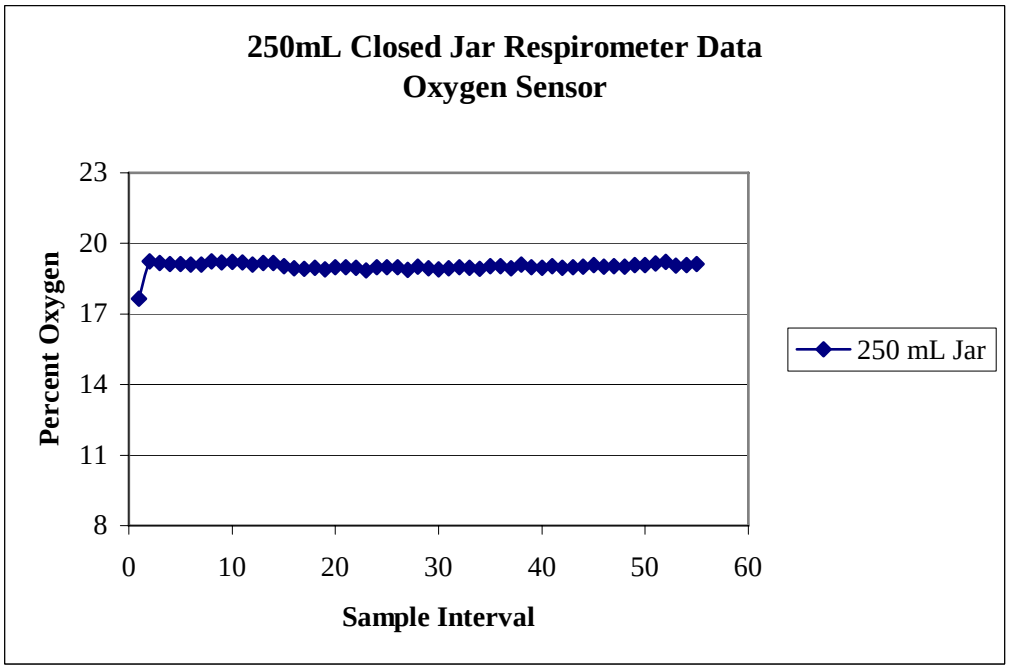

Figure B.38 250 mL Closed Jar Respirometer Data, Oxygen Sensor

References

Ahmed, Farid E. “Toxicology and human health effects following exposure to oxygenated or reformulated gasoline,” *Toxicology Letters,* 123: 89-113 (2001).

American Conference of Governmental Industrial Hygienists (ACGIH). *Documentation of the threshold limit values and biological exposure indices.* : American Conference of Governmental Industrial Hygienists, 2001.

American Conference of Governmental Industrial Hygienists (ACGIH). *TLVs & BEIs: Threshold limit Values for Chemical Substances and Physical Agents and Biological Exposure Indices for 2002*. Cincinnati: American Conference of Governmental Industrial Hygienists, 2002.

American Petroleum Institute (API). *Strategies for Characterizing Subsurface Releases of Gasoline Containing MTBE.* API Publication 4699. February 2000.

Arce, Alberto, Alberto Arce, Jr., Jose Martinez-Ageitos, Eva Rodil, Oscar Rodriguez, Ana Soto. “Physical and equilibrium properties of diisopropyl ether+alcohol+water system,” *Fluid Phase Equilibria,* 170: 113-126 (2000).

Boggan, Bill. "Sources and Uses of Ethyl Alcohol." Electronic Resource. n. pag. http://chemcases.com/alcohol/alc-03.htm. 19 January 2005.

Brown, Theodore L., H.Eugene LeMay, Jr., Bruce E. Bursten. *Chemistry The Central Science.* New Jersey: Prentice Hall, 1997.

40 CFR 136, Appendix B (1993)

Clark, Mark M. *Transport Modeling for environmental engineers and scientists.* New York: John Wiley & Sons, Inc, 1996.

Da Silva, Marcio L. B., and Pedro J.J. Alvarez. “Effects of Ethanol Versus MTBE on Benzene, Toluene, Ethylbenzene, and Xylene Natural Attenuation in Aquifer,” *Journal of Environmental Engineering,* 128(9): 862-868 (2002).

Day, Robert W. *Geotechnical Engineer's Portable Handbook.* New York: McGraw-Hill, 2000.

Delta Environmental Consultants. "Groundwater Oxygenate Cleanup Levels for LUST Sites." Electronic Resource. n. pag. http://www.epa.gov/swerust1/mtbe/oxytable.pdf. 19 January 2005.

Domenico, Patrick A. and Franklin W. Schwartz. *Physical and Chemical Hydrogeology.* New York: John Wiley & Sons, 1998.

Francois, Alan, Hugues Mathis, Davy Godefroy, Pascal Piveteau, Francoise Fayolle, and Frederic Monot. "Biodegradation of Methyl tert-Butyl Ether and Other Fuel Oxygenates by a New Strain, *Mycobacterium austroafricanum* IFP 2012," *Applied and Environmental Microbiology*, 68(6): 2754-2762 (2002).

Godish, Thad. *Air Quality.* New York: Lewis Publishers, 2004.

Grady, Steven J. and George D. Casey. *Occurrence and Distribution of Methyl tert-Butyl Ether and Other Volatile Organic Compounds in Drinking Water in the Northeast and Mid-Atlantic Regions of the United States, 1993-98.* Water Resources Investigations Report 00-4228; U.S. Geological Survey, 2001.

Howard, Carlton J., Armistead Russell, Roger Atkinson, Jack Calvert. *Interagency Assessment of Oxygenated Fuels.* National Science and Technology Council (NSTC), June 1997.

Kovarik, William. "The 1920's Environmental Conflict Over Leaded Gasoline and Alternative Fuels." Electronic Resource, Paper to the American Society for Environmental History. n. pag. http://www.radford.edu/~wkovarik/papers/ethylconflict.html. December 5, 2003.

Liu, Catherine Y., Gerald E. Speitel, Jr., and George Georgiou. "Kinetics of Methyl t-Butyl Ether Cometabolism at Low Concentrations by Pure Cultures of Butane-Degrading Bacteria," *Applied and Environmental Microbiology,* 67(5): 2197-2201 (2001).

Lovanh, Nanh, Craig S. Hunt, and Pedro J.J. Alvarez. "Effect of Ethanol on BTEX biodegradation kinetics: aerobic continuous culture experiments," *Water Research,* 36: 3739-3746 (2002).

Mares, Kevin A. *Aerobic Biodegradation of Alternative Fuel Oxygenates in Unsaturated Soil Columns*. MS thesis, AFIT/GEM/ENV/04M-13. School of Engineering, Air Force Institute of Technology (AU), Wright-Pattterson AFB OH, March 2004 (AD-A422919).

Masters, Gilbert M. *Introduction to Environmental Engineering and Science.* Upper Saddle River: Prentice Hall, 1998.

Mormile, Melanie R., Shi Liu, and Joseph M. Suflita. "Anaerobic Biodegradation of Gasoline Oxygenates; Extrapolation of Information to Multiple Sites and Redox Conditions," *Environmental Science and Technology*, 28(9): 1727-1732 (1994).

Padilla, Ingrid Y., T.-C. Jim Yeh, and Martha H. Conklin. "The Effect of Water Content on Solute Transport in Unsaturated Porous Media," *Water Resources Research,* 35(11): 3303-3313 (1999).

Park, J., Y.-M. Chen, J.J. Kukor, and L.M. Abriola. "Influence of substrate exposure history on biodegradation in a porous medium," *Journal of Contaminant Hydrology,* 51: 233-256 (2001).

Pauling, Linus. *General Chemistry.* New York: Dover Publications, 1988.

Ruiz-Aguilar, Graciela M.L, Jose M. Fernandez-Sanchez, Staci R. Kane, Donguk Kim, and Pedro J.J. Alvarez. "Effect of Ethanol and Methyl-*Tert*-Butyl Ether on Monoaromatic Hydrocarbon Biodegradation: Response Variability for Different Aquifer Materials Under Various Electron-Accepting Conditions," *Environmental Toxicology and Chemistry,* 21(12): 2631-2639 (2002).

Schirmer, Mario, Barbara J. Butler, Clinton D. Church, James F. Barker, and Nalina Nadarajah. "Laboratory Evidence of MTBE Biodegradation in Borden Aquifer Material," *Journal of Contaminant Hydrology,* 60: 229-249 (2003).

Schmidt, Torsten C., Mario Schirmer, Holger Weiβ, Stefan Haderlein. "Microbial degradation of methyl tert-butyl ether and tert-butyl alcohol in the subsurface," *Journal of Contaminant Hydrology,* 70: 173-203 (2004).

Sedran, Marie A., Amy Pruden, Gregory J. Wilson, Makram T. Suidan, and Albert D. Venosa. "Effect of BTEX on Degradation of MTBE and TBA by Mixed Bacterial Consortium," *Journal of Environmental Engineering,* 128(9): 830-835 (2002).

Squillace, Paul J., John S. Zogorski, William G. Wilber, and Curtis V. Price. "Preliminary Assessment of the Occurrence and Possible Sources of MTBE in Groundwater in the United States, 1993-1994," *Environmental Science and Technology,* 30(5): 1721-1730 (1996).

United States Environmental Protection Agency (USEPA). *A Review of the Reference Dose and Reference Concentration Processes.* 630/P-02/002F. Washington, DC: 2002.

United States Environmental Protection Agency (USEPA). *Achieving Clean Air and Clean Water: The Report of the Blue Ribbon Panel on Oxygenates in Gasoline.* 420/R-99/021.

United States Environmental Protection Agency (USEPA). *Assessment of Potential Health Risks of Gasoline Oxygenated with Methyl Tertiary Butyl Ether (MTBE).* 600/R-93/206. Washington, DC: 1993.

United States Environmental Protection Agency (USEPA). *Drinking Water Advisory: Consumer Acceptability Advice and Health Effects Analysis on Methyl Tertiary-Butyl Ether (MtBE).* 822-F-97-009. December 1997.

United States Environmental Protection Agency (USEPA). *Health Risk Perspective on Fuel Oxygenates.* 600/R-94/217. Washington, DC: 1994.

United States Environmental Protection Agency (USEPA). *MTBE Fact Sheet #3, Use and Distribution of MTBE and Ethanol.* 510-F-97-016. January 1998.

United States Environmental Protection Agency (USEPA). *State Actions Banning MTBE (Statewide).* 420-B-04-009; June 2004.

United States Environmental Protection Agency (USEPA). *Summary of Workshop on Biodegradation of MTBE, February 1-3 2000.* 625-R-01-001A; February 2001.

United States Environmental Protection Agency (EPA). "EPA Takes Final Step in Phaseout of Leaded Gasoline." Online Press Release for January 29, 1996. n. pag. http://www.epa.gov/otaq/regs/fuels/additive/lead/pr-lead.txt. 3 December 2003.

United States Environmental Protection Agency (EPA). "MTBE in Fuels." Online Information Sheet. n. pag. http://www.epa.gov/mtbe/gas.htm. 3 December 2003.

United States Environmental Protection Agency (USEPA). "State Winter Oxygenated Fuel Program Requirements for Attainment or Maintenance of CO NAAQS." Electronic Resource. n pag. http://www.epa.gov/otaq/regs/fuels/oxy-area.pdf. January 19, 2005.

Vita

Major David A. Torres graduated from Jesuit High School in Sacramento, California. He entered undergraduate studies at California State University Sacramento where he graduated with a Bachelor of Science degree in Civil Engineering and was commissioned through the Detachment 088 AFROTC in May 1993. In August 2003, he entered the Environmental Engineering and Science program at the Air Force Institute of Technology.

REPORT DOCUMENTATION PAGE

Form Approved
OMB No. 074-0188

1. REPORT DATE *(DD-MM-YYYY)*	**2. REPORT TYPE**	**3. DATES COVERED** *(From – To)*
21-03-2005	**Master's Thesis**	Sep 2004 – Mar 2005

4. TITLE AND SUBTITLE

Evaluation of Fuel Oxygenate Degradation in the Vadose Zone

5a. CONTRACT NUMBER

5b. GRANT NUMBER

5c. PROGRAM ELEMENT NUMBER

6. AUTHOR(S)

Torres, David A., Major, USAF, BSC

5d. PROJECT NUMBER

5e. TASK NUMBER

5f. WORK UNIT NUMBER

7. PERFORMING ORGANIZATION NAMES(S) AND ADDRESS(S)
Air Force Institute of Technology
Graduate School of Engineering and Management (AFIT/EN)
2950 Hobson Way
WPAFB OH 45433-7765

8. PERFORMING ORGANIZATION REPORT NUMBER

AFIT/GES/ENV/05M-05

9. SPONSORING/MONITORING AGENCY NAME(S) AND ADDRESS(ES)
Dr Carl G. Enfield COMM: (513)569-7489
National Risk Management Research Laboratory
U.S. Environmental Protection Agency
Cincinnati, Ohio 45628

11. SPONSOR/MONITOR'S REPORT NUMBER(S)

12. DISTRIBUTION/AVAILABILITY STATEMENT
APPROVED FOR PUBLIC RELEASE; DISTRIBUTION UNLIMITED

13. SUPPLEMENTARY NOTES

14. ABSTRACT

Groundwater contamination by petroleum products poses a potential human health and safety risk. Methyl tert-butyl ether (MTBE) was a commonly used fuel oxygenate that was added to gasoline to meet environmental regulations. The widespread use of MTBE resulted in significant contamination of drinking water supplies across the United States.

This research evaluated the degradation characteristics of potential alternative fuel oxygenates in the vadose zone. One fuel oxygenate being considered as an alternative to MTBE is diisopropyl ether (DIPE). Specifically, this thesis sought to answer three research questions: what is the potential for DIPE degradation in soil without prior microbial augmentation, how does the presence of co-contaminants, such as ethanol and toluene, impact the biodegradation of DIPE, and will the increased use of DIPE represent a potential environmental risk? Previous research related to fuel oxygenates has focused primarily on oxygenates currently used, such as MTBE and ethanol. This research focused on a potential alternative to MTBE prior to its widespread implementation and use.

An experiment was run for 30 days to assess degradation characteristics for DIPE, ethanol, and toluene in the vadose zone. Due to the short length of the experiment it is not possible to determine if DIPE degradation occurred.

15. SUBJECT TERMS
Fuel Oxygenates, Ethanol, DIPE, Isopropyl Ether , Toluene, Soil Column Study

16. SECURITY CLASSIFICATION OF:			**17. LIMITATION OF ABSTRACT**	**18. NUMBER OF PAGES**	**19a. NAME OF RESPONSIBLE PERSON**
REPORT	**ABSTRACT**	**c. THIS PAGE**			Charles A. Bleckmann
U	**U**	**U**	**UU**	138	**19b. TELEPHONE NUMBER** *(Include area code)* (937) 255-3636, ext 4721; e-mail: Charles.Bleckmann@afit.edu